

AN ASYMMETRIC μ -OXO TECHNETIUM COMPLEX

M. J. Clarke, Lisa Podbielski, Dept. of Chemistry, Boston College, Chestnut Hill, MA 02167

Margaret E. Kastner, Department of Chemistry, Bucknell University, Lewisburg, PA 17837

John Schreifels, Department of Chemistry, University of Missouri, St. Louis, MO

A dinuclear, asymmetric technetium complex in which the two Tc atoms appear to be in intimate electronic communication has been synthesized and structurally characterized. The complex shown in Figure 1 forms spontaneously on heating either $[\text{OCl}_4\text{Tc}]^-$ or $[\text{TcCl}_6]^{2-}$ in neat picoline. Upon standing in nonaqueous solvents, the complex undergoes a linkage isomerization reaction involving the exchange of the single equatorial picoline on one Tc and the single equatorial chloride on the second to yield the previously reported dissymmetric complex, $[\text{Cl}(\text{Pic})_4\text{Tc}-\text{O}-\text{Tc}(\text{Pic})\text{Cl}_4]$.¹ The compound crystallizes in the monoclinic space group $P2_1/n$ with unit cell parameters: $a = 12.421 \text{ \AA}$, $b = 15.471 \text{ \AA}$, $c = 18.764 \text{ \AA}$ and $\beta = 93.174^\circ$, $Z = 4$. The geometry is essentially octahedral around each Tc, which are linked by a μ -oxo bridge, with the equatorial ligands on each Tc being staggered relative to those on the other. The average equatorial Tc(1)-N bond distance is $2.143(4) \text{ \AA}$, while the Tc(1)-Cl(equatorial) distance is $2.421(2) \text{ \AA}$ and the axial Tc(1)-Cl distance is $2.407(2) \text{ \AA}$. On the second technetium the equatorial Tc(2)-N distance is $2.150(4) \text{ \AA}$, while the axial Tc(2)-N distance is somewhat longer at $2.188(4) \text{ \AA}$ due to a slight *trans* influence exerted by the bridging oxygen. The Tc(1)-O and Tc(2)-O bond lengths are $1.800(3) \text{ \AA}$ and $1.837(3) \text{ \AA}$, respectively. Electrochemical measurements made by cyclic and square-wave voltammetry indicate single-electron redox processes at 0.54 V and -0.54 V . EPR reveals a complicated spectrum suggesting a rhombic pattern strongly split by one ^{99}Tc ($I=9/2$) and more weakly split by a second ^{99}Tc . ESCA results show that the ionization potential for the $3d$ electrons on both Tc's are $254.4(1) \text{ eV}$, suggesting that the probable best formulation of the oxidation states is as $[\text{Tc}(\text{III}),\text{Tc}(\text{IV})]$ or as $[\text{Tc}(3.5),\text{Tc}(3.5)]$. The comproportionation constant for this complex is 4.0×10^{18} , which indicates substantial electronic communication between the two Tc's mediated by the bridging oxygen. This is consistent with substantial Tc-O π -bond formation, as indicated by the relatively short Tc-O bond distances, which are intermediate between that expected for Tc-O (1.98 \AA) and Tc=O (1.75 \AA).² The presence of planar aromatic ligands in this type of complex offers the possibility of intercalation into DNA as either a mono- or bisintercalator. The internuclear separation of 3.6 \AA is also suitable to allow intercalation through a ligand on one Tc and covalent binding via the second.

¹ Kastner, M.E.; Fackler, P.H.; Charkoudian, J.; Podbielski, L.; Charkoudian, J.; Clarke, M.J., *Inorganica Chimica Acta*, 114, L11-15 (1986).

² Fackler, P.H.; Kastner, M.E.; Clarke, M.J.; Deutsch, E., *Inorganic Chemistry*, 23, 4683 (1984).

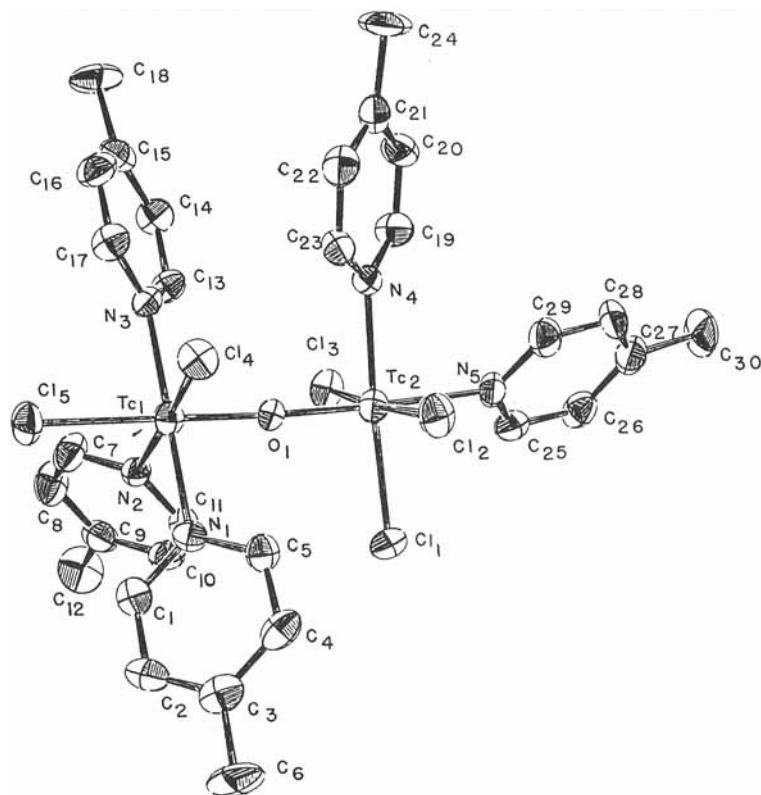


Figure 1.

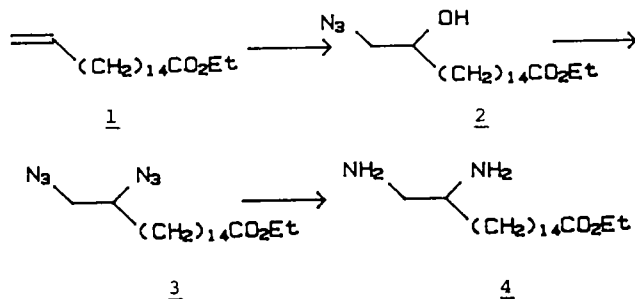
SYNTHESIS AND BIODISTRIBUTION OF Tc-99m BAT-PDA: A POTENTIAL HEART IMAGING AGENT FOR SPECT.

RH Mach, HF Kung, X-J Xu, Y-Z Guo and M. Blau*
 Department of Nuclear Medicine, SUNY/Buffalo and VA Medical Center, Buffalo, NY 14215 and *Department of Radiology, Harvard Medical School, Boston, MA 02115

The use of both I-123- labelled w-iodo fatty acids and w-(p-iodophenyl) fatty acids as potential SPECT imaging agents for the evaluation of regional myocardial perfusion and fatty acid metabolism has been well documented¹⁻³. Although several promising agents in this class have been prepared, the limited supply and high expense of uncontaminated I-123 has diminished the feasibility of the use of these agents in a clinical setting. The ready availability, cost effectiveness, and optimal half-life and gamma ray energy of Tc-99m make this isotope the radiolabel of choice in SPECT imaging. At this time we would like to report the synthesis and biodistribution of a novel Tc-99m- labelled fatty acid, bis(2-methyl-2-mercaptopropane)-16,17- diaminoheptadecanoic acid (BAT-PDA) as a potential SPECT heart imaging agent.

The synthesis of the title compound can be divided into two phases: a) conversion of the terminal olefin of ethyl 16-heptadecenoate⁴ (**1**) to the corresponding vicinal diamine; b) introduction of the bis(2-methyl-2-mercaptopropane) moiety. Introduction of the vicinal diamine was achieved by using a modification of the methodology described by Swift and Swern⁵ (Scheme 1). Epoxidation of **1** with *m*-chloroperbenzoic acid followed by SN₂ opening of the oxirane ring with sodium azide afforded the vicinal azido alcohol, **2**. Treatment of **2** with *p*-toluenesulfonyl chloride in pyridine followed by nucleophilic displacement of the tosyl group with sodium azide gave the vicinal diazide, **3**; catalytic hydrogenation of **3** with Adam's catalyst in ethanol gave the desired vicinal diamine, **4**.

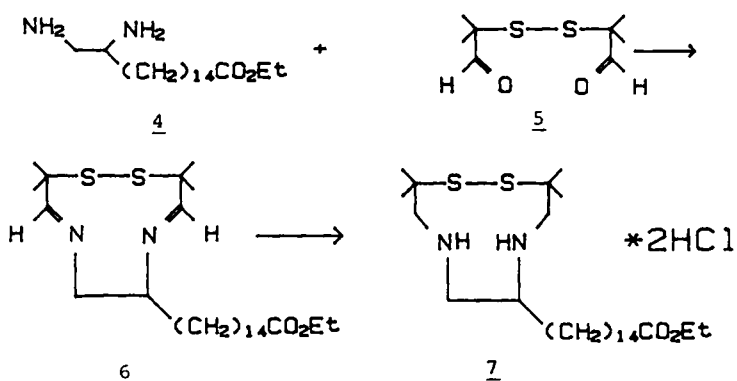
SCHEME 1



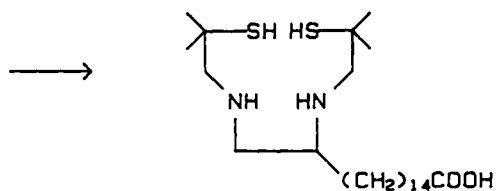
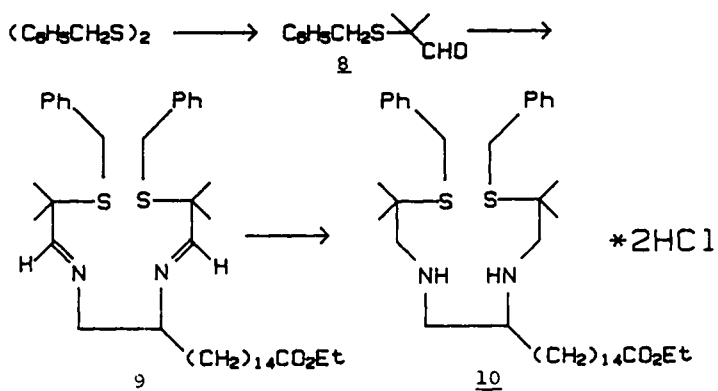
Introduction of the bis(2-methyl-2-mercaptopropane) moiety was achieved by two methods. Condensation of **4** with dialdehyde **5**⁶ (Scheme 2) afforded the diimine, **6**. Reduction of **6** with sodium borohydride in ethanol gave the corresponding disulfide analog, **7**. An alternative method for this conversion is outlined in Scheme 3. Treatment of benzylsulfenyl chloride⁷ with isobutyraldehyde in carbon tetrachloride at 50°C gave 2-methyl-2-benzylthiopropionaldehyde (**8**) in 76% yield. Condensation of **4** with two

equivalents of **8** gave the intermediate diimine, **9** which was reduced with sodium borohydride in ethanol to give the *S*-benzyl analog, **10**. Hydrolysis of the ester group of **10** with ethanolic sodium hydroxide followed by removal of the *S*-benzyl groups with sodium in liquid ammonia produced BAT-PDA.

SCHEME 2



SCHEME 3



BAT-PDA

Radiolabeling of BAT-PDA with Tc-99m was achieved by mixing the ligand with Tc-99m Sn(II)/pyro solution and heating at 100°C for 15 minutes. After extraction with chloroform, the organic layer was washed with water. The chloroform extract was condensed and the residue was redissolved in ethanol-saline (30-70). Radiochemical purity was determined by HPLC (purity >95%, labeling yield 50%). The partition coefficient (n-Octanol/pH7.0 buffer) was 1121, suggesting a neutral Tc-99m complex was formed.

Biodistribution of the Tc-99m BAT-PDA was evaluated in rats using I-125 w-(p-iodophenyl)-pentadecanoic acid (IPPA) as the internal standard. The initial heart uptake of the Tc-99m compound (0.3 %dose/organ at 5 min after injection) was lower than that for I-125 IPPA (0.5 %dose/organ). At 15 minutes after injection, the heart uptake was 0.1 and 0.6 %dose/organ for the Tc-99m BAT-PDA and I-125 IPPA, respectively. High liver uptake (30-40 %dose/organ) was observed for both compounds. This preliminary data suggested that the Tc-99m BAT-PDA itself may not be suitable for heart imaging. Attempts have been made to modify the fatty acid side chain to improve the uptake and retention in the heart.

REFERENCES

1. Otto, C.A.; Brown, L.E.; Wieland, D.M.; Beierwaltes, W.H. J of Nucl Med, **22**, 613-618 (1981)
2. Poe, N.D.; Robinson, G.D.Jr; Zielinski, F.W., et al Radiology, **124**,419-424 (1977)
3. Reshe, S.N.; Saver, W.; Machula, H.J.; et al Europ J Nucl Med, **10**, 228-234 (1985)
4. Tulloch, A.P. Chemistry and Physics of Lipids, **18**,1-6 (1977)
5. Swift, G, Swern, D. J Org Chem, **32**, 511-517 (1967)
6. Kung H.F.; Molnar, M.; Billings, J.B. et al J Nucl Med, **25**, 326-332, (1984)
7. Harpp, D.N.; Friedlander, B.T.; Smith, R.A. Synthesis, 181-182, (1979)

COMPLEXING OF ^{99}Tc WITH 1,4-DITHIA-8,11-DIAZACYCLOTETRADECANE

E. Ianovici, S. Truffer, M. Kosinski, P. Lerch

Institut d'électrochimie et de radiochimie, Swiss Federal Institute of Technology, Lausanne, Switzerland

The cationic complex of $^{99}\text{Tc(V)}$ with the ligand 1,4,8,11-tetraazaundecane (2,3,2 tet) was prepared recently (1). It has been shown that it contains $[\text{TcO}_2]^+$ core like the complex of Tc(V) with 1,4,8,11-tetraazadecane (2). In solution both complexes are positively charged and stable in air.

This report concerns the complexing of Tc with cis 1,4-dithia-8,11-diazacyclopentadecane (cis[14]ane N_2S_2).

The synthesis of this ligand and the corresponding Cu^{2+} complex was presented recently by T. Kaden (3).

1. Experiments with ^{99}Tc

Ligand dihydrochloride cis[14]ane N_2S_2 (5.21×10^{-2} mmol) was dissolved in 0.1M NaOH and extracted three times with CH_2Cl_2 . The free amine was added to a solution of $\text{TBA}[\text{TcOBr}_4]$ (1.41×10^{-2} mmol) in THF. After the evaporation of organic solvents the residue was dissolved in water and the separation was performed on a column packed with Bio-Gel P2 resin. The yellow coloured fractions eluted with water were combined and concentrated under nitrogen stream. Species present in solution before and after the separation on the column are presented in Fig.1.

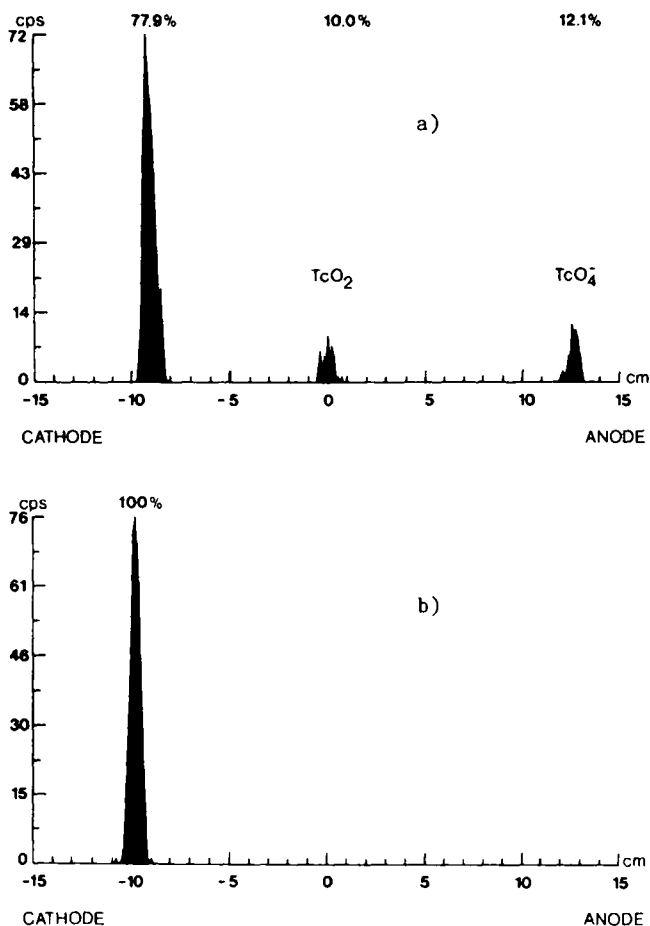


Figure 1. Species separated by electrophoresis. a) solution before separation on the Bio-Gel P2 column; b) solution after separation

Electrophoresis and paper chromatography showed a single cationic product which characteristics are presented in Table 1.

TABLE 1. Electrophoretic Behaviour of $^{99}\text{Tc}[14]\text{ane N}_2\text{S}_2$ *

System N°	Solution	Electrolyte	Migration distance (cm) cathode
1	H ₂ O	0.05 M phosphate buffer pH 8.5 or 7.0	9.8 ± 0.8
2	H ₂ O	0.1 M NaHCO ₃ pH 8.6	3.3 ± 1.0
3	0.1 M phosphate buffer pH 7.0	0.1 M phosphate buffer pH 7.0	9.4 ± 0.6
4	0.1 M phosphate buffer pH 8.5	0.05 M Na ₂ HPO ₄ pH 8.5	9.3 ± 0.7
5	0.1 M NaHCO ₃ pH 8.6	0.1M phosphate buffer pH 7.0	9.5 ± 0.5
6	0.05 M HCl	0.05 M Na ₂ HPO ₄ pH 8.5	10.0 ± 0.5

* Electrophoresis conditions : 2000 V for 30 min. except system N°2 : 300 V for 1 h (4)

In paper chromatography using 65/35 : acetonitril/water or 0.9% NaCl, the R_f values of the yellow complex were 0.6 + 0.07 and 0.84 + 0.02, respectively. The complex exhibits UV-vis absorptions at 240nm ($\epsilon = 10230 \text{ l.M}^{-1}.\text{cm}^{-1}$), 320nm ($\epsilon = 858 \text{ l.M}^{-1}.\text{cm}^{-1}$), 430nm ($\epsilon = 66 \text{ l.M}^{-1}.\text{cm}^{-1}$) and 570nm ($\epsilon = 4 \text{ l.M}^{-1}.\text{cm}^{-1}$) in aqueous solution. The stability of the complex in various solutions over different periods of time is shown in Table 2.

TABLE 2. Stability of $^{99}\text{Tc}[14]\text{ane N}_2\text{S}_2$ *

Solution	[^{99}Tc] M	Time d	Yield %
H ₂ O	4 x 10 ⁻⁴	8	100
0.1 M phosphate buffer pH 7.0	5 x 10 ⁻⁵	1	100
0.1 M phosphate buffer pH 8.5	5 x 10 ⁻⁵	0.8	98
0.1 M phosphate buffer pH 8.5	5 x 10 ⁻⁵	2	87
0.05 M HCl	2 x 10 ⁻⁵	0.8	98

* Methods used : electrophoresis and paper chromatography.

Dry yellow residue allowed to stand for ca. 24 h changed its colour into red-brown. Redissolution in water gave an instable red-orange product which absorption spectrum (320,365,474,730 nm) changed continuously. The final product was the yellow coloured compound with absorptions at 320 and 430nm. A comparison with previous results on [TcO₂(2,3,2-tet)]⁺ and [TcO₂cyclam]⁺ is made.

2. Experiments with ^{99m}Tc

The following labelling method was found to be optimal: To a vial containing 50 μl of ligand solution (10 mg/ml H_2O) were added consecutively: 500 μl 0.1M phosphate buffer pH 11.5, 100 μl physiological saline with $^{99m}\text{TcO}_4^-$ and 20 μl SnCl_2 (0.5 mg/ml 0.1M HCl). After shaking for 1 minute, 500 μl of 0.1M NaH_2PO_4 were added to set the pH at 7.0–7.5. Electrophoresis and paper chromatography showed a cationic species (96%) with the same characteristics as for ^{99}Tc . The impurities were 1% TcO_2 and 3% a cation which migration distance was 2cm from the start. The solution was repetitively analysed during 24 h after labelling. No decomposition was observed. The complex is not stable at pH higher than 8.0. The formation of TcO_4^- was observed.

The influence of the pH on the labelling was investigated; at pH 7.0 the cationic yield was only 30%.

It seems that the complex formed by technetium with cis[14]ane N_2S_2 is the same for ^{99}Tc and ^{99m}Tc but more detailed investigations are necessary.

1. Bläuenstein, P., Pfeiffer, G., Schubiger, P.A., Anderegg, G., Zollinger, K., May, K., Proso, Z., Ianovici, E., and Lerch, P., *Int. J. Appl. Radiat. Isot.*, 36, 315–317 (1985).
2. Zuckman, S.A., Freeman, G.M., Troutner, D.E., Volkert, W.A., Holmes, R.A., Deveer, D.G., and Barefield, E.K., *Inorg. Chem.*, 20, 2386–2389 (1981).
3. Siegfried, L., and Kaden, T., *Helv. Chim. Acta*, 67, 29–37 (1984).
4. Volkert, W.A., Troutner, D.E., and Holmes, R.A., *Int. J. Appl. Radiat. Isot.*, 33, 891–896 (1982).

PREPARATION OF Tc-PnAO BY LIGAND EXCHANGE

G. Ergun and D.E. Troutner

Department of Chemistry, University of Missouri, Columbia, MO 65211

Technetium propyleneamine oxime, {Oxo[3,3'-(1,3 propanediyl)diimino]bis(3-methyl-2-butanone oximato) (3-)-N,N,N'',N'''}technetium (V), formula $[TcO(C_{13}H_{25}N_4O_2)]$, TcPnAO) was the first of a series of amine oxime complexes of ^{99m}Tc found to be useful radiopharmaceuticals (1,2). It was of interest to develop a ligand exchange method for production of the complexes so that we would prepare them for radiochemical studies from stock solutions of ^{99m}Tc without a direct reduction step. Earlier work (3) had shown that ^{99m}Tc -amine complexes were readily formed from ^{99m}Tc -citrate solutions so that complex was chosen for the initial study.

First experiments were performed using solutions of 10^{-8} to $10^{-7}M$ $Na^{99}TcO_4$ to simulate approximate total technetium concentrations expected for 1 to 10-mCi/ml ^{99m}Tc solutions prepared from generators at daily intervals (4,5). Solutions were spiked with small amounts of ^{99m}Tc for a tracer. Formation of the Tc-PnAO complex was easily monitored by ascending solvent paper chromatography using diethyl ether as a solvent. In this system, all species except the lipophilic Tc-PnAO remain at the origin. In a typical experiment, Tc-cit was prepared by the method of Ref. 3 in saline at pH 6 using a saturated solutions of Sn(II)tartrate as a reducing agent. An aliquot was added to a $NaHCO_3$ -buffered solution of PnAO at pH ~ 8.5 . The resulting solution was analyzed for Tc-PnAO at times from 1 min to 24 hours. For some samples, the yield of Tc-PnAO was confirmed by extraction into $CHCl_3$, TcO_4^- was estimated by acetone paper chromatography and electrophoresis, and reduced, hydrolysed Tc by saline paper chromatography. Results of some experiments are shown in Table 1.

TABLE 1. Percent Complex Formation

[Tc] $\times 10^9$	[Cit] $\times 10^4$	[PnAO] $\times 10^6$	Percent Yield	
			0.5 hr	1 hr
100	70	1000	92	93
45	32	1000	87	87
14	10	5000	93	92
14	10	3000	93	92
14	10	1000	95	94
14	10	100	96	97
14	10	10	91	95
14	10	1	14	22

Blank experiments in which citrate, reducing agent, PnAO, or combinations of those were omitted gave zero yield as expected. Yields at pH 5 and 11 were only 5 and 50%, respectively. The order of addition of reagents had little effect on final yields. The highest yields were obtained when the pH of a

saline solution of Tc-cit was changed from pH 6 to 8.5 followed by addition of PnAO. The basic solution of Tc-cit eventually oxidized to TcO_4^- but yields of 95% were obtained when the PnAO was added as long as 3 hrs after making the Tc-cit solution basic. Yields from ligand exchange were equal to or higher than those from direct reduction at all PnAO concentrations from $1 \times 10^{-5} \text{M}$ to $5 \times 10^{-3} \text{M}$. Measurement of the yield as a function of time for the run at 10^{-6}M PnAO gave a final yield of $\sim 65\%$ after 24 hrs. The half-time was ~ 2 hr for the formation reaction. Uncomplexed Tc was present as TcO_4^- after 24 hrs.

These results suggest that $^{99\text{m}}\text{Tc}$ amine oxime radiopharmaceuticals might be prepared by reconstituting kits containing only PnAO and buffer with previously prepared Tc-cit solutions. Yields of $>95\%$ were obtained by adding 1 ml of $1.4 \times 10^{-7} \text{M}$ Tc-cit solutions to vials containing 10 ml of 10^{-3} or 10^{-4}M PnAO. These Tc-cit stock solutions were prepared at a Sn/Tc of ~ 10 or $\sim 10^{-4} \mu$ moles Sn/mCi $^{99\text{m}}\text{Tc}$. A 20 mCi final dose would require only $2 \times 10^{-3} \mu$ moles or $\sim 0.5 \mu\text{g}$ of Sn tartrate. Ligand exchange may also be useful in labeling antibodies to which PnAO chelating groups have been attached since it can be done under mild conditions and low Sn concentrations.

The experiments were extended to higher concentrations to learn if the method is suitable for preparation of ^{99}Tc amine oximes for chemical studies. A series of runs at Tc concentrations from $(5.6 - 560) \times 10^{-7} \text{M}$ gave yields of up to $\sim 70-80\%$ but yields depended greatly on the conditions under which the Tc-cit was prepared. Best results were obtained when Tc-cit was prepared by the method of Munze (6). A $6 \times 10^{-3} \text{M}$ solution of TcO_4^- was reduced with $1.1 \times 10^{-2} \text{M}$ Sn tartrate in $6 \times 10^{-2} \text{M}$ citrate. Five ml of this solution was combined with 6 ml of 10^{-2}M PnAO, made basic, and extracted into 10 ml ether. Solid Tc-PnAO was recovered from the ether. FTIR, UV-vis, and proton NMR spectra were consistent with those previously reported (7). The fraction of total Tc extracted into ether was $\sim 70\%$, comparable to a 74% yield when TcPnAO was prepared by direct reduction from the same TcO_4^- and PnAO concentrations. The Tc fraction which was not extracted into ether has not been fully characterized but appears to consist of reduced hydrolyzed Tc and a hydrophilic Tc-PnAO species.

1. Troutner, D.E., Volkert, W.A., Hoffman, T.J., and Holmes, Int. J. Appl. Radiat. Isot. 35, 467 (1984).
2. Fair, C.K., Troutner, D.E., Schlemper, E.O., Murmann, R.K., and Hoppe, M.L., Acta Cryst. C40, 1544 (1984).
3. Volkert, W.A., Troutner, D.E. and Holmes, R.A., Int. J. Appl. Radiat. Isot. 33, 891 (1982).

4. Holland, M.E., Deutsch, E., Heineman, W.R. and Holland, E.M., *Int. J. Appl. Radiat. Isot.* 37, 165 (1986).
5. Holland, M.E., Duetsch, E., and Heineman, W.R., *Int. J. Appl. Radiat. Isot.* 37, 173 (1986).
6. Munze, R., *Radiochem. Radioanal. Ltrrs.* 30, 61 (1977).
7. Jurisson, S., Schlemper, E.O., Troutner, D.E., Canning, L.R., Nowotnik, D.P., and Neirinckx, R.D., *Inorg. Chem.*, in press.

SYNTHESIS AND RENAL EXCRETION CHARACTERISTICS OF ISOMERIC METHYL DERIVATIVES OF ^{99m}Tc -MERCAPTOACETYLTRIGLYCINE

A. Verbruggen, P. Dekempeneer, B. Cleynhens, M. Hoogmartens, and M. De Roo

Radiopharmacy and Nuclear Medicine, University Hospital Gasthuisberg, B-3000 Leuven, BELGIUM

As recently described (1), ^{99m}Tc -mercaptoacetylglycylglycylglycine (^{99m}Tc MAG₃) is a technetium-99m labeled agent that is efficiently excreted by the kidneys, mainly by tubular secretion, and therefore it may be a useful alternative to ^{131}I -o-iodohippurate. In order to come to a better understanding of the interaction of hippurate-like substances with the renal tubular transport mechanisms we have synthesized and studied the biodistribution of isomeric derivatives of ^{99m}Tc MAG₃, differing by the position (C₁, C₃, C₅ or C₇, Table 1) and the orientation (D or L) of a methyl substituent on one of the methylene groups.

The ligands were synthesized as the S-benzoyl protected precursors by one of the synthetic routes outlined in Figure 1 starting from the appropriate di- or tripeptide. The compounds were labeled with ^{99m}Tc in high yield by heating 1 mg of the protected precursor with sodium pertechnetate in the presence of stannous tartrate. Radiolabeling reaction mixtures were purified by HPLC on a 250 mm x 0.5 inch Zorbax RP 8 column eluted with ethanol-0.05 M phosphate buffer, pH 6.0 (15:85). Diastereomers were separated for L- and DL- ^{99m}Tc -IV (Table 1) and observed but not resolved for DL- ^{99m}Tc -I. Biodistribution of the ^{99m}Tc complexes was studied in male mice 10 min after intravenous injection. The values of urinary excretion and accumulation in kidneys and liver are summarized in Table 1.

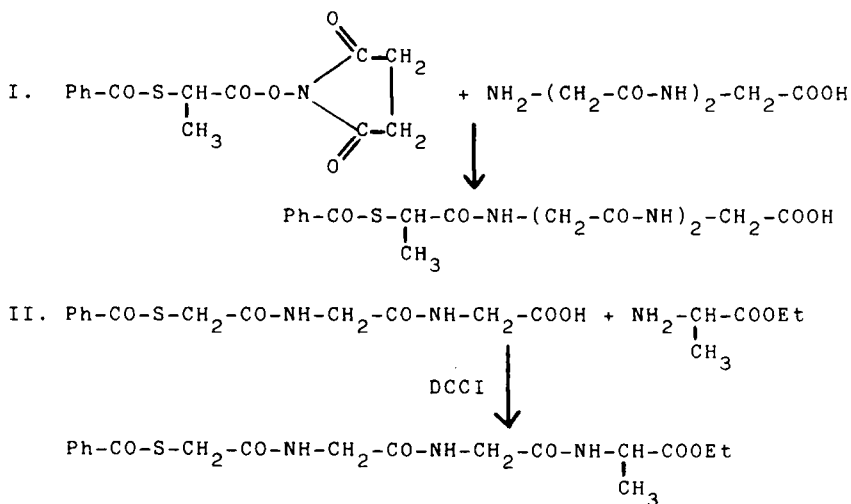
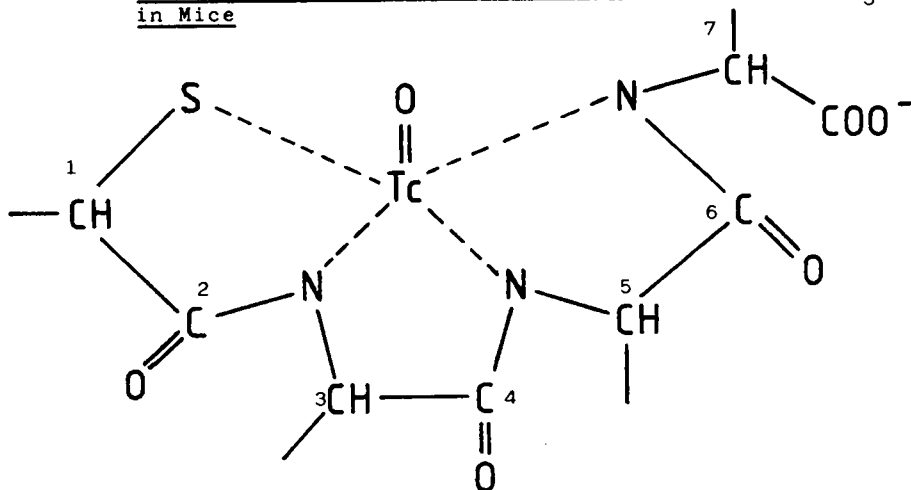


Figure 1. Examples of Synthetic Routes for S-Benzoyl Protected Methyl derivatives of MAG₃

For the racemic DL methyl derivatives of ^{99m}Tc MAG₃ it appears that introduction of a methyl substituent at C₃, C₅ or C₇ in ^{99m}Tc MAG₃ (DL-compounds I, II and III) results in agents with clearly inferior renal excretion characteristics in comparison with ^{99m}Tc MAG₃, as shown by the higher uptake in liver and renal retention. From the observed biodistribution of the D- and L-isomers of II and III one can conclude that these isomers are extracted by the kidneys to about the same extent, but their transport to the urine is completely different: the D-isomers are efficiently transported to the urine whereas the L-isomers are retained in the kidneys.

Table 1. Biodistribution of Methyl Derivatives of ^{99m}Tc MAG₃ in Mice



Compound	Methyl at	Percentage of injected dose/organ 10 min after injection as mean \pm s.e.m. (n=6)		
		Urine	Kidneys	Liver
MAG ₃ (1)	-	79.9 \pm 0.9	3.5 \pm 0.3	2.9 \pm 0.1
DL I	C ₁	43.6 \pm 5.2	28.9 \pm 2.5	14.6 \pm 1.3
DL II	C ₃	36.3 \pm 5.1	37.5 \pm 2.6	6.0 \pm 0.8
D II	C ₃	68.4 \pm 2.1	8.6 \pm 1.9	-
DL III	C ₅	37.1 \pm 2.1	36.2 \pm 2.7	7.2 \pm 0.8
D III	C ₅	69.2 \pm 2.0	9.3 \pm 0.8	7.2 \pm 0.6
L III	C ₅	8.9 \pm 1.2	72.6 \pm 4.0	7.6 \pm 1.1
DL IV*	C ₇	68.8 \pm 2.9	3.6 \pm 0.4	12.9 \pm 1.6
L IV*	C ₇	68.2 \pm 2.7	3.9 \pm 0.5	13.6 \pm 0.2

* Similar results for both diastereomers

Replacement of the terminal glycine moiety of ^{99m}Tc MAG_3 by alanine (compound IV) affects renal handling to a much smaller degree, although the uptake in the liver is increased moderately. For this derivative we observed that the L- and DL-isomer and their respective diastereomers show the same biological behaviour.

It seems that substitution of ^{99m}Tc MAG_3 with a methyl group in the part of the molecule involved in the complex formation with ^{99m}Tc does not reduce significantly the renal extraction efficiency. However the renal transport of the ^{99m}Tc complex can drastically be altered depending on the orientation (D or L) of the substituent. We have reported (2) similar observations for the four isomers of $^{99m}\text{Tc}-\text{CO}_2-\text{DADS}$, where the asymmetric carbon atom is also at a site involved in the complex formation. It is striking that for compounds II and III and for $^{99m}\text{Tc}-\text{CO}_2-\text{DADS}$ each time the D-isomer is excreted by the kidneys more efficiently than the L-isomer.

Addition of a methyl substituent in ^{99m}Tc MAG_3 on the carbon in α -position of the terminal carboxylate group, thus outside the technetium binding SN_3 core, results in a slight increase of lipophilic properties. This can be deduced from the longer retention time in the HPLC purification and leads to a higher uptake in the liver. However, the efficiency of renal extraction and tubular transport is almost completely maintained, regardless the orientation of the substituent and the geometrical constitution (syn or anti) of the ^{99m}Tc complex.

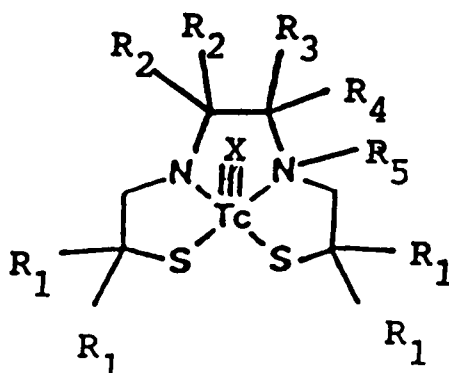
1. Fritzberg, A.R., Kasina, S., Eshima, D., and Johnson, D.L., *J. Nucl. Med.*, 27, 111 (1986)
2. Verbruggen, A., Cleynhens, B., José, D., Hoogmartens, M., and De Roo, M., *J. Nucl. Med.* P26, 19 (1985).

THE CHEMISTRY AND PHARMACOLOGY OF TRIAMINEDITHIOL
TECHNETIUM-BASED BRAIN PERFUSION AGENTS.



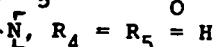
A.D. Watson, R.C. Walovitch, B.Q. Belonga, and E.H. Cheesman.
E.I. DuPont de Nemours & Co., Biomedical Products,
N. Billerica, MA 01862

Tchnetium complexes based on amine derivatives of the quadridentate ligand N,N'-bis(2',2'-dimethyl-2''-mercaptoethyl)-2,2-dimethylethylenediamine have been shown to cross the blood-brain barrier [J. Nucl. Med. 26: P105 (1985)]. We have examined the effects of converting the technetium(V)oxo core to the technetium nitrido core first described by Baldas [J.C.S. Dalton, 1981, 1798]. Five neutral complexes containing the technetium (V) oxo core were prepared and brain uptake indices (modified Oldendorff) and biodistributions were carried out in rats. This data is compared with that obtained for corresponding complexes containing the technetium nitrido core, prepared using a modification of a published procedure [Int. J. Appl. Rad. Isot., 36, 133 (1985)]. To determine the factors influencing retention of these complexes within the brain, in vivo subcellular distribution studies in rat brain tissue homogenates were carried out. Dual labeled autoradiographic studies using ¹⁴C antipyrine as a perfusion reference standard have also been conducted to quantitate the distribution of these complexes in rat brain. Contrary to earlier reports with other ligand systems (ibid.), we observe only a small variation in the pharmacological properties of the complexes examined when the technetium core is altered from Tc=O to Tc=N.

Table I



X=O X=N

(1) (6) $R_1 = \text{Me}, R_2 - R_5 = \text{H}$ (2) (7) $R_1 = R_2 = \text{Me}, R_3 - R_5 = \text{H}$ (3) (8) $R_1 = R_2 = \text{Me}, R_3 = R_4 = \text{H}, R_5 =$ (4) (9) $R_1 = R_2 = \text{Me}, R_3 = R_4 = \text{H}, R_5 =$ (5) (10) $R_1 = \text{Me}, R_2 = \text{H}, R_3 =$ , $R_4 = R_5 = \text{H}$

	BUI (a)	30 s Biodistribution (% ID) (b)	HPLC RT
X = O			
(1)	46 ± 19	0.80	9.0
(2)	97 ± 3	0.90	12.4
(3)	124 ± 10	1.60	12.0
(4)	106 ± 17	1.05	8.0
(5)	114 ± 6	1.80	7.5
X = N			
(6)	35 ± 3	0.74	6.3
(7)	80 ± 5	0.70	8.7
(8)	99 ± 7	1.40	12.2
(9)	83 ± 7	1.13	7.9
(10)	107 ± 9	1.74	7.0

(a) Determined according to a published modified Oldendorff procedure

(b) Carried out according to a previously described protocol

(c) HPLC conditions have been previously described.

COMPARISON OF THIOUREA COMPLEXES OF ^{99}Tc AND $^{99\text{m}}\text{Tc}$ AND POSSIBLE USE TO PREPARE
RADIOPHARMACEUTICALS

K. Zollinger, P. Bläuenstein, P.A. Schubiger and L. Helm*

Swiss Federal Institute for Reactor Research, 5303 Würenlingen; *Inst. of Inorganic and Analytical Chemistry, University Lausanne, 1005 Lausanne; Switzerland

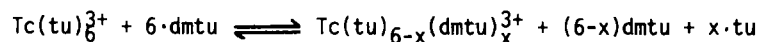
Thiourea (tu), Dimethylthiourea (dmu) and Tetramethylthiourea (tmtu) complexes of ^{99}Tc are well characterized (1,2). Paramagnetic complexes are formed with Tc(III) and tu or dmu ($\mu=2.7$ B.M.) and a diamagnetic complex with Tc(V) and tmtu. Despite the paramagnetism of the former complexes it was possible to obtain proton NMR spectra with surprisingly narrow lines (line width 10 to 30 Hz for methyl protons). The spectra were taken in deuterated Nitromethane and the results are given in table 1. The diamagnetism of the tmtu complex was not experimentally determined. Theoretical reasons and the comparison of the chemical shifts of the NMR signals are pointing to the different character of the complex.

TABLE 1.

Chemical shifts of the ^1H -NMR resonances of the Tc complexes with thiourea (tu), N,N-dimethylthiourea (dmu) and tetramethylthiourea (tmtu) as well as the free ligands in CD_3NO_2 . All values are given in ppm relative to TMS; CD_3NO_2 was taken as internal reference (4.30 ppm relative to TMS (3)).

	complexes		free ligands	
	CH ₃	NH	CH ₃	NH
$\text{Tc}(\text{tu})_6^{3+}$	-	-6.7, -11.8	-	6.15
$\text{Tc}(\text{dmu})_6^{3+}$	26.1	6.3	2.91, 2.94	6.2
$\text{TcO}(\text{tmtu})_4^{3+}$	3.44, 3.95	-	3.06	-

The aim of the ^1H -NMR study performed with these Tc-99 complexes was the determination of ligand exchange rates. No line broadening or chemical shift changes were observed when free ligands were added to solutions containing the complexes only. The exchange rates are therefore considered to be slow compared to the NMR time scale ($k < 10 \text{ s}^{-1}$). To get nevertheless an idea of the exchange rates we recorded ^1H -NMR spectra immediately after mixing $\text{Tc}(\text{L})$ with L^* ($\text{L} = \text{tu}, \text{dmu}$; $\text{L}^* = \text{dmu}, \text{tu}$). All spectra show the complicated pattern of mixed ligand complexes and mixed free ligands L, L^* . This shows that exchange rates for reactions like



are fast compared to the time between mixing and the recording of the spectra (less than 1 min.).

During the synthesis of these complexes a further reduction of the tmtu complex was observed and the product characterized as a Tc(IV) complex: $\text{Tc}(\text{tmtu})_2\text{Cl}_4$.

We tried to obtain the same compounds with $^{99\text{m}}\text{Tc}$, but the *rf* values obtained with paper chromatography (Whatman I, Acetonitrile/Water=72:28) showed a slightly different behavior of the complexes. The conditions were always pH=1 and ligand = 0.1 M. In case of tu the Tc(IV) oxidation state was observed and only

little of the Tc(III) complex, in case of dmtu no Tc(III) but Tc(IV) and Tc(V) and in the case of tmtu mainly the Tc(V) complex was obtained.

This observation together with the short time necessary for ligand exchange led to the idea to use these complexes as educts for ligand exchange reactions to produce radiopharmaceuticals. In a few tests with polydentate amine ligands promising results were obtained. A fast change of the colour was observed after mixing 2,12-Dimethyl-2,5,9,12-Tetraazatridecane (edtt) to the ^{99}Tc -tmtu-complex UV-Spectra proved the presence of $^{99}\text{TcO}_2(\text{edtt})^+$. In case of $^{99\text{m}}\text{Tc}$ the ligand exchange was analyzed using paper chromatography. The final goal of the study is the specific labelling of proteins to which a chelating ligand (like edtt) is covalently bound. Our interest was directed to the labelling of neoplasminogen used for the detection of deep vein thrombosis, a protein which is stable between pH 7 and pH 9. In contrast to the coupled DTPA, where the best results are obtained if the labelling is done in slightly acidic solutions, this type of amine ligand needs alkaline conditions (4) and is therefore preferred together with neoplasminogen. The first attempt using such a tetraamine ligand showed only a low percentage of specific binding of $^{99\text{m}}\text{Tc}$. Improvement is necessary to apply it in the nuclear medicine practice.

We thank K. May (Lab. for Radiochemistry, ETH Zürich) where the ^{99}Tc complexes were synthesized.

1. M.J. Abrams, A. Davison, R. Faggiani, A.G. Jones and C.J.L. Lock, *Inorg. Chem.*, **23** (1984) 3284.
2. M.J. Abrams, D. Brenner, A. Davison and A.G. Jones, *Inorg. Chim. Acta*, **77** (1983) L127.
3. Bruker Almanac 1986, p 107.
4. P. Bläuenstein, G. Pfeiffer, P.A. Schubiger, G. Anderegg, K. Zollinger, K. May, Z. Proso, E. Inaovici and P. Lerch, *Int. Z. Appt. Radiat. Isot.*, **36** (1985) 315.

EFFECTS OF SOME TRANSITION-METALLIC IONS ON THE PREPARATION OF TC-99m-PINGYANGMYCIN

J-X Wang, Y-H Zhang, W-Z Gau, and X.Li

Department of Nuclear Medicine, Beijing Institute for Cancer Research, Western District, Beijing

We have acquired some good results studying the technetium-99m labelling reaction of Pingyangmycin (PYM) without N_2 in recent years. (PYM is a clinically effective anticancer drug in China) The labelling yield has reached 96.7(\pm 0.3)% that the 94% labelling yield can be obtained only under N_2 (1), and the biodistribution experiments in mice indicated that except for Kidney the level of Tc-99m-PYM is highest in tumor (2) which has been reported (3-6) is only second or third high. In view of the sometimes dropping yield of Tc-99m-PYM, we supposed it maybe presented the microamounts of some metallic ions such as Al^{3+} , Ca^{2+} and Fe^{2+} in the reaction mixture while the glass shell of the stirring bar is broken. The effects of these three ions were studied and it was shown that adding Al^{3+} or Ca^{2+} has no influence but Fe^{2+} (maybe containing Fe^{3+}). To keep the high yield in preparing Tc-99m-PYM, the title project was undertaken.

The Tc-99m-labelling reaction was carried out as follows: various microamounts of common transition-metallic ions such as Cr^{3+} , Mn^{2+} , Fe^{3+} , Fe^{2+} , Co^{2+} , Ni^{2+} , Cu^{2+} , Cu^+ , Zn^{2+} , and Cd^{2+} were mixed respectively into the mixture of PYM and pertechnate eluate. Under vibration, the freshly prepared $SnCl_2$ solution was added rapidly and adjusted with $NaHCO_3$ to pH 4-5, then the total volume of 1.2ml was made with normal saline. At the end of vibrating, the sample was analyzed on silica gel by TLC with 10% NH_4OAc , MeOH (1:1, vols) as solvent and by electrophoresis with a buffer solution of 0.2M sodium phosphate at pH 5.8.

The results that are given in the table and the figure show the effects of common transition-metallic ions on the yield of Tc-99m-PYM.

The results showed that the ions from chromium, manganese, zinc and cadmium as high as 100 micrograms have no influence on this labelling reaction but Cu^+ , Cu^{2+} and Fe^{3+} have a greater effect than others due to the different abilities of metal-complexing, i.e the stability of forming complex of metallic ions from former four elements are lower than those from others. In other words the ions of Cu^+ , Cu^{2+} and Fe^{3+} can compete with Tc-99m for PYM complexing.

There is the oxidizing property of certain metallic ions like Fe^{3+} that may oxidize Sn^{2+} and affects on the labelling yield besides of complexing ability. So we conclude that it is important to avoid contaminating any ion from iron, cobalt, nickel and copper especially Cu^+ , Cu^{2+} , and Fe^{3+} to keep high yield of Tc-99m-PYM.

The complexing ion of (Tc-99m-PYM) moved toward the cathode as the unlabelled PYM did in the electrophoresis analysis. PYM is an alkaline peptide (p) carrying a positive charge in neutral solution shown as $\text{P} \begin{matrix} \text{NH}_3^+ \\ \diagdown \\ \text{COOH} \end{matrix}$, therefore Tc-99m-PYM should be suggested as a metal complex of peptide. Because the mole ratio of Sn^{2+} and $^{99\text{m}}\text{TcO}_4^-$ is 92, much higher than 1.5 in mononuclear complex and 5-10 in dinuclear complex (7), we think Tc-99m-PYM is a polynuclear complex, not so stable under the oxidizing effect of air, and that Tc-99m-PYM should be used immediately after preparing.

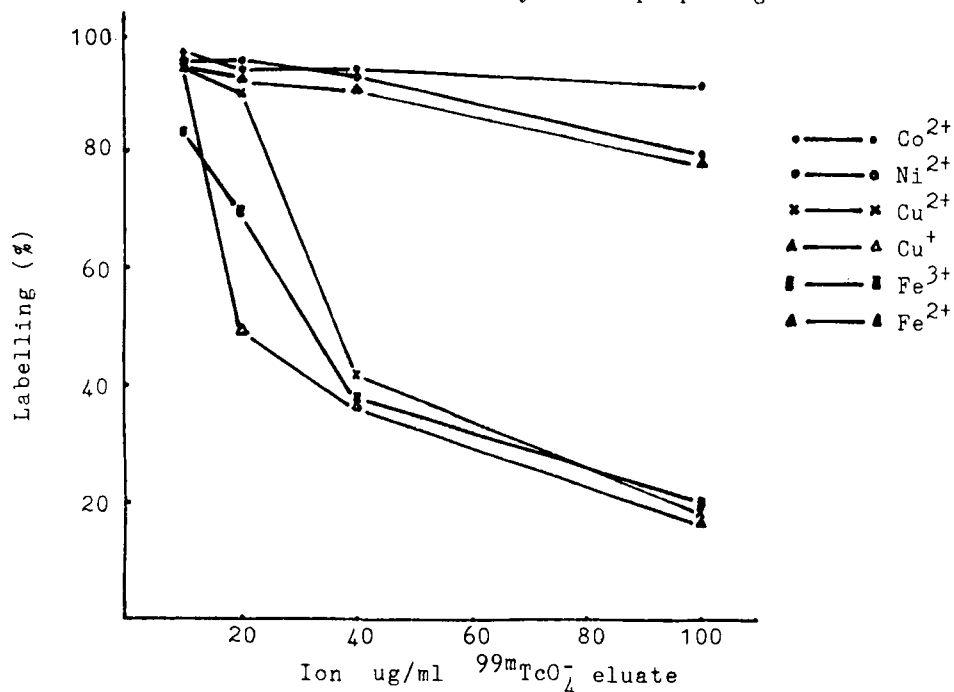


Fig. Effect of some transition-metallic ions
 10 μl SnCl_2 (1.77×10^{-9} mol in 0.1N HCl) is added to a mixture of PYM (0.5mg in 50 μl N.S.), $^{99\text{m}}\text{TcO}_4^-$ eluate (1ml) and various microamounts of every metallic ion respectively. After 10min vibrating without N_2 , the reaction mixture is analyzed on TLC. The labelling yield of Tc-99m-PYM are plotted against each amount of every relevant metallic ion.

Table. Effect of several metallic ions on Tc-99m labelling of Pingyangmycin

Ions	Labelling %	Value
100ug	$\bar{x} \pm S.D$	(t test)
None	96.7 \pm 0.3	
Cr ³⁺	96.6 \pm 0.3	> 0.05*
Mn ²⁺	96.2 \pm 0.4	> 0.05*
Zn ²⁺	96.0 \pm 0.7	> 0.05*
Cd ²⁺	96.7 \pm 0.3	> 0.05*

* No significant difference with "None"adding

1. Bartels P.J;Dekker B.G; Ligny C.L.DE;and Oldenburg S.J;Int.J. Appl.Radiat. Isotopes; 29, 15 (1978)
2. J-X Wang,S-Q Zhao, X.Li and B-H Lin; Chinese J. Nucl Med;5, 101 (1985)
3. Mori T; Hamamoto K;Onoyama Y;and Torizuka K;J.Nucl.Med;16,414 (1975)
4. Zimmermann. M;and Halc.T;Nuklearmedizin;15, 176(1976)
5. Tragl.K.H;Pils P; Angelberger. P;Hruby.R; and Imhof. H;Wien. Klin. Wshr; 87,308 (1975)
6. Yokoyama A; Terauchi Y;Horiuchi K; Okumura S;Saito Y;Tanaka H; Odori T;Morita R;Mori T; and Torizuka K; Int. J. Appl. Radiat. Isotopes; 29,549 (1978)
7. Horiuchi K; Yokoyama A; Fujibayashi Y; Tanaka H; Odori T; Saji H;Morita R; and Torizuka K; ibid; 32, 47 (1981)
8. Yokoyama A; and Horiuchi K; ibid; 33, 929 (1982)

UPTAKE OF ^{99m}Tc -ACRIDINYL IMINODIACETATES IN MELANOMAS

F.C. Hunt, J.H. Turner, and A.A. Martindale.

Isotope Divn; A.A.E.C; Lucas Heights Research Laboratories, PMB, Sutherland, NSW 2232 and Dept. of Nuclear Medicine, Fremantle Hospital, Fremantle, WA 6160, Australia.

Because of its DNA intercalating properties, the acridine moiety has been incorporated in the design of a series of chemotherapeutic agents effective against leukaemia (1), and a number of other animal tumours including melanomas (2).

One of these agents, (4'-(9'-acridinylamino)methanesulphon-m-anisidine, m-AMSA, labelled with carbon-14, was shown to bind strongly to B16 melanoma cell nuclei (3).

In a previous study, technetium- 99m acridinyl iminodiacetates were synthesised, and their biodistribution studied in rats bearing lymphatic leukaemias (4). This study extends the earlier work, by investigating the uptake of the compounds in melanomas, with the object of identifying a melanoma-specific radiopharmaceutical.

The ^{99m}Tc chelates (Figure 1) were synthesised as before (4) and injected into mice bearing melanotic and amelanotic strains of the B16 melanoma in C57 mice. Scintigraphic studies were performed using a gamma camera fitted with a pin-hole collimator.

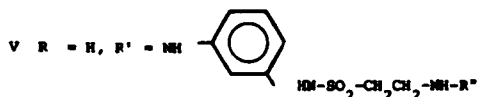
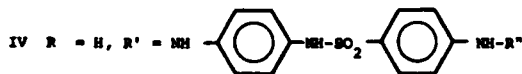
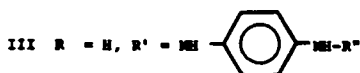
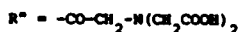
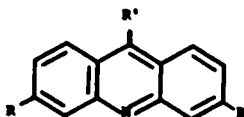


Fig. 1. Structural formulae of acridinyl iminodiacetic acids

Table 1. Biodistribution of Tc-acridinyl-IDA chelates in melanotic and amelanotic mice, 6 hours post injection

	Tc-I		Tc-II		Tc-III		Tc-IV		Tc-V	
	Mel	Amel	Mel	Amel	Mel	Amel	Mel	Amel	Mel	Amel
Liver	7.1	2.2	12.9	15.2	5.3	4.2	16.8	15.8	18.0	8.7
Spleen	3.6	0.9	2.6	3.2	1.4	1.8	6.6	9.1	8.9	3.6
Kidney	3.7	5.7	18.9	31.5	13.5	12.0	17.7	16.7	10.8	12.3
Muscle	0.1	0.1	0.2	0.3	0.3	0.2	0.5	0.3	0.2	0.3
Blood	0.5	0.6	0.9	0.8	1.6	1.5	2.3	2.1	1.9	1.6
Tumour	0.5	0.8	1.9	4.3	1.5	1.6	1.8	1.5	1.3	1.1
Eye	0.1	0.1	0.3	0.4	0.1	0.2	0.4	0.3	0.2	0.2
T/B	1.0	1.3	2.1	5.4	1.0	1.0	0.8	0.7	0.7	0.4
T/M	5.0	8.0	9.5	14.3	5.0	8.0	3.6	5.0	6.5	3.7

* Percentage of injected dose per gram. Means for 3 animals. Standard deviations omitted for clarity.

T/B = tumour/blood, T/M = tumour/muscle

The results of the biodistribution studies, 6 hours after injection, are shown in Table 1. Compound II had the best uptake with respect to tumour concentration and tumour-to-blood ratios, particularly in the amelanotic strain. Scintigraphic studies showed faint delineation of amelanotic tumours in the case of compound II, with good delineation and persistence of compound IV in amelanotic tumours at 24 hours post injection.

These results indicate selective tumour uptake with some of the ^{99m}Tc -acridinyl iminodiacetates. The localisation is structure dependent, and with the compounds having positive uptake, is more pronounced in amelanotic tumours. This result is the reverse of that found with the localisation of ^{14}C -m-AMSA, where higher uptake was found in melanotic tumours (3).

1. Ferguson, L.R; and Denny, W.A; *J. Med. Chem*; 22, 251 (1979).
2. Cain, B.F; and Atwell, G.J; *Ur. J. Cancer*, 10, 539 (1974).
3. Shoemaker, D.D; Legha, S.S; and Csyk, R.L; *Pharmacology*, 16, 211 (1978).
4. Hunt, F.C; McLaren, A.B; Maddalena, D.J; and Wilson J.G; *Int. J. Nucl. Med. Biol*; 11, 64 (1984).

STUDY OF BROMO-OXOTECHNETATE(V) COMPOUNDS

E. Ianovici, D. Mantegazzi, P. Lerch

Institut d'électrochimie et de radiochimie, Swiss Federal Institut of Technology, Lausanne Switzerland

Five-coordinated monooxo[TcOX_4]⁻ ion (X = Cl, Br) obtained by the reduction of TcO_4^- with cold concentrated HCl or HBr were isolated as tetraalkylammonium salts (1,2). A single crystal X-ray structure analysis was completed and it was reported that the [TcOCl_4]⁻ ion is square pyramidal (1). It has been shown that this ion can bind a fifth chloride forming a six-coordinate monooxo [TcOCl_5]²⁻ complex. The salts of this ion were isolated only with small cations : NH_4^+ , K^+ , Cs^+ and were characterised by infrared and UV-vis. spectroscopy (3). Recently the $\text{Cs}_2[\text{TcOCl}_5]$ and $\text{Cs}_2[\text{TcOBr}_5]$ were prepared and the X-ray structure analysis was completed (4). The crystal system of these complexes is cubic. Similar crystal data were found previously for $\text{Cs}_2[\text{ReOCl}_5]$ and $\text{Cs}_2[\text{ReOBr}_5]$ analogues (5,6), but an orthorhombic structure type was found for $\text{Rb}_2[\text{ReOCl}_5]$ (4).

As the nature of the cation has determined the isolation of one or another of the two ions, the formation of [TcOBr_5]²⁻ or [TcOBr_4]⁻ was investigated with the following cations : NH_4^+ , K^+ , Rb^+ , Cs^+ , Et_4N^+ and Me_4N^+ . For comparison the Bu_4N^+ salt was also prepared.

The K^+ and NH_4^+ salts being too soluble, they could not be isolated from the solution. Their absorption spectra in 4M HBr are given in Figure 1.a).

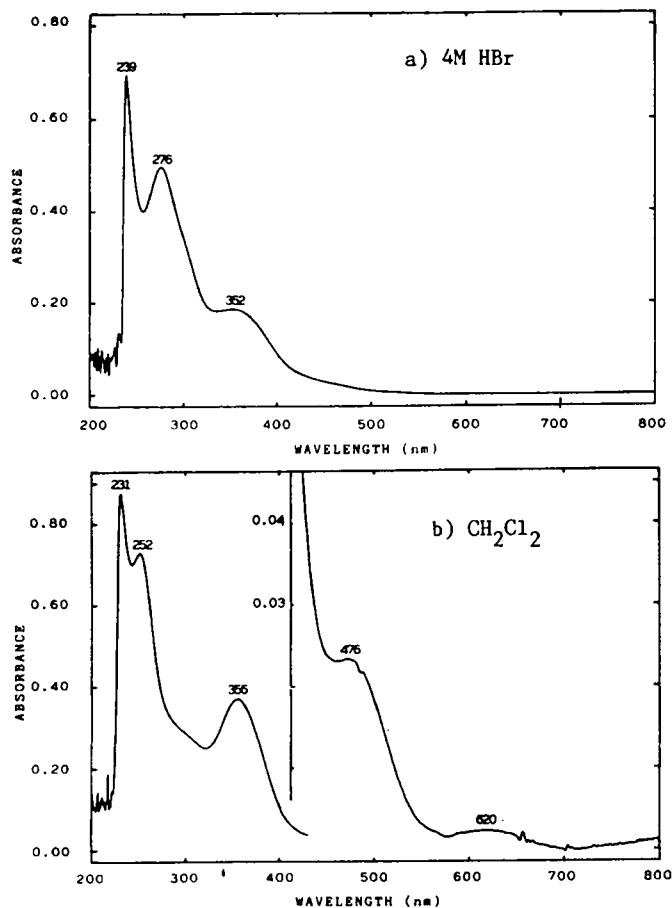
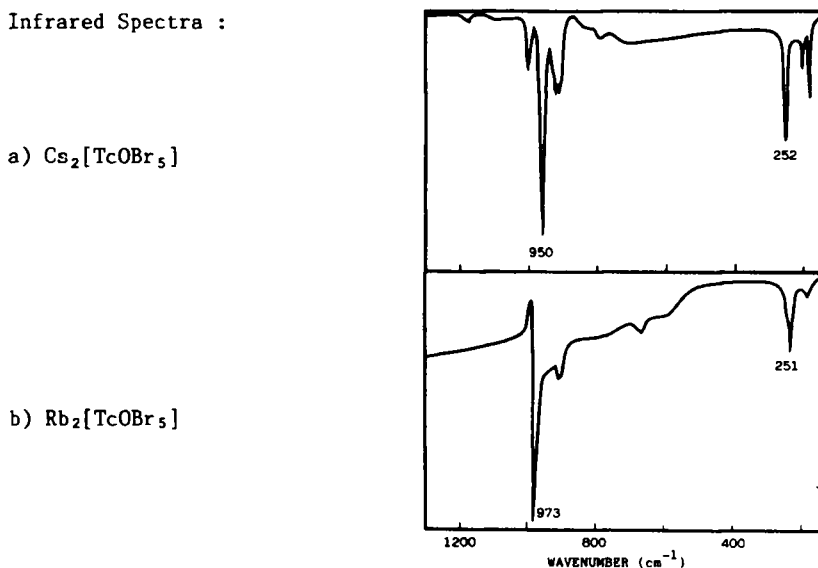


Figure 1. UV-vis. spectra of bromo-oxotechnetate(V) : a) NH_4^+ , K^+ , Rb^+ , Cs^+ , Me_4N^+ , Et_4N^+ , Bu_4N^+ , b) Me_4N^+ , Et_4N^+ , Bu_4N^+

Cs^+ and Rb^+ salts were isolated as red crystalline powder. The UV-vis. spectra in 4M HBr exhibit the same absorptions as for nonisolated NH_4^+ and K^+ complexes (Figure 1.a)). The infrared spectra of Cs^+ and Rb^+ salts are presented in Figure 2.

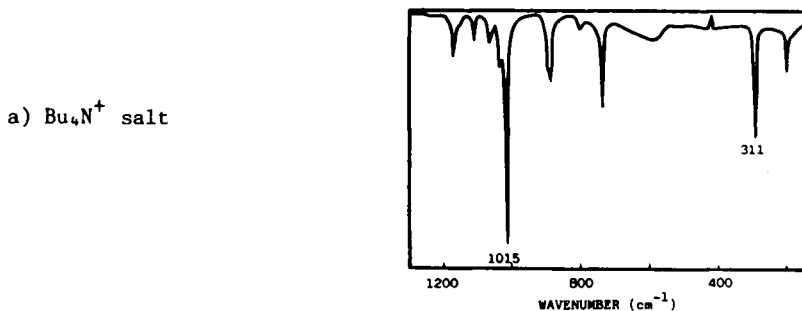
Figure 2. Infrared Spectra :

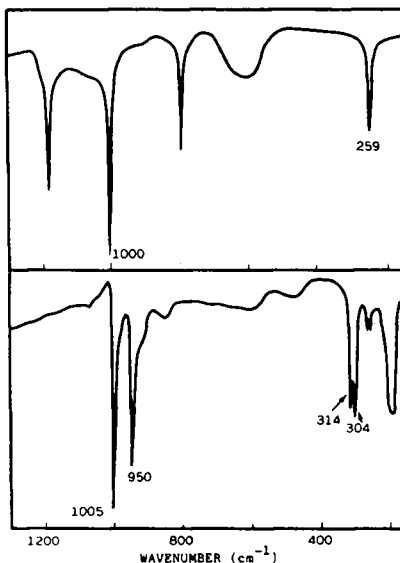


The comparison with previously reported data on the $\text{M}_2[\text{ReOX}_5]$ (4-6) and $\text{M}_2[\text{TcOX}_5]$ (4) shows that the Cs^+ and Rb^+ salts isolated in this work are $\text{Cs}_2[\text{TcOBr}_5]$ and $\text{Rb}_2[\text{TcOBr}_5]$.

The freshly prepared Et_4N^+ and Me_4N^+ salts were green-pale yellow. The UV-vis. spectra in dichloromethane are presented in Figure 1.b). These products and the Bu_4N^+ salt are soluble in 4M HBr and their spectra are the same as for $\text{Cs}_2[\text{TcOBr}_5]$ and $\text{Rb}_2[\text{TcOBr}_5]$ (Figure 1.a)). Their similar behaviour in aqueous solution could not be verified in organic solvents as Cs^+ and Rb^+ salts are not soluble. The infrared spectra of Bu_4N^+ , Et_4N^+ and Me_4N^+ salts are presented in Figure 3.

Figure 3. Infrared Spectra of bromo-oxotechnetate(V) salts



b) Et_4N^+ saltc) Me_4N^+ salt

In all three compounds a strong absorption is observed in the range $1015\text{--}1000\text{ cm}^{-1}$ which is assigned to $\text{Tc}=\text{O}$ stretch. However in the spectrum of Me_4N^+ salt a second band at 950 cm^{-1} is found which corresponds to the $\text{Tc}=\text{O}$ stretch in $\text{M}_2[\text{TcOBr}_5]$ (Figure 2.). Some differences in spectra can also be observed in the range between 400 and 200 cm^{-1} . With Et_4N^+ like with Bu_4N^+ only one type of ion is formed i.e. $[\text{TcOBr}_4]^-$. With the smaller cation Me_4N^+ both $[\text{TcOBr}_4]^-$ and $[\text{TcOBr}_5]^{2-}$ are in equilibrium and with NH_4^+ probably only the $[\text{TcOBr}_5]^{2-}$ ion is formed but the salt being too soluble it could not be isolated.

1. Cotton, F.A., Davison, A., Day, V.W., Gage, L., and Trop, H., *Inorg. Chem.*, **18**, 3024 (1979).
2. Thomas, R., Davison, A., Trop, H., and Deutsch, E., *Inorg. Chem.*, **19**, 2840 (1980).
3. Baluka, M., Hanuza, J., and Jezowska-Trzebiatowska, B., *Bull. Akad. Sci. Polon. Sci.*, **20**, 271 (1972).
4. Fergusson, J., Greenaway, A., and Penfold, B., *Inorg. Chim. Acta*, **71**, 29 (1983).
5. Padalia, B., Gupta, S., and Krishnan, V., *J. Chem. Phys.*, **58**, 2084 (1973).
6. Edwards, D., and Ward, R., *J. Mol. Struct.*, **6**, 421 (1970).

QUALITY CONTROL OF Tc-99m - DEXTRAN IN VITRO AND IN VIVO

Karin Wingårdh, S-E. Strand

Radiation Phys Dept, University of Lund, Lund, Sweden.

Lymphoscintigraphy is currently performed with radiolabelled colloids in the particle size range of 5–500 nm, commonly injected subcutaneously (1). Because of the slow outflow from the injection site of the colloid particles a high absorbed dose can be received (1). Also dynamic studies are difficult to perform. Dextran labelled with $^{99}\text{Tc}^{\text{m}}$ was reported to have a faster clearance from the injection site and perhaps also better reflects the lymph flow (4). Two different labelling techniques have been reported in the literature by Henze (2) and Ercan (3) respectively.

In the present study Dextran preparations, with three different molecular weights (70000, 90000 and 500000), have been tested for evaluating its potential as lymphoscintigraphic agents. Two labelling techniques have been reported. The aim was to compare these methods and to find an optimal technique for determining the labelling efficiency.

Applying to the method of Henze, 1 ml 10% Dextran-solution was mixed with 0.15 mg of SnCl_2 dissolved in 5 μl of concentrated HCl. Using the labelling method of Ercan, 1 ml 5% dextran-solution was mixed with 0.5 mg $\text{SnCl}_2 \cdot 2\text{H}_2\text{O}$ dissolved in 0.5 ml distilled water. The Dextran-solutions were added with pertechnetate and left for 10 and 60 min to incubate at room temperature. The pH-value was about 2 for the method of Henze and about 4.5 for the method of Ercan.

The labelling efficiency after different incubation times, 10 and 60 min, was measured with gel chromatography scanning(GCS), thin-layer chromatography(TLC) and paper chromatography(PC). For GCS Sephadex G-25 Fine was used. As mobile phase for PC 0.9% saline solution was used and for TLC 85% aqueous methanol.

The labelling efficiency (%) depending on the incubation time

		Dextran 70		Dextran 90		Dextran 500	
		Henze	Ercan	Henze	Ercan	Henze	Ercan
Sephadex G-25 fine	10'	17	18	16	36	23	32
"	60'	47	55	33	59	70	63
ITLC-SG	10'	32	96	21	99	22	95
"	60'	57	96	78	96	81	96
PC	10'	63	94	72	92	50	92
"	60'	60	88	61	76	77	78

Table 1: Labelling efficiency for the different Dextran molecules and incubation time.

To verify that the $^{99}\text{Tc}^{\text{m}}$ was labelled to the Dextran, an UV-monitor (214 nm) for monitoring the sugar content and a CdTe-detector for recording the $^{99}\text{Tc}^{\text{m}}$ -activity were used at the separation of the labelled Dextran on a Sephadex G-25 Fine column. Fractions of 1–4 ml were then collected in test tubes and measured for activity in an automatic sample-changing NaI(Tl) well detector. The Anthron-test was used to verify the sugar content in the eluate.

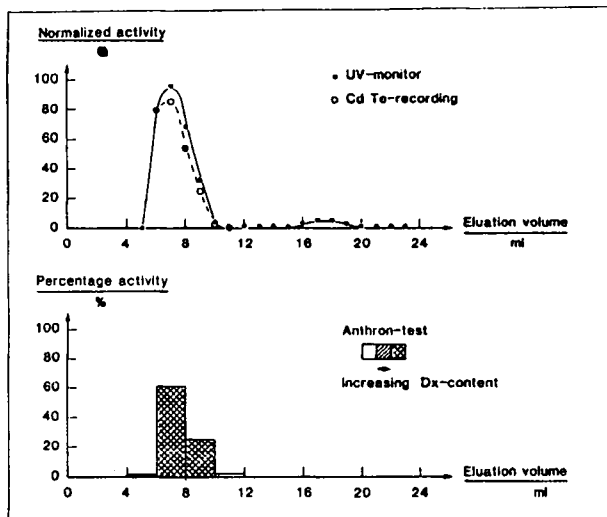


Figure 4: The radioactivity and the sugar content measured in the eluate of a Sephadex G-25 Fine column with a CdTe - detector respectively an UV - monitor. Also including the results from the Anthrone - test.

The GCS-technique shows a much lower labelling efficiency in comparison with TLC and PC, which may be due to a better separation of the radioactive components. The method according to Ercan gave a higher labelling efficiency compared to the method of Henze.

Experiments have been performed on rabbits. The $^{99}\text{Tc}^{\text{m}}$ - labelled Dextran-solution was injected subcutaneously bilaterally just below the xiphoid process. The Dextran was mixed with 100 IE hyaluronidase to stimulate the outflow from the injection site. Dynamic images were taken with a scintillation camera equipped with a parallel hole collimator and after 2 and 5 hours static images were taken. After this studies the animals were sacrificed and dissected. The activity content in the parasternal lymph nodes and the other organs were measured in an automatic sample-changing NaI(Tl) well detector.

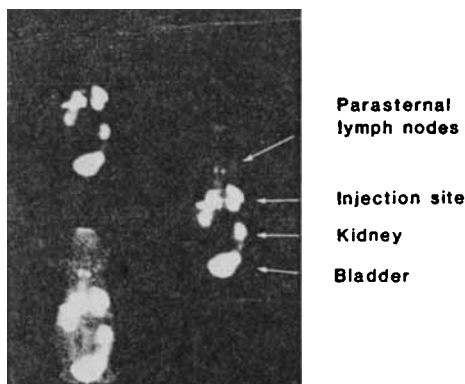


Figure 2. Scintillation camera image of Dextran 90 in a rabbit measured after 2 hours.

The specific activity uptake of the parasternal lymph nodes were about 30%/g.

In conclusion, the method of Ercan is the best and the labelling efficiency should be checked with the GCS-technique in combination with the Anthron-test. Also the pH of the Dextran when labelling according to the method of Ercan is better for subcutaneously injection.

1. L. Bergqvist et al. *Semin Nucl Med* 13:9-19, 1983
2. E. Henze et al. *J Nucl Med* 23:348-353, 1982
3. M. Ercan et al. *Eur J Nucl Med* 11, 1985
4. E. Henze et al. *J Nucl Med* 23:923-929, 1982

Tc-99m-HYDROXYMETHYLENE SODIUM DIPHOSPHONATE (Tc-99m-HMDP) - AN IMPROVED
SYNTHESIS AND ITS BIODISTRIBUTION IN RATS

Zhou, Y. G., Zhu, T., Zhao, H. Y., Wang, L. M., Shi, Q. X.
Shanghai Medical University, Shanghai, China

Tc-99m-Hydroxymethylene sodium diphosphonate (Tc-99m-HMDP) was reported to be a superior bone imaging agent. It has high bone affinity, low blood and soft tissue background in primary and metastatic bone tumors. Tc-99m-HMDP was synthesized through several steps including pyrolysis and high pressure catalytic hydrogenation. We report here an improved synthesis of Tc-99m-HMDP and its biodistribution in rats along with its whole body bone imaging in patients.

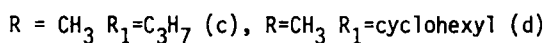
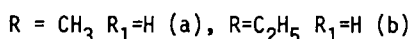
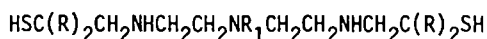
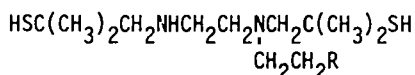
HMDP was synthesized according to the literature procedure except using HCl hydrolysis and sodium borohydride reduction for the pyrolysis and high pressure catalytic hydrogenation steps. Thus it simplifies the reaction procedures and increases the overall yield. Tc-99m-HMDP was synthesized by adding Tc-99m sodium pertechnetate into a sterile, pyrogen-free vial containing 2 mg of HMDP, 0.16 mg of stannous chloride and 0.5 mg of vitamin C with pH between 6.0 - 6.2 in greater than 95% radiochemical yield. The radiochemical purity of Tc-99m-HMDP was checked by TLC with two solvent systems (85% MeOH and saline) and showed to be greater than 96%.

The biodistribution of Tc-99m-HMDP in rats revealed that relative bone concentrations were in the order of Tc-99m-HMDP > -MDP > -PYP. The soft tissue was found in the order of Tc-99m-HMDP < -MDP < -PYP. The Tc-99m-HMDP bone/soft tissue ratios was 311 and the Tc-99m-MDP bone/soft tissue ratio was 113. We also have applied Tc-99m-HMDP in clinical studies (22 patients) and found that we were able to obtain a clear image 3 hrs post-injection.

STRUCTURE ACTIVITY RELATIONSHIP OF ^{99m}Tc -LABELED TRIAMINE DITHIOLES

E. Chiotellis, A. Varvarigou, C.I. Stassinopoulou, Th. Maina
 Radiodiagnostic products and Biology Departments, Nuclear Research Center
 "Demokritos", 153 10 Aghia Paraskevi Attiki, Greece

Recently, emphasis has been given in synthesizing ^{99m}Tc -chelates suitable for brain perfusion imaging. Such agents must be neutral, lipid soluble, presenting prolonged retention of activity in brain tissue. Bis amino ethanedithiol (BAT) labeled with ^{99m}Tc (1) and several BAT derivatives (2,3) showed promising properties in experimental animals, suggesting that such agents may be useful in brain scintigraphy. The ability of BAT moiety to penetrate the BBB is not yet fully explained. Except lipophilicity or protein binding capacity, several structural parameters are probably involved in brain passage or retention. In this work we studied comparatively various ^{99m}Tc -triamine dithiol derivatives, analogs of BAT, in order to obtain information concerning the influence of the structure of the ligand on brain uptake. The compounds studied fall into two groups:

1 Derivatives of 4,7,10 triaza,1-13 tridecane dithiol:2 Derivatives of 4,7 diaza, 1-10 decane dithiol(BAT)

R=piperidine* (a), morpholine (b), pyrrolidine (c) cyclopentylamine (d), dipropylamine (e).

The derivatives of group 1 were prepared by condensing the substituted dithio-dialdehydes with the corresponding dimethylenetriamines. The Schiff bases obtained were reduced to the corresponding dithiols by H_4LiAl in THF. Compounds of group 2 were synthesized by similar methods to those reported by Lever et al (2). The ligands formed readily complexes with Tc-99m using sodium borohydride in an aqueous solution of the ligand. The ^{99m}Tc -complex was removed from the aqueous phase by chloroform and after evaporation the residue was redissolved in alcohol 30% for the biological studies. Partition coefficient (P.C.) measurements were performed in octanol/phosphate buffer. HPLC purification of the complexes revealed more than one peak in certain BAT derivatives.

*Similar compound was reported in literature (2).

In these cases mice studies were performed on the more lipophilic components. Mice data and P.C. values are listed in Table 1. Compounds of group 1 (a-d) were not localized in brain tissue in significant amounts. Thus, by increasing the length of the chain between the two nitrogens which carry the -SH groups, brain affinity was not maintained. The data remained almost unchanged even when heavy substituents were used (1, comp. c,d). Regarding the compounds of group 2, brain uptake or retention depended on the structure of the amine coupled with one nitrogen of BAT moiety. Cyclic secondary amines with one heteroatom (2 comp. a,c) seemed to exhibit longer retention time. Lipophilicity of the compounds studied was not always correlated to BBB penetration. In conclusion, for this class of compounds BAT moiety seems indispensable in preparing ^{99m}Tc -complexes with high brain uptake and long retention time.

TABLE 1. % Dose per g in Mice Brain*

Compound		2 min	15 min	Brain/Blood 15 min	P.C.
<u>1</u>	a	1.074±0.36	0.479±0.11	0.056	2.99
	b	0.657±0.01	0.270±0.15	0.032	9.18
	c	0.527±0.07	0.222±0.02	0.037	3.87
	d	0.835±0.19	0.563±0.17	0.091	11.65
<u>2</u>	a	11.560±1.43	2.798±0.56	1.723	30.46
	b	7.746±0.95	1.049±0.06	0.564	28.11
	c	11.454±1.17	4.110±0.99	2.526	28.85
	d	8.361±1.12	3.008±0.15	0.721	9.04
	e	9.240±1.44	1.486±0.39	1.140	72.40
BAT		9.635±1.63	2.864±1.80	0.777	17.12

*each value is the average of 5-7 animals

1. Kung, H.F., Molnar, M., Billings, J., Wicks, R., Blau, M., J. Nucl. Med. 25, 326 (1984).
2. Lever, S.Z., Burns, H.D., Kervitsky, T.M., Goldfarb, H.W., Woo, D.V., Wong, D.F., Epps, L.A., Kramer, A.V., Wagner, H.N. Jr., J. Nucl. Med. 26, 1287 (1985).
3. Kung, H.F., Yu, C.C., Billings, J., Molnar, M., Blau, M., J. Med. Chem., 28, 1280 (1985).

IONISATION CONSTANTS OF RADIOPHARMACEUTICALS BY HPLC.

C.G. Stylli and A.R. Theobald, Chelsea Department of Pharmacy
King's College, London, U.K.

It has long been recognised that the pK_a of drugs and radiopharmaceuticals is an important determinant of their biological distribution. The brain uptake of some ionogenic radiopharmaceuticals such as IMP and HIPDM may be explained on the basis of a pH shift theory⁽¹⁾. In the case of Technetium-99m labelled radiopharmaceuticals, determination of the pK_a by conventional methods is impossible due to the tracer quantities of complexes actually formed. Although "shake-flask" partition methods may be used for the estimation of pK_a as well as $\log P$, chromatographic methods have an advantage in separating the ionogenic radiolabelled species from other components in the samples.

In this study an HPLC method for pK_a measurement, based on the work of Horvath et al.⁽²⁾, has been developed for radiotracers. It has been validated with several amines and used to estimate the pK_a values of some Tc-99m PnAO⁽³⁾ complexes [3,4,5] by observing the change in chromatographic retention (and hence capacity factor k') with change in mobile phase pH. A plot of pH against k' has the typical sigmoid shape encountered in pK_a determinations (Fig.1). The pK_a values were estimated from the data by three methods: derivative analysis (by locating the pH of maximum difference in k'), quadratic regression (best fitting quadratic to k' values), and the Henderson - Hasselbalch equation (using k' values for protonated and unprotonated species).

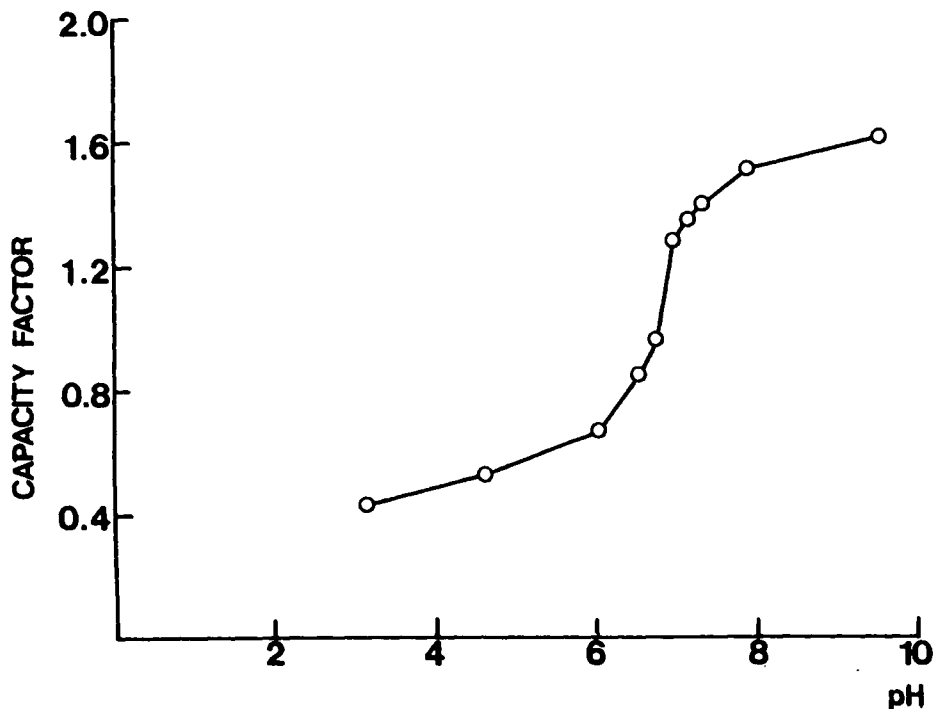


Figure 1. Change in capacity factor k' of morpholinyl ethyl PnAO with mobile phase pH, TSK-5PW column.

Initial experiments employed PLRP and PRP columns which required addition of 30% MeCN to the buffered mobile phase as an organic modifier. The reference amine pK_a values were estimated (literature values in parentheses) in this system as:-

m-anisidine	4.9 (4.2)	aniline	4.7 (4.6)
N-ethylaniline	4.6 (5.1)	2,4,6-collidine	7.2 (7.4)

The non-ionogenic Tc-99m complexes with PnAO [1] Diethyl-PnAO [2] showed constant k' values while the ionogenic complex with morpholino ethyl PnAO [3] had an estimated pK_a of 6.6.

Subsequent experiments employed a TSK-phenyl-5PW column and aqueous mobile phases to avoid the inevitable complications arising from the definition and measurement of pH and pK_a in mixed solvents (4,5). This system (Table 1) gives more satisfactory pK_a values of the reference amines and Tc-complexes with morpholino ethyl PnAO [3], N-phenyl ethyl PnAO [4], and N-isopropyl methyl PnAO [5].

The method is reproducible and is applicable to nearly all ionogenic radiopharmaceuticals.

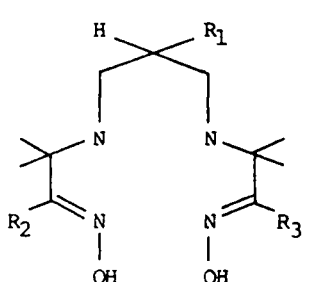

	R_1	R_2	R_3
	<u>1</u>	H	Me Me
	<u>2</u>	H	Et Et
	<u>3</u>	CH ₂ .CH ₂ .N 	Me Me
	<u>4</u>	CH ₂ .CH ₂ .N(Et).C ₆ H ₅	Me Me
	<u>5</u>	CH ₂ .NH.CH(CH ₃) ₂	Me Me

TABLE 1 Ionisation Constants determined with a TSK phenyl-5PW column.

sample	pK_a of substituent*	observed pK_a by methods		
		deriv	quadr	Henderson
N-ethylaniline	5.12	5.05	5.35	5.35
2,4,6-collidine	7.43	7.43	7.40	7.46
3	7.62	6.9	6.92	6.82
4	6.61	6.15	6.15	6.2
5	11.16**	9.17	9.26	9.07

* pK_a values for reference amines and values for PnAO substituents (as R-H) taken from ref (6)

** calculated from Taft constants according to ref.(7)

ACKNOWLEDGEMENT

We thank Amersham International for the gift of the PnAO ligands and Mr R. Bird for his invaluable technical assistance during the course of this work. One of us (CGS) acknowledges the receipt of an SERC/CASE award sponsored by Amersham International plc.

1. Kung H.F., and Blau M., *J. Nucl. Med.*, **21**, 147 (1980)
2. Horvath Cs, Melander W, and Molnar I, *Anal. Chem.*, **49**, 142 (1977)
3. Nechvatal G., Canning L., Cumming S.A., et al., *J. Nucl. Med. Allied Sci.*, **29**, 208 (1985)
4. Benet L.Z. and Goyan J.E., *J. Pharm. Sci.*, **56**, 665 (1967)
5. Pashankov P.P., Zikolov P.S. and Budevsky O.B., *J. Chromatog.*, **209**, 149 (1981)
6. Perrin D.D. *Dissociation Constants of Organic Bases in Aqueous Solution*, London, Butterworth, (1965)
7. Clark, J., and Perrin D.D., *Quart. Rev. Chem. Sci.* **18**, 295 (1964)

TECHNETIUM(V) OXOCOMPLEXES WITH POTENTIALLY PENTADENTATE SCHIFF BASE TYPE LIGANDS

F. Tisato, F. Refosco, U. Mazzi:

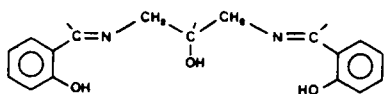
Istituto di Chimica e Tecnologia dei Radioelementi del CNR, Padova, Italy.

G. Bandoli, M. Nicolini:

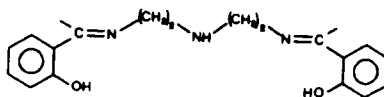
Dipartimento di Scienze Farmaceutiche, Università di Padova, Padova, Italy.

One of the numerous possibilities to stabilize $Tc=O^{3+}$ core is to close technetium in a hexacoordination with a suitable ligand with five donor groups.

From our experience working with Schiff base ligands⁽¹⁻⁵⁾ we designed the two following potentially pentacoordinate ligands containing ONONO and ONNNO donor atoms.

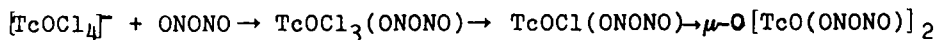


ONONO



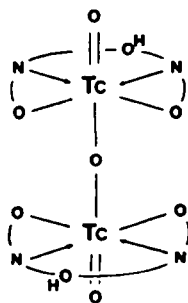
ONNNO

The ONONO ligand follows similar pathways both starting from $[TcOCl_4]^-$ and from $[TcO(eg)_2]^-$ (eg=ethylenglycol). This was defined using $[TcOCl_4]^-$ as starting material as follows:

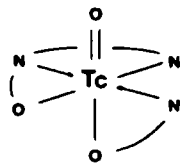


The ONNNO ligand reacts with $[TcOCl_4]^-$ to produce a compound in which the ligand is partially hydrolyzed and of which no sure formulation has yet been established, while starting from $[TcO(eg)_2]^-$ the $TcO(ONNNO)$ complex, in which the ligand completely surrounds the $Tc=O$ core, is produced.

The $\mu-O[TcO(ONONO)]_2$ (I) and $TcO(ONNNO)$ (II) complexes were completely characterized and their X-ray structure determination confirms the different ways of coordination of the two ligands.



μ -oxobis{[N,N'-2-hydroxypropane-1,3-diy]bis(salicylideneimine)} oxotechnetium(V)



N,N'-(3-diethyleneaminate)-1,5-diybis(salicylideneimine)} oxotechnetium(V)

Complex (I) shows the hydroxylic group removed from the inner core and the ligand acts as tetradentate in the same way as μ -O[Tc(salpd)]₂ (salpd = N,N'-[propane-1,3-diylbis(salicylideneimine)]⁽³⁾). The detailed structure determination is in progress. Complex (II) molecular structure shows, in particular, the Tc-N bond length (1.89 Å) of the aminate nitrogen atom very short. This suggests a multiple character of this bond; the Tc atom is displaced 0.30 Å from the mean basal plane on the opposite side to Tc=O. Tc=O distance (1.68 Å) is longer in respect to other analogue complexes, in agreement with a very low ν (Tc=O) stretching vibration (888 cm⁻¹).

The configurations previously illustrated suggest that the TcOL structure is not possible, for steric reasons, when ONONO is used and the possibility to find the alchooxy group of ONONO bond around the Tc=O position is withdrawn for the more thermodynamically stable formation of the μ -oxo compound.

The formation of TcO(ONNNO) using [TcO(eg)₂]⁻ is due to the deprotonation of amine group of the ONNNO ligand in basic medium.

REFERENCES

1. Bandoli G., Mazzi U., Clemente D.A., Roncari E., J.Chem.Soc. Dalton, 2455 (1982)
2. Bandoli G., Mazzi U., Wilcox B.E., Jurisson S., Deutsch E., Inorg.Chim.Acta, 95, 217 (1984)
3. Bandoli G., Nicolini M., Mazzi U., Refosco F., J.Chem.Soc. Dalton, 2505 (1984)
4. Mazzi U., Refosco F., Tisato F., Bandoli G., Nicolini M., J.Chem.Soc.Dalton, in press
5. Bandoli G., Mazzi U., Moresco A. Nicolini M., Refosco F., Tisato F., In Nicolini M., Bandoli G. and Mazzi U. Eds, Technetium in Chemistry and Nuclear Medicine, Verona, Cortina International, 1986, in press.

[¹⁸F]FLUORIDE ION: A VERSATILE REAGENT FOR RADIOPHARMACEUTICAL SYNTHESSES

M.R. Kilbourn, J.W. Brodack, D.Y. Chi*, C.S. Dence, P.A. Jerabek, J.A. Katzenellenbogen,* T.B. Patrick, and M.J. Welch
Mallinckrodt Institute of Radiology, Washington University School of Medicine, St. Louis, MO, and *University of Illinois, Urbana, IL

With the development of small volume [O-¹⁸]water targets for cyclotron production of fluorine-18 (1,2), large amounts of [F-¹⁸]fluoride ion have become available for use in radiopharmaceutical syntheses. This [F-¹⁸]fluoride ion has become a vital precursor to the synthesis of new radiopharmaceuticals (e.g., [F-¹⁸]neuroleptics (3,4) and [F-¹⁸]estrogen (5)), as well as an important part of improved methods for the synthesis of established radiopharmaceuticals (e.g., [F-¹⁸]2-FDG (6,7)).

We have gained considerable expertise in the production and use of [F-¹⁸]fluoride ion (600 target irradiations, over 1500 chemical reactions). Our initial target (1) has undergone several improvements, and in its present form (8) is of simple design and constructed of inexpensive materials (Havar foils and stainless steel). In daily use, it produces 900 mCi (1 h beam) in 0.8-1.0 ml of water.

This fluoride has been used in a diverse array of chemical reactions (Table 1) to produce a large number of compounds (Table 2). Reactions used have varied from the simple (nucleophilic substitutions (3,5,9)) to new reactions such as halofluorination (10) and fluorodecarboxylation (11). Products include both simple (fluoroalkanes) and complex (spiperone) compounds. In the course of this work, we have made numerous observations on the use of cyclotron-produced [F-¹⁸]fluoride ion in organic syntheses.

Specific Activity. The [F-¹⁸]fluoride ion obtained in our target is of high specific activity (50,000 Ci/mmol) but not carrier-free. The effective specific activity of one product, 16-fluoroestradiol, has been measured at more than 7000 Ci/mmol (EOB, by radioreceptor assay), indicating that the high specific activity fluoride can be used with minimal isotopic dilution. (12)

Counterions. In all our work we routinely use the tetrabutylammonium cation as a means of solubilizing fluoride ion in organic solutions. Other workers have used metal ions (Cs, Rb) (4) or metal ions with aminopolyethers (K⁺, Kryptofix)(7). Despite claims that tetraalkylammonium salts decompose at high temperatures, we find that TBAF can be successfully used at elevated temperatures, as evidenced by very good yields in aromatic nucleophilic substitutions. Decomposition, if occurring, is either slow, or the products so formed must include a reactive form of [F-¹⁸]fluoride ion. We have found absolutely no need for the use of metal ions and polyethers to obtain soluble and highly reactive [F-¹⁸]fluoride ion.

Water. Much has been said of the need for "anhydrous" fluoride ion in organic syntheses. In fact, several of our reactions are remarkably tolerant of water: in the reaction of 3-bromopropyl triflate with TBAF, the addition of small amounts (1-2 μ l) of water does not diminish the radiochemical yields. On a molar scale, for 1 μ l water and 1 mCi fluorine-18, this is a water-to-fluoride ratio of 270000.

Vessel. Problems with "sticking" of high specific activity fluoride ion to vessel surfaces have often been reported. Most of our reactions are conducted in ordinary borosilicate or pyrex glass vessels, with minimum losses due to "sticking". We have found, however, that the evaporation of target water and resublimation of the fluoride proceeds reliably and in high yield (90%) in Vacutainers, a commercial source of siliconized glass (12).

Table 1. Chemical Reactions Using Cyclotron-Produced [F-18]Fluoride Ion.

aromatic nucleophilic substitution
 aliphatic nucleophilic substitution
 epoxide opening to fluorohydrins
 triazene decompositions
 halofluorinations
 fluorodecarboxylation

Table 2. Compounds prepared with Cyclotron-Produced [F-18]Fluoride Ion.

fluoroalkanes (methane, ethane, propane)
 fluorotrimethylsilane
 1-bromo-2-fluoroalkanes (ethane, propane, pentane, butane, hexane)
 1-bromo-3-fluoroalkanes (propane, butane)
 spiperone (also N-methyl, N-ethyl, N-propyl, N-2-fluoropropyl)
 haloperidol
 16-fluoroestradiols
 1-fluorohexestrol
 1-fluoronorhexestrol
 hypoxic radiosensitizers:
 1-(2-nitroimidazolyl)-3-fluoro-2-hydroxypropane
 1-(2-fluoroethyl)-2-nitroimidazole
 1-(2-fluoroethyl)-2-methyl-5-nitroimidazole
 N-fluoroalkylspiperones (2-fluoroethyl, 2-fluoropropyl, 3-fluoropropyl, 2-fluorobutyl, 4-fluorobutyl, 2-fluoropentyl, 2-fluorohexyl)

Metal Ion Contaminants. Metal ions are always present after irradiation of water in a metal target, and the contaminants mirror the composition of the target body and foils (e.g., Fe, Cr, Co from Havar foils (13)). Many metal ions have a high affinity for fluoride ion, and could interfere with organic reactions. Levels of contaminants depends on target design, beam current, and length of irradiation. Our current target produces [F-18]fluoride which can be resubolized with small amounts of base (2 μ mol), and it is extremely reactive (80% reactive). Metal ions, although certainly present, appear to be of minimal concern. Our double foil target, we feel, helps minimize metal ions; we routinely change the foils after 50 hours of beam.

Reaction times and Yields. Reaction times vary from instantaneous (triflates) to 20-30 min (aromatic substitutions). Yields, although often quite good (60-80%), are never 100%.

In summary, we have developed targetry suitable for producing large amounts of [F-18]fluoride ion, which can be rapidly and easily converted to reactive [F-18]TBAF in a dry organic solvent, and then used in a wide variety of chemical reactions. These procedures are straightforward, and we have even automated such through the use of laboratory robotics, as exemplified by the synthesis of 16- α -[F-18]fluoroestradiol. (14,15)

This work was supported by National Institutes of Health grant HL-13851 and Department of Energy grant DE-FG02-84ER60218.A000.

1. Kilbourn MR, and Welch MJ, *J. Nucl. Med.* 24, P120 (1983).
2. Wieland BW, and Wolf AP, *J. Nucl. Med.* 24, P122 (1983).
3. Kilbourn MR, Welch MJ, Dence CS, Tewson TJ, Saji H, and Maeda M, *Int. J. Appl. Radiat. Isot.* 35, 591 (1984).

4. Shiu C-Y, Fowler JS, Wolf AP, McPherson DW, Arnett CD, and Zecca L, *J. Nucl. Med.* 27, 226 (1986).
5. Kieseletter DO, Kilbourn MR, Landvatter SW, Heiman DR, Katzenellenbogen JA, and Welch MJ, *J. Nucl. Med.* 25, 1212 (1984).
6. Tewson TJ, *J. Nucl. Med.* 24, 718 (1983).
7. Hamacher K, Coenen HH, and Stocklin G, *J. Nucl. Med.* 27, 235 (1986).
8. Kilbourn MR, Jerabek PA, and Welch MJ, *Int. J. Appl. Radiat. Isot.* 36, 327 (1985).
9. Jerabek PA, Patrick TB, Kilbourn MR, Dischino DD, and Welch MJ, *Int. J. Appl. Radiat. Isot.* (in press)
10. Chi DY, Kieseletter DO, Katzenellenbogen JA, Kilbourn MR, and Welch MJ, *J. Fluorine Chem.* (in press).
11. Patrick TB, Johri KH, White DH, Bertrand WS, Mokhtar R, Kilbourn MR, and Welch MJ, *Can. J. Chem.* (in press).
12. Brodack JW, Kilbourn MR, Welch MJ, and Katzenellenbogen JA, *Appl. Radiat. Isot.* 37, 217 (1986).
13. Jerabek PA, Kilbourn MR, and Welch MJ, *Book of Abstracts, 187th National Meeting of the American Chemical Society, 1984, St. Louis, NUCL-61.*
14. Brodack JW, Welch MJ, Kilbourn MR, and Katzenellenbogen JA, *Book of Abstracts, 190th National Meeting of the American Chemical Society, 1985, Chicago, NUCL-137.*
15. Brodack JW, Kilbourn MR, Welch MJ, and Katzenellenbogen JA, *J. Nucl. Med.* (in press).

EFFECTS OF TARGET DESIGN ON THE PRODUCTION AND UTILIZATION OF [F-18]-FLUORIDE FROM [O-18]-WATER

M.S. Berridge and T.J. Tewson

University of Texas Medical School, Houston, TX 77225

The $^{18}\text{O}(p,n)^{18}\text{F}$ reaction is an attractive one for the production of fluorine-18, using oxygen-18 enriched water as the target material. Over the last few years a number of target systems have been reported using this reaction^{1,2,3,4}. All the targets operate within the constraints of using the smallest possible amounts of water and producing fluorine-18 that can be successfully utilized in further synthesis. Using a target similar to one described in the literature¹ we encountered two major problems. First the gas produced by radiolysis during bombardment forced about half of the water out of the target and so within the first few minutes of bombardment the target was half-empty. Secondly, although small scale reactions to incorporate the fluorine-18 using small fractions of the bombarded water gave high yields when these reactions were repeated using the entire volume of water, the incorporation yields were very low. It was established that these low yields were due to metal ions that dissolved in the water during bombardment. This resulted in the formation of fluoride salts that were insoluble in the organic solvent used for the synthesis reactions. However, the fluoride was not irreversibly bound in that dissolving these salts in water, adding more base and treating this solution in the same fashion as the original solution gave essentially the same results as that obtained with the original solution i.e. incorporation yields of 20~30%, and the majority of the activity was insoluble in organic solvents. Deliberate addition of micromolar quantities of metal salts to small quantities of the original aqueous solution of fluorine-18 produced essentially similar results. It is likely that many of the difficulties that have been encountered in using fluorine-18 fluoride can be ascribed to similar problems of metal ion impurities.

The extent of metal ion contamination became significantly worse as the target was used. After approximately thirty bombardments it was impossible to obtain incorporation yields of fluorine greater than 10%.

To overcome these problems we have constructed a target with a keyhole shape, the circular portion of which is filled with oxygen-18 water and the upper portion constitutes a head space which allows the bubbles to clear the water without removing it permanently from the beam strike region. The target is made of silver and also uses a silver window. The rationale is that silver is an excellent conductor of heat and that as fluorine-18 fluoride reactions have been performed successfully in the presence of silver⁵ and silver oxide⁶, any metal that does dissolve should not interfere with the reactions of the fluoride.

This target consistently produces close to the theoretical quantity of fluorine-18 and of the fluorine-18 made on a production basis 80% is typically available in the final product.

BIBLIOGRAPHY

1. Kilbourn M.R., Hood J.T., and Welch M.J. Int. J. Appl. Radiat. Isot. 35 599, 1984.
2. Wieland B.W. and Wolf A.P. J. Nucl. Med. 24, P 122.
3. Nickles R.J. and Daube M.E. J. Nucl. Med. 24, P 121.
4. Kilbourn M.R., Jerabek P.A., and Welch M.J. Int. J. Appl. Radiat. Isot. 36 328. 1095.
5. Tewson T.J., Welch M.J. and Raichle M.E. J. Nucl. Med. 19, 1339, 1979.
6. Gatley S.J., Hichwa R.D., Shaughnessy W.J., and Nickles R.J. Int. J. Appl. Radiat. Isot. 32 211, 1981.

ELECTROPHILIC RADIOFLUORINATION OF AROMATIC COMPOUNDS WITH $[^{18}\text{F}]\text{-F}_2$ AND $[^{18}\text{F}]\text{-CH}_3\text{CO}_2\text{F}$ AND REGIOSELECTIVE PREPARATION OF L-p- $[^{18}\text{F}]\text{-FLUOROPHENYLALANINE}$

H.H. Coenen, K. Franken, S. Metwally, G. Stöcklin

Institut für Chemie 1 (Nuklearchemie), Kernforschungsanlage Jülich GmbH, 5170 Jülich, FRG

Molecular fluorine is known to be a highly reactive electrophile but still exhibits distinct selectivity when used in a highly diluted state (1). Acetyl hypofluorite is a milder electrophilic reagent for aromatic fluorination (2) and is expected to show a higher selectivity. Both the compounds are successfully used for direct radiofluorination of aromatic compounds. In this study the reactivity and selectivity of gaseous $[^{18}\text{F}]\text{-F}_2$ and $[^{18}\text{F}]\text{-CH}_3\text{CO}_2\text{F}$ in a series of benzene derivatives ($\text{C}_6\text{H}_5\text{X}$, X = CF_3 , I, Br, Cl, F, H, CH_3 , OCH_3 , OH) are compared under practical labeling conditions.

The effect of reactant concentration, the influence of the reaction solvent and of the various substituents on the radiochemical yield and positional selectivity have been studied. As shown in Table 1 low substitution yields are found in "reactive" solvents such as CH_3OH and CHCl_3 , whereas in the acid $\text{CF}_3\text{CO}_2\text{H}$ efficient fluorination is observed. This is similar to recent reactions in HF (3). The substitution yield generally increases with the acceptor number (AN) of the solvent. Correspondingly, the addition of the Lewis acid BF_3 enhanced the yields in all solvents except $\text{CF}_3\text{CO}_2\text{H}$. While F_2 is superior as fluorination reagent in CH_3OH and CHCl_3 in non-activated substrates like fluorobenzene, it is identical to that of $\text{CH}_3\text{CO}_2\text{F}$ in trifluoroacetic acid, when correcting for the 50 % loss of radioactivity in the formation step of $[^{18}\text{F}]\text{-CH}_3\text{CO}_2\text{F}$.

TABLE 1. Effect of Solvent on the Reactivity and Selectivity of the Radiofluorination of Fluorobenzene with $[^{18}\text{F}]\text{-F}_2$ and $[^{18}\text{F}]\text{-CH}_3\text{CO}_2\text{F}$ at 0°C

Solvent	Reagent	Radiochemical H-Subst. Yield	Relative Isomer Distribution (o+m+p = 100 %)		
			o	m	p
CH_3OH	F_2	4.2 ± 0.5	30	14	56
	$\text{CH}_3\text{CO}_2\text{F}$	1.8 ± 1	38	16	54
CHCl_3	F_2	17.5 ± 2.5	17	26	57
	$\text{CH}_3\text{CO}_2\text{F}$	2.2 ± 1	32	21	47
$\text{CF}_3\text{CO}_2\text{H}$	F_2	34 ± 3	30	12	58
	$\text{CH}_3\text{CO}_2\text{F}$	74 ± 5	24	6	70

TABLE 2. Effect of the Substituent on the para-to-meta Ratio (per position) in Substituted Benzenes ($\text{C}_6\text{H}_5\text{X}$) with $[^{18}\text{F}]\text{-F}_2$ and $[^{18}\text{F}]\text{-CH}_3\text{CO}_2\text{F}$ in $\text{CF}_3\text{CO}_2\text{H}$ as Solvent at 0°C

X	CF_3	Br	Cl	F	CH_3	OCH_3	OH
$[^{18}\text{F}]\text{-F}_2$	0.6	5	6.2	9.7	3.1	70	5.2
$[^{18}\text{F}]\text{-CH}_3\text{CO}_2\text{F}$	0.5	11	15	29	5.3	77	*

* no meta product formed

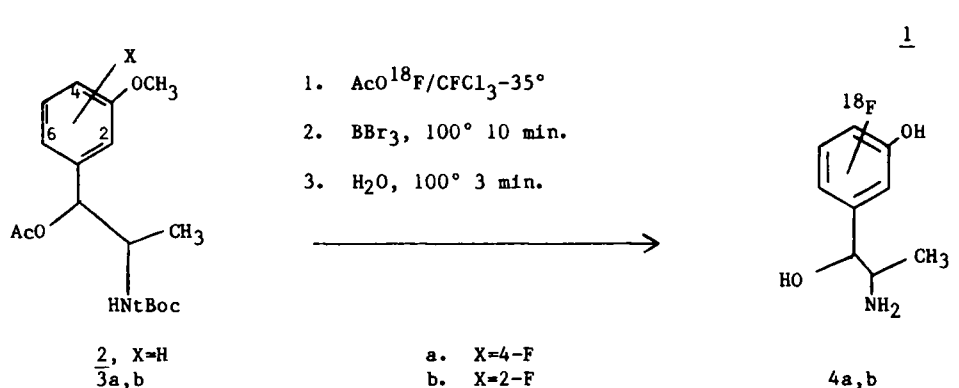
This is also true in the case of fluorine-18 labeling of L-phenylalanine, which can be carried out by direct fluorination with F_2 in CF_3CO_2H with a radiochemical yield of about 30 % (o:m:p = 60:15:25) without racemization (5). However, the separation of the desired para- from the meta-isomer has not been possible so far. Alternatively, para-substituted trimethyltin phenylalanine is prepared and used to achieve the L-para- $[^{18}F]$ -fluorophenylalanine with a corrected yield of about 25 % after HPLC (see Scheme). The amide protecting groups proved to be optimal for the metallation and radiofluorination step.

1. Cacace, F., Giacomello, P., Wolf, A.P., J.Am.Chem.Soc. 102, 3511 (1980)
2. Lerman, O., Tor, Y., Rozen, S., J.Org.Chem. 46, 4631 (1981)
3. Firnau, G., Chirakel, R., Garnett, E.S., J.Nucl.Med. 25, 1228 (1984)
4. Coenen, H.H., Moerlein, S.M., J.Chem.Soc., Perkin Trans. I, submitted
5. Coenen, H.H., Bodsch, W., Takahashi, K., Hossmann, A., Stöcklin, G., J. Neurochem., in press

RADIOFLUORINATION OF A BLOCKED METARAMINOL DERIVATIVE WITH [^{18}F] ACETYL HYPOFLUORITE. G.K. Mulholland, H. Lee, D.M. Wieland
University of Michigan, Ann Arbor, MI 48109

Metaraminol (MR, 1) is an adrenergic amine which resembles norepinephrine (NE) in its pharmacological profile. However, unlike NE, MR is not significantly metabolized by either monoamine oxidase or catechol-O-methyl transferase. Encouraging results from tritiated MR biodistribution studies (1) in rats and dogs have led us to search for a radiofluorinated MR analog as a potential P.E.T. agent for quantitatively mapping adrenergic nerve density.

The most promising route to ^{18}F -MR found to date is shown below.



Preliminary "cold" fluorination experiments with compound 2 were carried out using either gaseous acetyl hypofluorite (2) or gaseous R_fOF (principally CF₃CF(OF)₂, ref. 3) under various solvent and temperature conditions. The reaction mixtures containing 3 were directly examined by ^{19}F -NMR. The greatest selectivity was observed with acetyl hypofluorite in CFC₃ at -78°. In this case, the ^{19}F -NMR showed a 4:1 ratio of two ortho-to-the-methoxy fluorine products at CFC₃ - 139.15 (3a) and -136.41 ppm (3b). No 6-fluoro-3 could be observed by NMR but small amounts of this isomer were also present as indicated by GC-MS.

For radiosynthesis of 4, 50-75 μmol s of 2 was treated with 25 μmol s of [^{18}F]AcOF in 5 ml of CFC₃. The blocking groups were removed with excess BBr₃. Water (1.5 ml) was added next to complete hydrolysis of the blocking groups. The hydrolysate was drawn through sequential columns containing poly-4-vinyl pyridine to remove B(OH)₃, HBr, and alumina to remove ^{18}F . The final eluent, pH 6.2, contained 4a, 4b and 1 as a mixture which was homogeneous by radio TLC. An HPLC separation of these compounds is currently being evaluated. The overall radio yield (E.O.S.) of 4a and 4b at the end of a 45 min. synthesis was 12% (average of 5 runs) based upon the total amount of ^{18}F vented from the target (the theoretical maximum yield at 45 min. is 37.5%).

Research was supported by NCI #5-T32-CA-09015 and by NINCDS grant #P01-NS-15655.

- (1) Wieland DM, Lee H, Arjunan P, Mulholland K, Fisher SJ, Sherman PS: 33rd Annual Meeting of the Society of Nuclear Medicine, June 22-25, 1986.
- (2) Jewett DM, Potocki JF, Ehrenkauf RE: J Fluorine Chem 24:477, 1984.
- (3) Mulholland GK, Ehrenkauf RE: J Org Chem 51:1482, 1986.

ROBOTICS FOR THE PRODUCTION OF SEVERAL SHORT-LIVED POSITRON-EMITTING
RADIOPHARMACEUTICALS

J.W. Brodack, M.R. Kilbourn, M.J. Welch, and J.A. Katzenellenbogen*
Washington University School of Medicine, St. Louis, MO 63110; *University of
Illinois, Urbana, IL 61801

Routine production of radiopharmaceuticals labeled with short-lived radioisotopes (O-15, N-13, C-11, F-18, Ga-68) usually requires large amounts of radioactivity (on the order of several hundred millicuries) in order to produce sufficient amounts of the tracer with high specific activity for clinical use. Presently, three approaches have been used to obtain such radiopharmaceuticals: manual syntheses, manual operation of a remote apparatus, and use of an automated apparatus. The manual approach, being the simplest and most versatile, is labor intensive and results in excessive radiation dose to the chemist. The radiation dose can be reduced significantly through the use of a manually-operated remote apparatus, as in the preparation of 2-[F-18]fluoro-2-deoxyglucose (1), 1-[C-11]palmitic acid (2), and [C-11]glucose (3). These apparatus, however, are still labor intensive and are usually restricted to the preparation of a single, or a few closely related, radiopharmaceuticals. A totally automated apparatus, on the other hand, eliminates the need for operator presence by virtue of microprocessor control. Automated methods of this type have been reported for the preparation of 2-[F-18]fluoro-2-deoxyglucose (4) and [C-11]methionine (5). However, such devices have several disadvantages. They are often very complicated, entailing considerable time and labor in the construction of the hardware and software for the microprocessor. These apparatus are also limited to the synthesis of one or at best a few closely related radiopharmaceuticals. For an institution in need of several different radiotracers for clinical studies, this limitation requires the construction of several different automated devices. In addition, any changes in the synthesis due to improvements or alternate approaches are difficult to implement without significant overhaul of the apparatus.

We have recently shown the applicability of robotics to the synthesis of a positron-emitting radiopharmaceutical, namely 16 α -[F-18]fluoroestradiol-17 β , a breast tumor imaging agent (6). The production of this radiotracer requires the use of several hundred millicuries of activity at the start of synthesis due to the combination of half-life (110 min), low radiochemical yield, and long synthesis time (at least one half-life). The Zymate[®] Laboratory Automation System (Figure 1) is well suited for this type of synthesis, as it can perform the necessary sequence of chemical steps in a high radiation environment without operator intervention. The robot performs the fluoroestrogen synthesis from the preparation of the radionuclide for the labeling step to the isolation and preparation of the radiotracer for clinical use. These steps involve evaporating solvents to dryness, handling air-sensitive reagents, heating and cooling, liquid-liquid extractions, and injecting onto an HPLC column.

Since the above chemical manipulations are needed to produce most carbon-11 and fluorine-18 radiopharmaceuticals, the robot is an ideal device for the synthesis of several unrelated radiopharmaceuticals in limited laboratory space. Procedures that are programmed into the robot for one type of synthesis can be readily used by the robot in another synthesis with minimal additions in hardware. We now report the application of the robot to the synthesis of two additional radiopharmaceuticals, [F-18]spiroperidol and [C-11]butanol. Through the construction of small stations and careful planning of work space, the robot is now able to synthesize the three unrelated radiotracers in the same area available to the robot. This achievement shows the power of a robot as a multifunctional automated device for the synthesis of several positron-emitting radiopharmaceuticals in limited laboratory space.

Acknowledgement. This work was supported by Department of Energy Contract No. DE-FG02-84ER60218 and National Institutes of Health Grant No. HL13851.

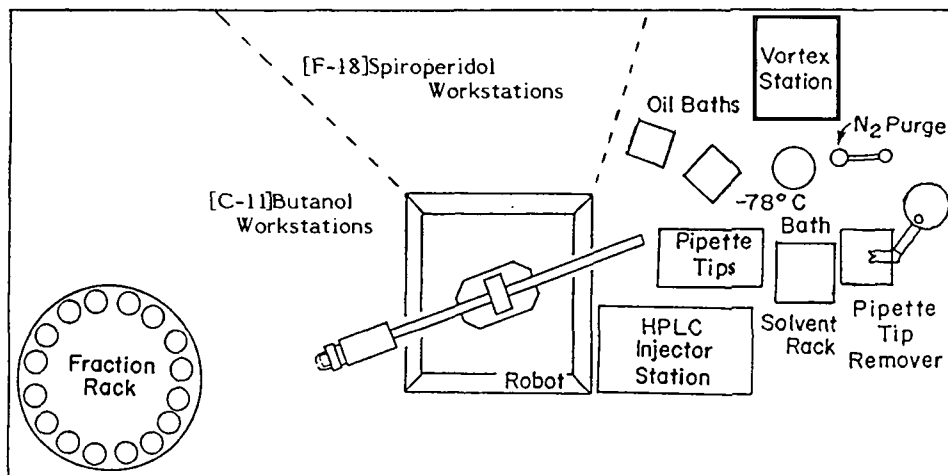


Figure 1. Zymate™ Laboratory Automation System used in the synthesis of 16α -[F-18]fluoroestradiol-17 β , [F-18]spiroperidol, and [C-11]butanol. The robot table (28 x 58 in.) is located in a hot cell. The Master Laboratory Station, Power and Event Controller, and HPLC are situated below the robot, while the System Controller, printer, and chart recorder are located outside the hot cell.

1. Fowler, J.S., MacGregor, R.R., Wolf, A.P., Farrell, A.A., Karlstrom, K.I., and Ruth T.J., *J. Nucl. Med.*, **22**, 376 (1981).
2. Welch, M.J., Dence, C.S., Marshall, D.R., and Kilbourn, M.R., *J. Labelled Compd. Radiopharm.*, **20**, 1087 (1983).
3. Dence, C.S., Lechner, K.A., Welch, M.J., and Kilbourn, M.R., *J. Labelled Compd. Radiopharm.*, **21**, 743 (1984).
4. Iwata, R., Ido, T., Takahashi, T., and Monma, M., *Int. J. Appl. Radiat. Isot.*, **35**, 445 (1984).
5. Davis, J., Yano, Y., Cahoon, J., and Budinger, T.F., *Int. J. Appl. Radiat. Isot.*, **33**, 363 (1982).
6. Brodack, J.W., Kilbourn, M.R., Welch, M.J., and Katzenellenbogen, J.A., *In Advances in Laboratory Automation Robotics*, Zymark Corp., Hopkinton, 1985, p 663.

MICROPROCESSOR CONTROLLED SYSTEM FOR AUTOMATIC AND SEMI-AUTOMATIC SYNTHESSES

OF RADIOPHARMACEUTICALS T.J. Ruth, M.J. Adam, D. Morris and S. Jivan
TRIUMF and UBC Program on Positron Emission Tomography, University of British
Columbia, Vancouver, Canada V6T 2A3

A computer based system has been constructed to control the automatic synthesis of 2-deoxy-2-(^{18}F)fluoro-D-glucose and is also being used in the development of an automatic synthesis of L-6-(^{18}F)fluorodopa.

The 2FDG synthesis uses gas phase acetylhypofluorite in a reaction with tri-acetyl-glucal (TAG). The system controls the emptying of the target gas (^{18}F -F₂ in Neon) at a prescribed flow rate (180 mL/min) through the acetate salt column (1) and into the reaction vessel containing the TAG in freon. When the target is empty as determined by the flow rate dropping below the preset value (50 mL/min) the next step is initiated (evaporation of freon). The next step is to add 2.5 mL of 1N HCl followed by raising the heater to hydrolysis temperature. The solution is refluxed for 20 min while the temperature is maintained at $122^\circ\text{C} \pm 7^\circ\text{C}$ through a feedback loop. At the end of hydrolysis the solution is passed through a series of columns consisting of an ion-retardation resin, a SEP-PAK alumina cartridge and a SEP-PAK C-18 cartridge which remove, in turn, excess HCl, (^{18}F)-fluoride and organics/polymeric materials. The solution then passes through a 0.2 μm filter into a sterile/pyrogen-free multi-injection vial. The reaction vessel is rinsed twice with 3-4 mL of USP water with each washing passing through the column chain and filter into the vial.

The entire process is initiated by a key on the computer keyboard. There are three radioactivity monitors to check radiation levels at the salt column, the reaction vessel and the final vial. Stainless steel solenoid valves control the flow of gases and the vacuum system while teflon solenoid valves control the flow of liquids. Liquid level sensors monitor the addition of liquids. Transfers are effected by air pressured (10 psi) or vacuum.

A schematic of the system (Fig. 1) is displayed on the CRT screen with the valves and transducers highlighted when involved with a particular function. The software controlling the process has been written in 8080 assembler and FORTRAN. Each sequential step is a separate subroutine, making it easy to modify specific functions, and to expand or create new processes while keeping a similar structure. The computer hardware is based on the S100 buss, and one of two different terminals can be used for the user interface.

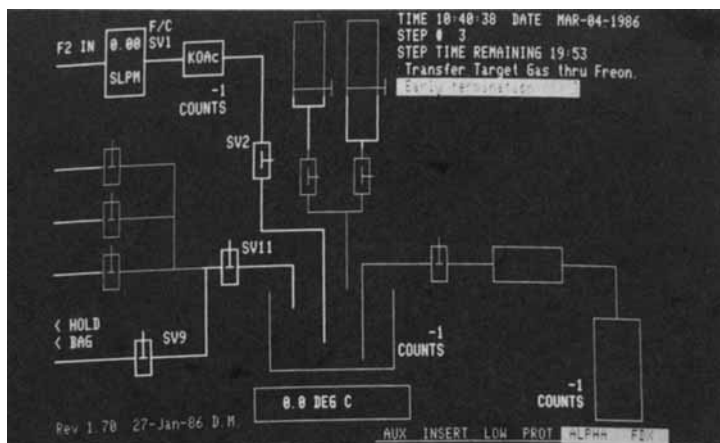


Fig. 1. Schematic of system displayed on CRT screen during automatic FDG run.

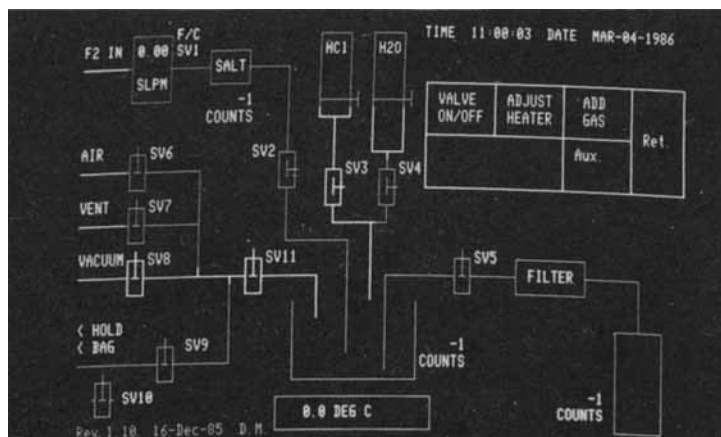


Fig. 2. Schematic of system displayed on CRT screen during interactive mode

An interactive mode also exists to facilitate the development of new procedures (Fig. 2).

We have begun the automation of L-6- (^{18}F) fluorodopa using this method as well. This compound is particularly attractive for this system since it also uses gas phase acetylfuorite (2).

The computer keeps records of the synthesis so that each radiopharmaceutical preparation has a printout of all the parameters for each step of the synthesis. The procedure for set-up before a run and clean-up after the run are done in an interactive mode as well.

This system has been in active use since late 1985 for 2FDG production. Total synthesis time is 45 minutes from EOB with a yield of ~20% EOS.

We wish to thank the Medical Research Council of Canada and TRIUMF for financial support.

- (1) Jewett, D.M. et al., *J. Fluorine Chem.* **24**, 477 (1984).
- (2) Adam M.J. et al., *J. Nucl. Med.* (in press).

DESIGN AND PERFORMANCE OF TARGETS FOR PRODUCING C-11, N-13, O-15 AND F-18 WITH 11 MeV PROTONS

B. W. Wieland*, **G.O. Hendry***, and **D.G. Schmidt[†]**

*Computer Technology & Imaging, Inc., 950 Gilman St., Berkeley, CA 94710

[†]UCLA School of Medicine, Division of Biophysics and Nuclear Medicine, Los Angeles, CA 90024

An economical system for producing required labeled compounds is a prerequisite for the widespread use of clinical positron tomography. The targetry reported here has been developed to enhance the efficiency of the integrated system with characteristics described in Table 1.

TABLE 1: Radionuclide Delivery System (RDS) Characteristics

CYCLOTRON: 11 MeV protons, negative ion with four separate extraction ports (option of two simultaneously) delivering homogeneous collimated 10 mm circular beams at 45 cm from vacuum tank, stable unattended operation up to 50 μ A.

SHIELDING: Compact self-shielded configuration for minimum facility requirements, targets (strong localized sources of radiation) surrounded on all sides by lead and hydrogenous shielding and mounted on removable shielding plugs for ease of maintenance, cyclotron (weak distributed source of prompt and residual radiation) surrounded by surface shield with removable sections for maintenance.

TARGETS: yields of C-11, N-13, O-15 and F-18 adequate for routine clinical studies, production and recovery times compatible with efficient patient scheduling, acceptable enriched stable isotope cost where expendable use is required, small physical size to accommodate economical shield design, simple reliable operation and ease of maintenance.

CHEMISTRY MODULES: high efficiency stressing minimum synthesis/processing time, adequate quantities of radiopharmaceuticals for clinical PET studies, operational reliability and quality control.

INSTRUMENTATION AND CONTROL: automated operation and monitoring of integrated cyclotron/target/chemistry systems using IBM PC/AT computer control to maximize unattended sequences, resulting in reduced personnel cost (number of technicians and level of training required).

Targets for the production of C-11, N-13, O-15 and F-18 which meet the RDS criteria have been built and tested at beam currents up to 30 μ A and bombardment times up to two hours. The physical parameters of these targets are given in Table 2. Details of the experiments on the individual targets have been submitted for publication. Examples selected from these experiments which are indicative of performance appropriate for clinical positron tomography are presented in Table 3.

TABLE 2. Target System Parameters

Radionuclide	C-11	N-13	O-15	F-18
Nuclear Reaction	N-14 (p, α)	C-13 (p,n)+ O-16 (p, α)	N-15 (p,n)	O-18 (p,n)
Recovered Form	CO ₂	Oxides	O ₂	Fluoride
Energy on Target (MeV)	10.1	10.1	8.5	10.4
Target Shape	Conical	Cylinder	Cylinder	Cylinder
Target Dia. (mm)	10 Front 15 Back	10	10	10
Target Length (mm)	100	1.0	50	1.0 and 2.0
Target Material	N-14 N ₂ (gas)	C-13 powder + O-18 H ₂ O	N-15 N ₂ (gas)	O-18 H ₂ O
Target Loading	9.8 mL at 16.7 atm	140 mg C-13 powder	4 mL at 16.7 atm	.200 and .325 mL
Loading Cost ^a	--	\$22 ^b	\$20	\$17

a Isotec, Inc., 7542 McEwen Rd., Dayton OH 45459, April 1985 price list.

b C-13 powder is not expended.

TABLE 3. Experimental Target Performance Results

Radionuclide	Beam Current (μA)	Bombardment Time (min)	EOB Activity (mCi)	Yield mCi/ μA @ Saturation
C-11	30	40	1,297	58.2
N-13 ^a	20	20	308	20.5
O-15 (Batch)	20	10	750	36.3
O-15 (On-Line) ^b	20	10	19.0 mCi/min	--
F-18 ^c	20	30	410	120.4
F-18 ^c	20	113	1,170	117.0

^a The N-13 target activity is recovered by flowing water at 1 cm³/min through a bed of C-13 powder. The recovered aqueous product has been converted to N-13 ammonia.

^b Target pressure: 200 psia, Flow: 4 standard mL/min, Cost: \$1/min.

^c The recovered aqueous product from the F-18 target has been converted to F-18-FDG using the Hamacher¹ synthesis.

A key factor in achieving the results of Table 3 has been the exceptional optics of the extracted cyclotron beam, allowing small diameter targets to be operated at high power because of the uniformity of the beam distribution. The increase in penetration of the beam due to heating in gas targets has been minimized by eliminating the dead volumes surrounding the beam strike and external to the target. The effects of beam dispersion due to multiple scattering in windows, degraders, and target gas are minimized by the use of short high pressure targets. All of the targets (gas and liquid) use a standard screw-together configuration of 25.4 micrometer aluminum beam window and 12.7 or 25.4 micrometer Havar target windows which are helium cooled and held in place by crush seals employing 25.4 micrometer thick gold foils.

The goal of these target experiments has been to demonstrate the ability of an 11 MeV negative-ion proton accelerator to economically produce adequate quantities of C-11, N-13, O-15 and F-18 for clinical positron tomography applications. The results presented establish that high levels of activity in short bombardment times with moderate beam currents are feasible and indicate that enriched isotope cost requirements are not substantial when compared with overall PET center costs. We expect to continue to increase yields and decrease costs as development of the targetry progresses.

1. Hamacher, K., Coenen, H.H., Stocklin, G., *J. Nucl Med* **27**, 235, 1986.

THE USE OF 50 MEV PROTONS TO PRODUCE C-11 AND O-15

K.A. Krohn, J.M. Link, T.K. Lewellen, R. Risler, J. Eenmaa, M. Maler
 Departments of Radiology and Radiation Oncology, University of Washington,
 Seattle, WA 98195 and Scanditronix AB, Uppsala, Sweden

Installation of a Scanditronix NT50 cyclotron at the University of Washington has provided a resource for production of radionuclides for PET. This machine currently has the capacity to accelerate protons at 32 to 50.5 MeV and deuterons at 16 to 25 MeV and can be adapted to accelerate alphas. The cyclotron was acquired under a National Cancer Institute contract for clinical neutron therapy of cancer; positron isotope production is a secondary use and must therefore accept certain restrictions. Patient irradiations require 50.5 MeV protons and between 7 am and 6 pm on weekdays only this energy particle is available. The time window available for irradiation between patient treatments ranges from 5 to 60 minutes, typically 15 minutes. The hours before 7 am and after 6 pm are available for acceleration of protons with lower energies and for deuterons. Our initial experience shows that this arrangement is satisfactory for supplying the radioisotopes needed for a positron emission tomography (PET) program; however some new methods have been required to adapt to the constraints of interfacing with a busy neutron therapy program.

Our radioisotope production system consists of a switching magnet which leads off of the main beam line to the radioisotope production targets which are mounted to a four-target support stand, switched remotely from the radioisotope laboratory. Beam switching between neutron therapy and radioisotope beam lines is completed in approximately 40 sec controlled by a computer system which uses NMR probes to measure magnetic field strength and then regulates the current to the switching magnet. The speed of switching enables radioisotope production of virtually unlimited ^{15}O and several ^{11}C runs daily during therapy.

These constraints do not allow production of ^{15}O by the commonly used $^{14}\text{N}(d,n)$ reaction; it is produced by the (p,pn) reaction on ^{16}O . The reaction has a threshold of 16.6 MeV with a maximum cross section of 75 mb at 50 MeV (1). Our target consists of a conical cylinder of aluminum 27 cm long with a volume of 0.36 L. The proton beam passes through a rectangular aluminum window 1.2×3.0 cm and 0.350 ± 0.005 cm (944 mg cm^{-2}) thick. Both the window and target are separately cooled using water at 5.7 and 6.6 L min^{-1} , respectively. The aluminum window is calculated to degrade the 50.5 MeV proton beam to 41 MeV (2).

For ^{15}O production the target is filled to 3.4 atmospheres (0.055 moles) with ultra high purity oxygen and irradiated for two to four minutes. The extracted yield is 900 mCi at the end of bombardment (EOB) for a four minute 43 uA irradiation, in quantitative agreement with cross-section calculations (1,2). Radionuclidic purity at EOB is greater than 96% with impurities of <2% as ^{13}N from the (p,α) reaction and <3% as ^{11}C from the $(p,\alpha pn)$ reaction. After passing the target product through a charcoal/NaOH trap, radionuclidic purity is as great as 99.8%. The radiochemical purity is greater than 99% with the activity in the form of O^{15}O as determined by radiogas chromatography using an Alltech CTR1 column (molecular sieve, Porapak double column). The chemical purity of the gas is greater than 98% as determined using a thermal conductivity detector and the gas chromatography system just described.

^{15}O water is made in our laboratory by the reaction of hydrogen with O^{15}O on a palladium catalyst and a yield of 21 mCi in 0.95 ml has been obtained at two minutes after a two minute 20 uA irradiation. Because of the carrier O_2 , the temperature in the tube furnace increases as the target content moves through the catalyst. The principal disadvantage associated with the (p,pn) method of production, low specific activity, has posed no difficulty for production of O^{15}O and H_2^{15}O . C^{15}O produced by this technique is unacceptable due to the high chemical level of CO ; our target contents convert to about 2L of CO . Production of radiochemically pure CO^{15}O and C^{15}O have proved difficult because of the large quantity of carrier O_2 .

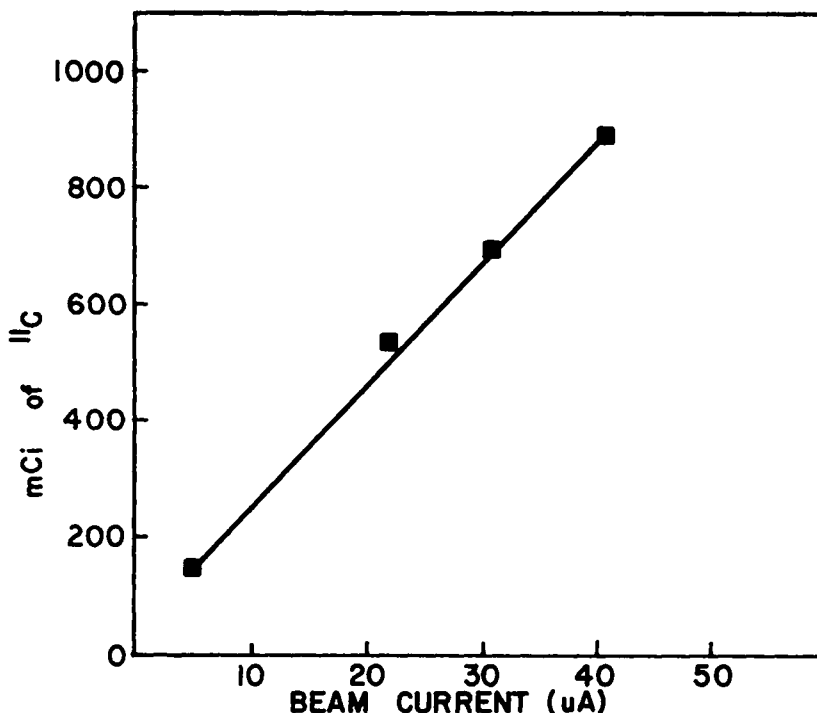


Figure 1. $^{11}\text{C}\text{O}_2$ extracted from target as a function of beam current for a 20 min. irradiation

Carbon-11 is produced by the commonly reported (p, α) reaction on ^{14}N . The reaction has a threshold of 3.1 MeV with a maximum cross section of 250 mb at 7.4 MeV, dropping to 100 mb at 13.7 MeV (1). The competing (p, pn) reaction to ^{13}N has a threshold of 11.3 MeV with a maximum cross section of 44 mb at 17.7 MeV (1). A 0.67 L aluminum target which is similar in shape to the oxygen target is used. For ^{11}C production the 1.2×3.0 cm window is 0.950 ± 0.005 cm (2560 mg cm^{-2}) of aluminum and is water cooled with the same flows as the oxygen target. Beam is degraded to 13.7 (FWHM 3.3 MeV) as measured with multichannel energy analysis of protons passing through the thick Al foil and elastically scattered by a gold foil onto a SILI solid state detector. This compares well with the proton energy degradation from 50.5 to 13 MeV (range 10 to 16 MeV) calculated for 0.95 cm of aluminum (2).

The ^{11}C target is filled to 5.8 atmospheres (0.17 moles) for a calculated proton energy entering the gas at an average of 13.7 MeV and exiting at about 11 MeV. The extracted target yield determined as CO_2 trapped on ascarite is presented in Figure 1 as a function of current on target, and is 890 mCi at the end of bombardment (EOB) for a 20 minute, 41 uA irradiation. This value is more than expected from cross section calculations but these calculations introduce uncertainties from the dispersion in our incident proton energy spectrum and the angular spread of our scattered beam. The radiochemical composition of the gas extracted from the target is 53% ^{11}C at EOB, with 47% ^{13}N and no detectable ^{15}O . The ^{13}N is N_2 and can be removed by passing the target gas in a stream of N_2 through a liquid nitrogen cold trap which collects only the $^{11}\text{C}\text{O}_2$. The ^{13}N yield is much higher than expected and, again, suggests that an appreciable portion of our proton beam is above the energy spectrum that we measured. We are continuing to improve this target and expect to eliminate ^{13}N radionuclidic impurity by modifying the window; however, the yield and quality of $^{11}\text{C}\text{O}_2$ from the present target is adequate for the radiopharmaceutical syntheses that we are planning.

In summary, we have found that the use of a 50 MeV proton beam for production of ^{11}C and ^{15}O is a workable solution for our PET program. We can make sufficient O^{15}O and H_2^{15}O for imaging and we use the ^{11}C to produce ^{11}CO of high specific activity and $^{11}\text{CO}_2$ for use in synthesis. The convenience of having the cyclotron maintenance, operation and physics support covered as a fixed cost for hourly use of the machine more than offsets any inconvenience associated with the use of a 50 MeV proton beam in radioisotope production.

This work was supported in part by PHS grant NO1 CM977282 awarded by the National Cancer Institute and S10 RR01765 by the Division of Research Resources, DHHS and by a Positron Emission Tomography Project Grant from the University of Washington School of Medicine.

1. Hellwege, K.H., ed. Landolt-Bornstein: Numerical Data and Functional Relationships in Science and Technology. New Series, Group 1: Nuclear and Particle Physics, Vol. 5. Q-values and Excitation Functions for Charged Particle Induced Nuclear Reactions. Berlin, Springer-Verlag, 1973.
2. Ziegler, J.F., ed. Handbook of Stopping Cross-Sections for Energetic Ions in All Elements. Vol. 5. New York, Pergamon Press, 1980.

VERTICAL TARGET SYSTEM FOR THE CYCLOTRON PRODUCTION OF
POSITRON EMITTERS FROM MELTED TARGETS

F. Helus, G. Wolber, I. Mahunka, K. Layer, W. Maier-Borst
Institut of Nuclear Medicine, DKFZ, Heidelberg, FRG

As part of a research program to produce biologically active compounds labelled with positron emitters for physiological tomographic studies of tumour metabolism with PET, a vertical target system was developed to produce radionuclides by irradiation on melted targets. The radionuclides produced are separated by thermochromatography from the melted target materials and recovered from the target chamber with a non-reactive carrier gas.

Advantages of this system are:

- use of the energy carried by the particle beam for melting of the target material,
- target may be used many times without recovery procedure,
- fast separation, which may be carried out on-line with the irradiation,
- high yield of produced radionuclides,
- system can be remotely controlled, automation is easily achievable.

B_2O_3 was chosen as target material to produce simultaneously by proton irradiation, the medically useful radionuclides ^{11}C and ^{13}N . The target material is placed in a small cavity constructed from Mo-metal (Figure 1).

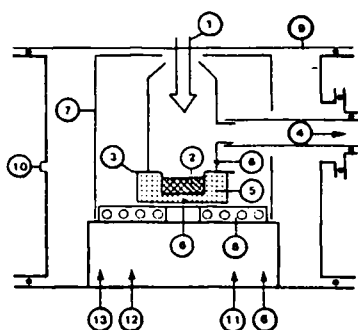


Figure 1 Schematic design of the target chamber

1. Beam inlet
2. Target material
3. Target backing disc
4. Outlet of carrier gas with radioactive products
5. Temperature controlled oven
6. Thermocouple probe
7. Heat reflector
8. Water cooled target mounting plate
9. Foil
10. Vacuum gauge
11. Current junction
12. Inlet of carrier gas
13. Cooling water

During the irradiation the target is partially heated by the energy of the particle beam (20 μA) up to 1,000 $^{\circ}\text{C}$. The temperature was measured by a thermocouple placed at position 6 inside the target backing plate. The produced gaseous products (^{11}CO , $^{11}\text{CO}_2$ and $^{13}\text{N-N}_2$) are transported to the traps by helium carrier gas.

In a typical run the yield of ^{11}C via $^{11}\text{B}(\text{p},\text{n})$ ^{11}C is about 330 $\text{mCi}/\mu\text{Ah}$, the yield of ^{13}N via $^{16}\text{O}(\text{p},\alpha)$ ^{13}N is about 70 $\text{mCi}/\mu\text{Ah}$ and ^{18}F is produced with a yield of 150 $\mu\text{Ci}/\mu\text{Ah}$ from $^{18}\text{O}(\text{p},\text{n})$ ^{18}F in non enriched material. If the target material is melted typically, more than 50% of the produced radioactivity is swept out by the helium carrier gas, using B_2O_3 with a natural oxygen-18 abundance ($\sim 0.2\%$). Even at 20 μA beam current, external electrical heating of the target is necessary to ensure that it is molten.

Higher yields of ^{18}F requires an enriched target ($^{18}\text{O-B}_2\text{O}_3$); the development of an appropriate separation procedure is under development.

;

YIELD RATIO OF $[^{13}\text{C}]\text{-CO}_2$, $[^{13}\text{C}]\text{-CO}$ and $[^{13}\text{C}]\text{-CH}_4$ FROM
THE IRRADIATION OF N_2/H_2 MIXTURES IN THE GAS TARGET

F. Helus, M. Hanisch, K. Layer, W. Maier-Borst
Institut für Nuklearmedizin, DKFZ, Heidelberg, FRG

The $^{14}\text{N}(p,\alpha)^{13}\text{C}$ reaction was studied in different N_2/H_2 -mixtures. The products are $[^{13}\text{C}]\text{-CO}_2$, $[^{13}\text{C}]\text{-CO}$ and $[^{13}\text{C}]\text{-CH}_4$. The yield ratio may be controlled by variation of the bombardement conditions. High pressure, high H_2 -content, high beam current and high proton energy, shift the ratio towards $[^{13}\text{C}]\text{-CH}_4$. Lower beam current and lower proton energy increase the yield of $[^{13}\text{C}]\text{-CO}_2$. The production of $^{13}\text{C}\text{-CO}$ is constant over a wide range of conditions (about 10%).

In recent works, Wolf et al (1,2), found $[^{13}\text{C}]\text{-HCN}$ to be the major product by bombarding N_2/H_2 -mixtures with protons. On the other hand NH_3 or NH_3/N_2 -mixtures as target gas lead to $[^{13}\text{C}]\text{-CH}_4$ and $[^{13}\text{C}]\text{-CH}_2\text{NH}_2$ (3,4), while liquid ammonia shows a wide spectrum of products (5). At high target gas pressure and high proton beam current, $[^{13}\text{C}]\text{-CH}_4$ is produced in a N_2/H_2 -mixture with 5,5% H_2 (6).

Carton-11 was obtained by the bombardement of N_2/H_2 -mixtures (N_2 5.5 H_2 3.5 both Messer Griesheim) with protons. The target gas chamber was a simple quartz liner (length 450 mm, 50 mm i.d.) closed at the rear end with 10 mm Al. At the front the liner is an Al-disc fixed to the beamline with a fast coupling system. In this way it is possible to wash out the liner after bombardement to identify non volatile products.

For product analysis an aliquot of the target gas was examined by radio-gaschromatography (Perkin Elmer 64 Gaschromatograph) on a Chromosorb 102 column (length 1,8 m). The radioactivity was measured on-line using a NaI-scintillation counter.

In the first experiment, the content of H_2 was varied from 0% up to 25%. The beam current was 1 μA , target pressure was $3 \cdot 10^5$ Pa and the proton energy was 14,4 MeV. Figure 1 shows that the major product is $[^{13}\text{C}]\text{-CO}_2$, if no H_2 is added. But a small amount of H_2 decreases the yield of $[^{13}\text{C}]\text{-CO}_2$, while the yield of $[^{13}\text{C}]\text{-CO}$ increases to 8 - 10%. At rising H_2 - concentrations the ratios of $[^{13}\text{C}]\text{-CO}_2$ and $[^{13}\text{C}]\text{-CH}_4$ are inversely proportional. At 25% H_2 a saturation is reached with 85% $[^{13}\text{C}]\text{-CH}_4$, 10% $[^{13}\text{C}]\text{-CO}$ and 5% $[^{13}\text{C}]\text{-CO}_2$.

In the second study, the beam current was varied from 0.5 μA to 3 μA , while the H_2 -content was kept constantly at 5%. The proton energy and the target pressure were the same as above. At a beam current of 0.5 μA only a small amount of $[^{13}\text{C}]\text{-CH}_4$ could be detected (< 1%), but the yield rose rapidly with increasing beam current. The maximum yield of $[^{13}\text{C}]\text{-CH}_4$ was reached at a beam current of 2,5 μA (about 75%, See Figure 2).

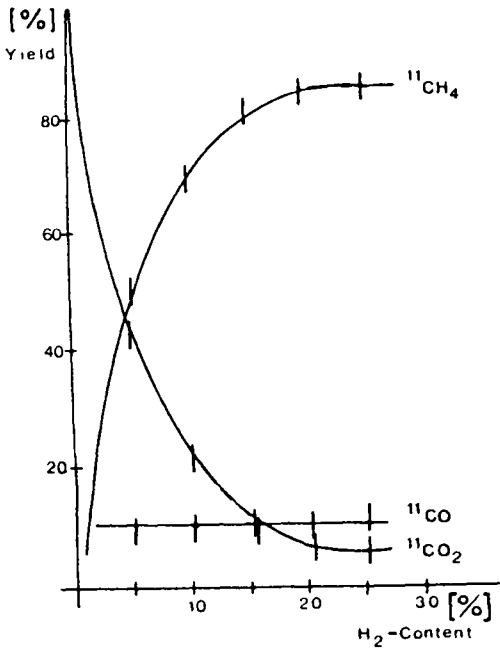


Figure 1: Yield ratio at different H₂-contents

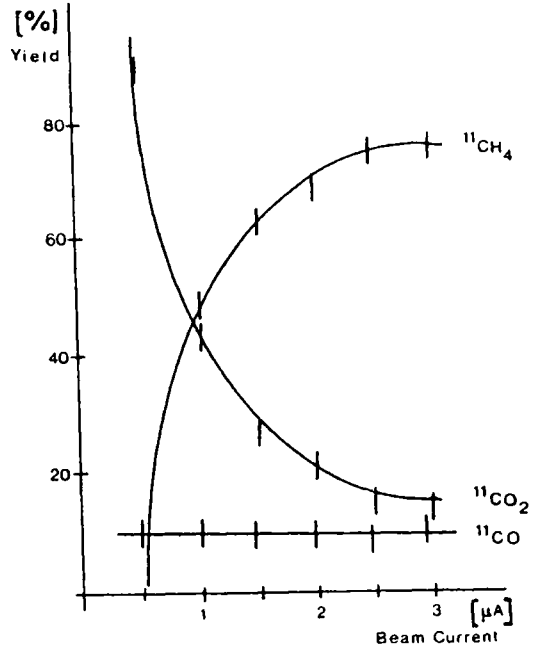


Figure 2: Yield ratio at different beam currents

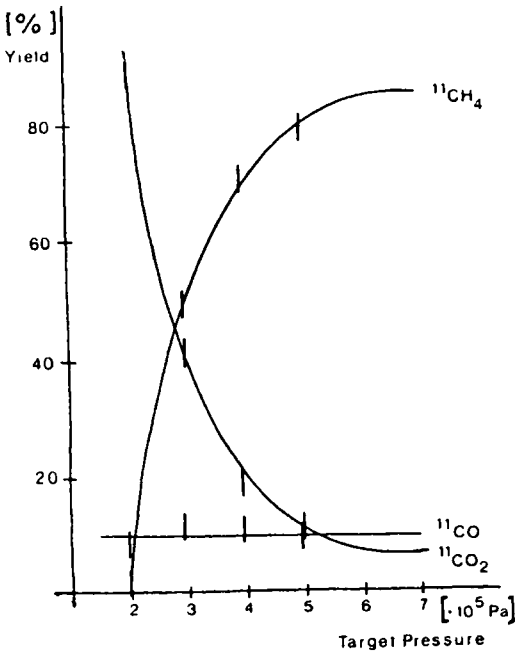


Figure 3: Yield ratio at different target pressures

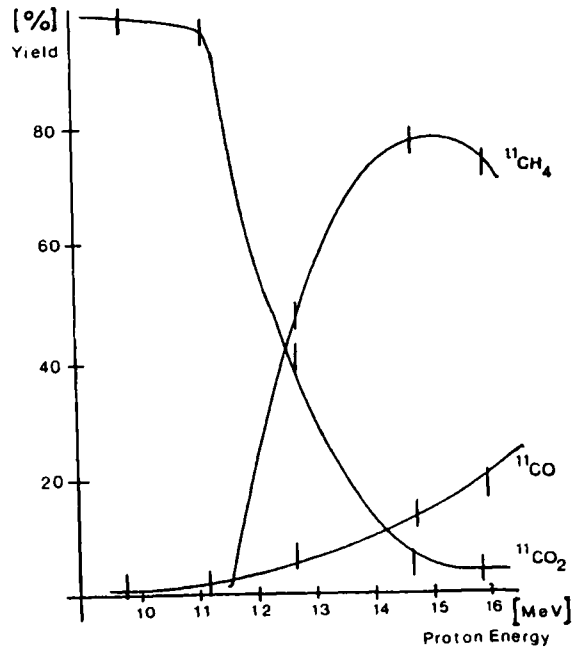


Figure 4: Yield ratio at different proton energies

Variation in target pressure were then made. In this part of the work a pressure of $2 \cdot 10^5$ Pa was necessary for the total absorption of the proton energy in the target. The beam current was kept constant at $1 \mu\text{A}$, the H_2 -content was 5% and the proton energy was 14,4 MeV. The product ratio is shown in Figure 3. A saturation could not be reached in this case, because the target gas holder was not constructed for pressures higher than $4 \cdot 10^5$ Pa. The saturation was estimated by linear extrapolation. It is reached at $7 \cdot 10^5$ Pa with about 85% $[^{13}\text{C}]\text{-CH}_4$, 10% $[^{13}\text{C}]\text{-CO}$ and 5% $[^{13}\text{C}]\text{-CO}_2$.

Finally the proton energy was varied. For this purpose different Al-foils were imposed in front of the target gas holder. The H_2 -content was 5%, the beam current was $1 \mu\text{A}$ and the target gas pressure was $3 \cdot 10^5$ Pa. At low energies, up to 11 MeV, the main product was $[^{13}\text{C}]\text{-CO}_2$ (99%). At energies higher than 11 MeV the yield of $[^{13}\text{C}]\text{-CO}$ is slowly increasing. The production of $^{13}\text{C-CH}_4$ is beginning at 11,5 MeV. At about 15 MeV a maximum is reached with a yield of 80% $[^{13}\text{C}]\text{-CH}_4$. At higher energies $[^{13}\text{C}]\text{-CO}_2$ is constant at 5%, $[^{13}\text{C}]\text{-CH}_4$ is decreasing again. The ratio is shown in Figure 4.

The aim of this work was to find out the optimum conditions to produce $[^{13}\text{C}]\text{-CH}_4$ of high purity by recoil synthesis. We found that there must be a H_2 -content of 5% in the target gas. At lower concentrations no saturation could be reached and at higher concentrations the N_2 as target gas is too dilute. The proton energy should be about 14 - 15 MeV to get a good yield of $[^{13}\text{C}]\text{-CH}_4$. At lower energies too much $[^{13}\text{C}]\text{-CO}_2$ is obtained. At higher energies the yield of $[^{13}\text{C}]\text{-CH}_4$ decreases and $^{13}\text{N-N}_2$, via the $^{14}\text{N}(\text{p,pn})$ ^{13}N , reaction is co-produced. Pressure and beam current should be as high as possible to get a good yield of ^{13}C -radioactivity.

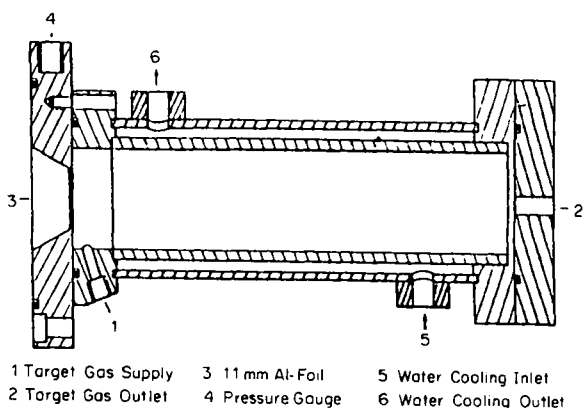


Figure 5: Target gas chamber for high pressures

For this purpose a target gas holder has been developed. Details are given in Figure 5. This target gas holder was filled with 5% H₂ in N₂ at 3.10⁶Pa. Irradiation with protons gave a typical yield of [¹¹C]-CH₄ of 400 - 500 mCi at a beam current of 15 - 20 μA. No other ¹¹C-labelled compound could be detected.

REFERENCES

- 1) H.J. Ache and A.P. Wolf, *Radiochimica Acta* 6, 32 (1966).
- 2) A.P. Wolf and C.S. Redvanly, *Int. J. Appl. Radiat. Isot.* 28, 29 (1977).
- 3) J.Y. Yang and A.P. Wolf, *J. Am. Chem. Soc.* 82, 4488 (1960).
- 4) F. Cacace and A.P. Wolf, *J. Am. Chem. Soc.* 87, 5301 (1965).
- 5) R. Iwada, T. Ido and T. Tominaga, *Radiochimica Acta* 33, 195 (1983).
- 6) J. Sambre, C. Vandecasteele, P. Goethals, N.A. Rabi, D. Van Haver and G. Slegers, *Int. J. Appl. Radiat. Isot.* 36, 275 (1985).

KINETIC STUDIES WITH F-18 FLUORIDE

S.J. Gatley, M. Kornguth, T.R. DeGrado, J. E. Holden

Franklin-McLean Institute, University of Chicago, Chicago, IL 60637 and Department of Medical Physics, University of Wisconsin, Madison, WI 53706

Fluorine-18 is one of the principal nuclides used in positron tomography. In the last several years, a fairly wide range of syntheses of F-18 labeled compounds has become available. One of the major routes to F-18 compounds is that of nucleophilic substitution of groups such as iodide or triflate. Several sources of F-18 "fluoride" are available, one of the most common now being the 0-18(p,n) reaction on 0-18 water. Water is evaporated after addition of a base to prevent loss of F-18 HF. The base may be, for example, Rb_2CO_3 (1), KOH plus 18-crown-6 (2) K_2CO_3 plus Kryptofix 2,2,2, (3) or TEA+ hydroxide (4). There are several significant reaction variables, such as: cation; bulk anion, and solvent. The nature of the target and foil also has a bearing on the reactivity of the F-18, because sputtering or leaching can introduce metal ions or other impurities into the F-18 preparation. Since different laboratories in addition are usually reporting the syntheses of different labeled compounds, it is hard to obtain a coherent picture of the subject.

We have recently described a method of purifying F-18 via synthesis and hydrolysis of gaseous fluorotrimethylsilane (5). This gives, after rotary evaporation of water, a highly reactive preparation of F-18 which we have used to prepare 2-deoxy-2-fluoro-D-glucose (2FDG) (6) and 16-fluoropalmitate (7). We have also been able to obtain excellent reproducibility in terms of reaction rates with individual batches of TEA+ fluoride and fair reproducibility between batches. Thus, we may now be in a position to probe mechanism of F-18 incorporation. By elucidating the factors which limit yields of tracers such as F-18 methyl spiperone, we may be able to circumvent them.

RESULTS AND DISCUSSION

Rates of incorporation of no carrier added F-18 were linear with time for the first few minutes and with the concentration of organic reactant (Fig. 1). Thus kinetic analysis may give useful information about the detailed mechanisms of the reactions.

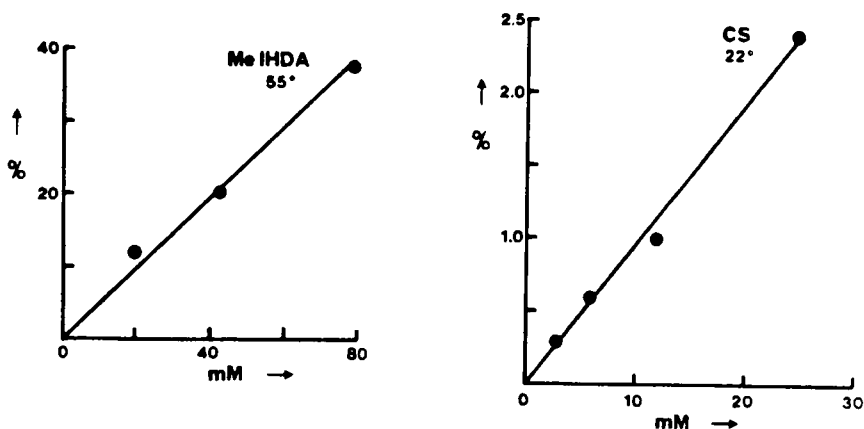


Fig. 1 Linearity of initial rate of F-18 incorporation with concentration of organic reactant. Left panel, methyl 16-iodohexadecanoate; right panel, beta-methyl cyclic sulfate.

The rate of reaction of the cyclic sulfate was decreased in the presence of spiroperidol (SP), chlorodinitrobenzene (chloroDNB) or water (Fig. 2). The extent of reaction of chloroDNB during the experiment was significant, thus the inhibition may be due to rapid removal of F-18 fluoride. However, spiroperidol did not show significant isotope exchange with F-18. The inhibition of the cyclic sulfate reaction by SP may be due to the formation of a hydrogen bonded complex with F-18, and may be relevant to the problem of poor yields obtained in attempts to substitute F-18 directly into molecules with the SP skeleton (8).

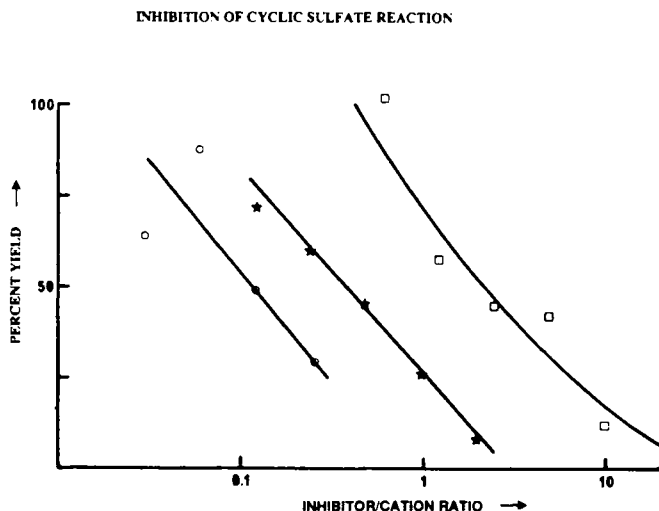


Fig. 2 Inhibition of reaction between F-18 fluoride and cyclic sulfate. Circles, spiropiperidol; stars, chlorodinitrobenzene; squares, water.

Water was less inhibitory to reaction of the cyclic sulfate than SP or chloroDNB. The results are consistent with those published earlier for reaction of diisopropylidene allose triflate (9); two molecules of water per mole of cation gives about 50% inhibition. In fact, normalized water inhibition curves were identical within experimental error for the cyclic sulfate, methyl iodopalmitate, and chloroDNB (data not shown). We previously hypothesized on the basis of observed identical time-courses of the cyclic sulfate and allose triflate reactions (6), that the rate of formation of an "active fluoride" species from bulk fluoride in acetonitrile rate limited nucleophilic substitution. It is not clear how this model would fit the water inhibition data, which imply that all three reactions share a rate determining step where water is involved. We also found that, although the Julich starting material for 2FDG (tetraacetyl mannose triflate) also reacts at the same rate as the cyclic sulfate at 55 degrees (10), chloroDNB reacts faster, while isotope exchange with FDNB is much faster. Thus three reactions at saturated carbon appear to share a rate determining step, but the aromatic substrates as well as chlorotrimethylsilane (5,6) can circumvent it.

The effects of excess TEA⁺ hydroxide were also studied; highest initial rates were found at approximately equal concentrations of hydroxide and cyclic sulfate or methyl iodopalmitate (not shown). TEA⁺ was somewhat less inhibitory than water, although 1 mol of TEA⁺ hydroxide contains about 2 mol of bound water (11). No carrier added F-18 fluoride ions would have a large hydration sphere in the presence of even a trace of adventitious water. Thus the optimum TEA⁺ concentration may represent a compromise between hydroxide pulling water off fluoride, on the one hand, and unavoidable addition of water, on the other.

We hope that continued detailed investigation of a range of F-18 substitution reactions will lead to more efficient syntheses of positron radiotracers.

1. Cacace, F., Speranza, M., Wolf, A.P., MacGregor, R.R., *J. Fluorine Chem.* 21, 145-158 (1982).
2. Spitznagel, L.A. and Marino, C.A., *Steroids* 30, 435-438, 1977.
3. Coenen, H.H., Colosime, M., Schuller, M., and Stocklin, G., *J. Nucl. Med.* 26, p37 (1985).
4. Gatley, S.J. and Shaughnessy, W.J., *Int. J. Appl. Radiat. Isotopes*, 31, 339-341 (1980).
5. Rosenthal, M.S., Bosch, A.L., Nickles, R.J., and Gatley, S.J., *Int. J. Appl. Radiat. Isotopes*, 36, 318-319 (1985).
6. Hutchins, L.G., Bosch, A.L., Rosenthal, M.S., Nickles, R.J., and Gatley, S.J., *Int. J. Appl. Radiat. Isotopes*, 36, 375-378 (1985).
7. Bosch, A.L., DeGrado, T.R., and Gatley, S.J., *Int. J. Appl. Radiat. Isotopes*, (in press).

8. Kilbourn, M.R., Welch, M.J., Dence, C.S., Tewson, T.J., Saji, H., and Maeda, M., *Int. J. Appl. Radiat. Isotopes* **35**, 591-598 (1984)
9. Gatley, S.J. and Shaughnessy, W.J., *J. Label. Comp. Radiopharm.*, **19**, 24-25 (1981).
10. Kornguth, M., DeGrado, T.R., Holden, J.E., and Gatley, S.J., *J. Nucl. Med.* (submitted abstract).
11. Gennick, I., Harmon, K.M., and Hartwig, J., *Inorg. Chem.* **16**, 224-248 (1977).
12. Landini, D., Maia, A., and Podda, G., *J. Org. Chem.*, **47**, 2264-2268 (1982).

Acknowledgements

This work was funded in part by National Institutes of Health awards 1-ROI-HL36534 and HL29046.

PRODUCTION OF $^{18}\text{F-F}_2$ FROM $^{18}\text{O}_2$

O.Solin and J. Bergman

Åbo Akademi Accelerator Laboratory and Turku Medical Cyclotron Project
Porthansgatan 3, SF-20500 Turku, Finland

With the small cyclotrons developed for production of shortlived positron emitting radionuclides the reaction of choice for ^{18}F production is $^{18}\text{O}(p, n)^{18}\text{F}$, using highly enriched ^{18}O as target material. Most systems in use produce ^{18}F from enriched H_2^{18}O (1), which gives the radionuclide in a chemical form suited for nucleophilic substitution reactions.

Nickles et al. (2) showed that it is possible to produce $^{18}\text{F-F}_2$, a chemical form suited for electrophilic addition reactions, from an $^{18}\text{O}_2$ gas target using a two-step technique, by first irradiating the $^{18}\text{O}_2$ gas in a F_2 passivated nickel target chamber, and after removal of the oxygen gas re-irradiate the target chamber containing a mixture of carrier F_2 and a noble gas. The reirradiation forces fluorine exchange between the carrier F_2 and and the ^{18}F adhering to the chamber walls.

We have tested this two-step technique with our target chamber, originally developed for production of $^{18}\text{F-F}_2$ with the reaction $^{20}\text{Ne}(d, \alpha)^{18}\text{F}$ — $^{18}\text{F-F}_2$. The target chamber is made of nickel. No initial F_2 -passivation procedure is used. The chamber body, front and end flanges, are water cooled. The inlet foil is a 25 μm Ni-foil, the inlet diameter is 14 mm. Silver O-rings are used at the front and back ends of the target chamber. The target performance using the reaction $^{20}\text{Ne}(d, \alpha)^{18}\text{F}$ can be seen in table 1. Data from (3) was used when calculating the absolute amounts of ^{18}F produced. The percentages and amounts of $^{18}\text{F-F}_2$ is expressed as amounts collected in the radiochemical laboratory corrected for decay to EOB. The time from EOB to the end of bubbling is about 18 min.

TABLE 1. The $^{20}\text{Ne}(d, \alpha)$ -reaction used for production of $^{18}\text{F-F}_2$ with the system described. $E_d = 8.9$ MeV incident on gas. The beam current was 10 μA in all runs. 100 μmol F_2 carrier was used.

Irradiation time (min)	Radioactivity $^{18}\text{F-F}_2$ (%)	Absolute amount (mean) as $^{18}\text{F-F}_2$ (mCi)
10	60 \pm 3 (n=17) ^a	19.6
30	71 \pm 4 (n= 9) ^b	65.5
90	65 \pm 5 (n=15) ^b	150.7

a) Pre-irradiations for longer runs

b) Before the irradiations a 10 min pre-irradiation was made

For the purpose of the test a SS bottle containing 970 ml (STP) of $^{18}\text{O}_2$ (98 % enriched, Isotech Inc., Ohio, USA) at a pressure of 3800 kPa was connected to the target chamber, see fig.1. The storage bottle also contains 7 g molecular sieve (4 Å). The gas-handling system and target chamber can be seen in fig.1 and 2. After the target chamber has been placed in the irradiation position at the cyclotron all further manipulations of the target are carried out using remote control from the radiochemical laboratory. When valve A (see fig.1) is actuated the pressure in the storage bottle equilibrates with the target chamber volume to a pressure of 750 kPa. After irradiation the $^{18}\text{O}_2$ gas is condensed back into the storage bottle at liquid nitrogen temperature (-196 °C). The loss of enriched gas per handling cycle was found to be about 12 ml (STP), about 1.2 % of the total inventory. The condensation is continued for 5 minutes, after which the target chamber is pumped empty a vacuum pump to a pressure of about 1 Pa. The chamber is then filled with Ne+100 μmol F_2 to a pressure of 900 kPa and reirradiated with the proton beam for 5 min at 10 μA . The gas is then bubbled through either a water solution of KI for iodometric titration of F_2 or used for radiochemical synthesis. The amount of radioactivity that remains in the bubbling vessel is assigned as $^{18}\text{F-F}_2$. After passing through the KI trap the gas is collected, and a

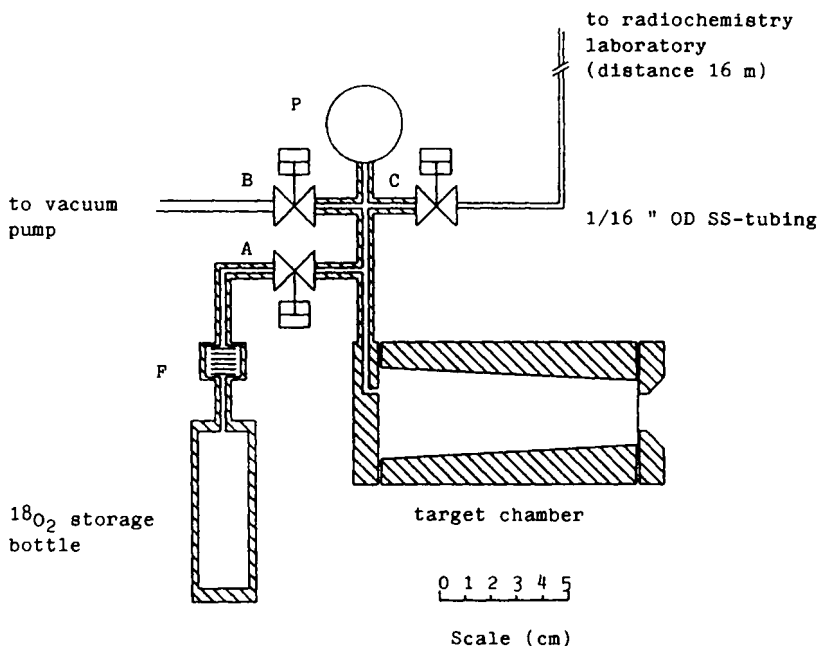


Figure 1. Schematic scale drawing of target chamber and $^{18}\text{O}_2$ storage bottle. A-C are air operated normally closed valves. F = filter. P = Bourdon type pressure gauge.

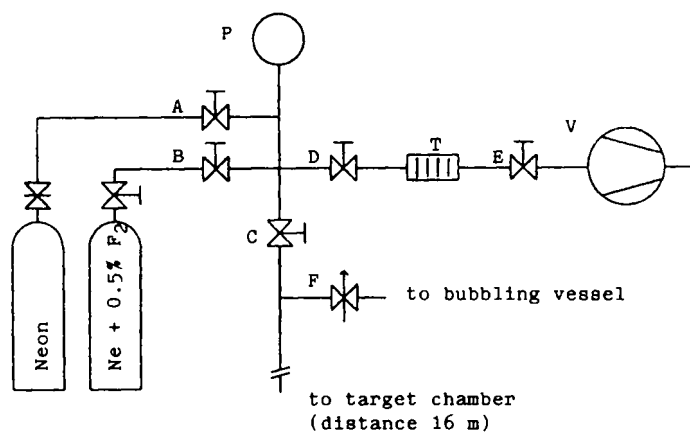


Figure 2. Gas handling system situated in the radiochemistry laboratory. A-E = hand operated valves (monel). F = needle valve (monel). T = NaOH trap. V = vacuum pump. P = Bourdon type pressure gauge (monel).

sample of the gas is injected on a gas chromatograph equipped with a thermal conductivity and a radioactivity detector (column Porapak Q, 80-100 mesh, length 2 m, temp. -30°C , He carrier). Only $^{18}\text{F-CF}_4$ and $^{18}\text{F-NF}_3$ (4) are detected in the chromatograms.

Table 2 shows the results from 5 experiments made with the system described. Data from (5) was used when calculating the absolute amounts of ^{18}F produced. The percentages and amounts of $^{18}\text{F-F}_2$ is expressed as amounts collected in the radiochemical laboratory corrected for decay to EOB. The time from EOB to the end of bubbling was about 35 min.

TABLE 2. The $^{18}\text{O}(p,n)$ -reaction used for production of $^{18}\text{F-F}_2$ with the system described. The beam current was 10 μA in all irradiations.

Run No	Irradiation time (min)	E_p (MeV)	Radioactivity as $^{18}\text{F-F}_2^a$ (%)	Absolute amount as $^{18}\text{F-F}_2$ (mCi)
1	30	10.1	22	57
2	30	7.6	25	44
3	90	8.5	24	126 ^b
4	30	8.5	13	27
5	30	8.5	14	28

a) No correction was made for density reduction in the target gas during irradiation.

b) This run was used for synthesis of $^{18}\text{F-FDG}$ (6) with a radiochemical yield of 22 % (mean for syntheses 21 ± 3).

A major part of the radioactivity not accounted for in the radiochemistry laboratory was found in the $^{18}\text{O}_2$ storage bottle. The decrease in yield of $^{18}\text{F-F}_2$ after run no 3 was associated with a proportional increase of radioactivity in the storage bottle. This work will be continued with studies on the chemical quality of the $^{18}\text{O}_2$ gas used in the system.

1. Kilbourn, M.R., Hood, J.T., and Welch, M.J., *Int. J. Appl. Radiat. Isot.*, 35, 599 (1984).
2. Nickles, R.J., Daube, M.E., and Ruth, T.J., *Int. Appl. Radiat. Isot.*, 35, 117 (1984).
3. Casella, V., Ido, T., Wolf, A.P., Fowler, J.S., MacGregor, R.R., and Ruth, T.J., *J. Nucl. Med.* 21, 750 (1980).
4. Bida, G.T., Ehrenkaufner, R.L., Wolf, A.P., Fowler, J.S., MacGregor, R.R., and Ruth, T.J., *J. Nucl. Med.* 21, 750 (1980).
5. Ruth, T.J., and Wolf, A.P., *Radichimica Acta*, 26, 21 (1979).
6. Haaparanta, M., Bergman, J., Solin, O., and Roeda, D., *Nuklearmedizin, Suppl.*, 21, 823 (1984).

EFFICIENT SMALL-VOLUME O-18 WATER TARGETS FOR PRODUCING F-18 FLUORIDE WITH LOW ENERGY PROTONSB.W. Wieland^a, G.O. Hendry^a, D.G. Schmidt^b, G. Bida^b, T.J. Ruth^c^aComputer Technology & Imaging, Inc., 950 Gilman St., Berkeley, CA 94710^bUCLA School of Medicine, Division of Biophysics and Nuclear Medicine, Los Angeles, CA 90024^cUBC/TRIUMF PET Program, University of British Columbia, Vancouver, BC VGT 1W5

Small, high-performance, static water targets for the production of aqueous F-18 fluoride from enriched O-18 water have been developed for use with a collimated 11 MeV proton beam extracted from a negative ion cyclotron. The beam current density distribution at the target entrance has been measured by activating 1 mm copper pins at the centerline and on 4 mm and 8 mm diameter circles. Counting the 38.1 min Zn-63 from the p,n reaction on Cu-63 indicates a uniform circular beam distribution with intensity of 84% of maximum at the 4 mm diameter and 49% at the 8 mm diameter. The 10 mm collimator is split assuring a centered beam when the collimator currents are balanced.

Targets were constructed of copper and plated with electroless nickel. A vacuum window of 25.4 micrometer aluminum and a target window of 12.7 micrometer Havar reduce the energy entering the target water to 10.5 MeV. 10 mm diameter cavity depths of 1.0 and 2.0 mm were used in the experiments, resulting in centerline water thicknesses of 1.15 and 2.15 mm due to outward deflection of the window with the target pressurized. The range of 10.5 MeV protons in water is 1.32 mm. This results in one target with predicted exit energies of 3.0 MeV centerline and 4.7 MeV at the perimeter, and one target which is 163% range thick at the centerline and 151% range thick at the perimeter. Both targets have a 0.300 mL reflux chamber above minimum loaded water level. Extra target water was loaded to insure make-up for radiolysis and reflux redistribution.

The targets have been remotely loaded through 15 meters of polyethylene tubing (0.86 mm I.D.). For these experiments the target was loaded through the bottom port via a zero dead volume Teflon slider-valve (necessary for pressurization). The radioactive water was recovered remotely in all runs. Transit time was approximately two minutes and the activity was recovered in a vessel located in a dose calibrator.

The "thick" target of Table 1 shows a relatively linear decrease in yield of about 1.6 mCi/uA per μ A of current increase (29% yield decrease at 25 μ A). The "thin" target of Table 2 shows 2.4 mCi/ μ A per μ A (43% decrease at 25 μ A). There is no significant difference between short runs (5 - 12 min) and long runs (26-113 min).

Table 3 indicates there was no significant increase in yield for the "thick" target run at 10 atmosphere pressure versus the 2 atmosphere condition of Table 1.

The target water loading was accurately weighed and compared to the recovered weight with and without bombardment. No decrease was observed without bombardment and an average decrease of 5% was observed with bombardment. The 10 mL volume of the pressurization tubing was valved off during each run and a pressure transducer was used to record the pressure increase. The increases in pressure correlated well with a calculation of hydrogen and oxygen resulting from the radiolysis of 5% of the target water.

Separate rinses were made of the "thin" target and of the recovery line after a 10 min run at 20 μ A (0.195 mL initial loading). 91% of the activity was recovered before the rinses, 7% from the target rinse, and 2% from the line rinse.

The target loadings used in these initial experiments were considerably above the amount needed to bring the water level to the top of the beam strike (185% for the "thick" target and 253% for the "thin" target). The cost of the 0.330 mL loading of Table 1 is \$24.

Table 1. Experiments with 2 mm Thick Water Target using 2 atm Helium Overpressure (average 0-18 water loading of 0.330 mL with 0.157 mL beam strike and 0.157 mL refluxing space above liquid level).

Beam Current (microamps)	Bombardment Duration (minutes)	Activity at EOB (millicuries)	Saturation Yield at EOB (millicuries/microamp)
1.0	10	7.9	129.4
5.2	10	45.3	142.2
10.0	10	76.6	125.2
10.0	60	408.3	129.4
12.5	10	91.4	119.5
12.4	33	273.2	117.1
15.0	10	101.2	110.2
15.2	30	290.7	110.8
20.0	10	131.8	107.7
19.7	30	409.4	120.4
19.6	113	1170.2	117.0
25.0	10	150.3	98.2

Table 2. Experiments with 1 mm Thick Water Target using 2 atm Helium Overpressure (average 0-18 water loading of 0.225 mL with 0.079 mL beam strike and 0.164 mL refluxing space above liquid level).

Beam Current (microamps)	Bombardment Duration (minutes)	Activity at EOB (millicuries)	Saturation Yield at EOB (millicuries/microamp)
1.0	10	8.9	144.8
5.0	5	20.8	132.7
5.2	10	43.0	134.9
8.7	12	70.9	111.7
15.0	10	89.8	97.8
15.2	26	264.0	114.6
20.0	10	124.2	101.4
20.0	60	546.5	86.6
23.5	10	129.7	90.2

Table 3. Experiments with 2 mm Thick Water Target using 10 atm Helium Overpressure (average 0-18 water loading of 0.340 mL with 0.157 mL beam strike and 0.147 mL refluxing space above liquid level).

BEAM Current (microamps)	Bombardment Duration (minutes)	Activity at EOB (millicuries)	Saturation Yield at EOB (millicuries/microamp)
25.0	10	171.1	111.8
25.0	29	371.7	88.8

Tables 1 and 2 give results for the "thick" (2 mm) target and the "thin" (1 mm) target as a function of beam current. These experiments were done with a 2 atmosphere initial pressure on the target chamber to keep the target window deflected outward against the helium window cooling pressure. Table 3 gives results for a 10 atmosphere pressure on the "thick" target.

The F-18 fluoride produced has been used to prepare 2-(F-18)-fluoro-2-deoxy-D-glucose (FDG) in approximately 50% radiochemical yield (EOB) using the synthesis described by Hamacher et al.¹. The final product, analyzed by TLC, gave appropriate R_f values.²

The results of these initial experiments indicate that an 11 MeV proton accelerator can economically produce sufficient quantities of F-18 fluoride to support a clinical PET program.

- 1) Hamacher, K., Coenen, H.H., Stocklin, G., *J Nucl Med* 27, 235, 1986.
- 2) Bida, G.T. Satyamurthy, N., Barrio, J.R., *J Nucl Med* 25, 1327, 1984

PRODUCTION OF ^{18}F -LABELED RADIOTRACERS WITH AN ELECTRON ACCELERATOR

S.-E. Strand, K. Ljunggren, L. Hallstadius, K. Jönsson, M. Ljungberg,
T. Ohlsson, O. Olsson, A. Sandell

Radiation Physics Department, University of Lund, University Hospital,
S-221 85 Lund, Sweden

The growing interest in positron-emitters in nuclear medicine has motivated an attempt to build a simple PET-system based on an electron accelerator and a dual-headed gamma camera. The newly developed race-track microtron (1) has made it possible to get a small electron accelerator with energy 50 MeV and $I=10\ \mu\text{A}$ suitable also for cancer therapy. The using of two gamma cameras as positron camera has been studied for many years in Groningen (2) successfully. The great advantage is the high sensitivity (50 times a PET-ring) and the main drawback the poor depth resolution (10 cm), the latter could probably be considerably improved by a more refined image-reconstruction technique. At our institute we have access to the described equipment and our first goal is to make studies with ^{18}F -labeled compounds. There are different ways to produce ^{18}F with photons eg $^{19}\text{F}(\gamma, n)^{18}\text{F}$, $^{23}\text{Na}(\gamma, \alpha n)^{18}\text{F}$ and $^{20}\text{Ne}(\gamma, 2n)^{18}\text{Ne} \rightarrow ^{18}\text{F}$. The last one is of no real interest due to the small activity being produced. The first reaction gives the highest activity but with the difficulty to achieve high specific activity. The $^{23}\text{Na}(\gamma, \alpha n)^{18}\text{F}$ reaction has been studied by (3, 4), however, their results differ considerably probably due to the different geometries used during the irradiations. By irradiating Na in the form of NaOH pellets we have confirmed the higher results (60 $\mu\text{Ci/gNa}$ μA at saturation) of (4). The ^{18}F is easily extracted by ion-exchange technique. Our next step will be to investigate the possibility to use the $^{19}\text{F}(\gamma, n)^{18}\text{F}$ reaction. An interesting method has been reported by (5) where the $^{19}\text{F}(n, 2n)^{18}\text{F}$ reaction was used. The target consists of perfluoro-n-hexane, where the produced ^{18}F leaves its chemical place and by shaking the solution (density 2.7) with water the ^{18}F activity was extracted. The yield of this reaction is approximately 10 times larger than the former one per gram of irradiated material, in this case also larger targets could be used. The chemical yield is 25 % and the F^- concentration was less than $10^{-5}\ \text{M}$. During summer 1986 a set-up for producing FDG starting from F^- in water based on the idea of (6) will be installed at our institute for biomedical studies.

1. Rosander, S., Sedlacek, M., and Wernholm, O., Nucl. Instrum. Meth., 204, 1 (1982).
2. Paans, A.M.J., De Graaf, E.J., Wallererd, J., Waalburg, W., and Woldring, M.G., Nucl. Instrum. Meth., 192, 491 (1982).
3. Donnerhack, A., and Sattler, E.L., Int. J. Appl. Radiat. Isotop., 31, 279 (1980).
4. Yagi, M., and Amano, R., Int. J. Appl. Radiat. Isotop., 31, 599 (1980).
5. Kushelevsky, A.P., Alfassi, Z.B., and Wolf, W., to be published.
6. Hamacker, K., Coenen, H.H., and Stöckling, G., to be published.

^{15}O -WATER CONSTANT INFUSION SYSTEM FOR CLINICAL ROUTINE APPLICATION

G. J. Meyer, A. Osterholz, H. Hundeshagen
 Medizinische Hochschule Hannover, F. R. Germany

^{15}O -water has been used widely for measurements of cerebral blood flow, cerebral oxygen utilization, and extravascular water (1,2). Except for very recent examples, where fast tomographs of the latest generation could be used, most of the clinically oriented measurements are carried out under steady state conditions. The common procedure for maintaining a steady state of ^{15}O -water is by constant inhalation of ^{15}O -carbonyl dioxide, which equilibrates to ^{15}O -water in the lungs instantaneously.

However, this procedure can not be used for measurements of extravascular water in the lungs. Furthermore the procedure gives rise to additional scattered radiation from the mouthpiece and the upper respiratory tract in CBF studies of the brain, especially below the OM-line, and finally the radiation dose to the trachea has been calculated to be critical.

We have therefore set up a constant infusion system for ^{15}O -water, which is an improved version of that described by Harper and Wickland (3). The system has been used in clinical routine studies on more than 200 patients during the past 3 years without adverse effects in any case.

^{15}O is produced by 8 MeV deuteron bombardment of nitrogen containing 0.2% oxygen. About 20m from the target the molecular oxygen passes a control station for calibration, purification and analysis and is then led on for about 30 m to the ^{15}O -water production and infusion system right besides the PET imaging device. The ^{15}O -water production and infusion system is housed in a 20x30x20 cm lead box of 5 cm wall thickness with a 10x10 cm leadglass window of equivalent thickness. The whole system is mounted on a laboratory wheel cart. As shown in Fig. 1 the leadbox contains a catalyst tube of 5x0.6 cm with ca 10 pellets of Pd on Aluminumoxide (Engelhardt) covered by an oven of equivalent length, a 4 necked flask (20ml) sealed with GC-septa (Perkin Elmer type), a cooling bath for the flask served by an external cryostat and a double head peristaltic pump. Hydrogen is mixed to the target gas before entering the leadbox. The peristaltic pump withdraws physiol. NaCl from an infusion bottle and pumps it into the 4 necked flask with one head, while the other head withdraws the active mixture from the 4 necked flask at the same rate, and pumps it via a calibration detector and a sterilization filter into the patient.

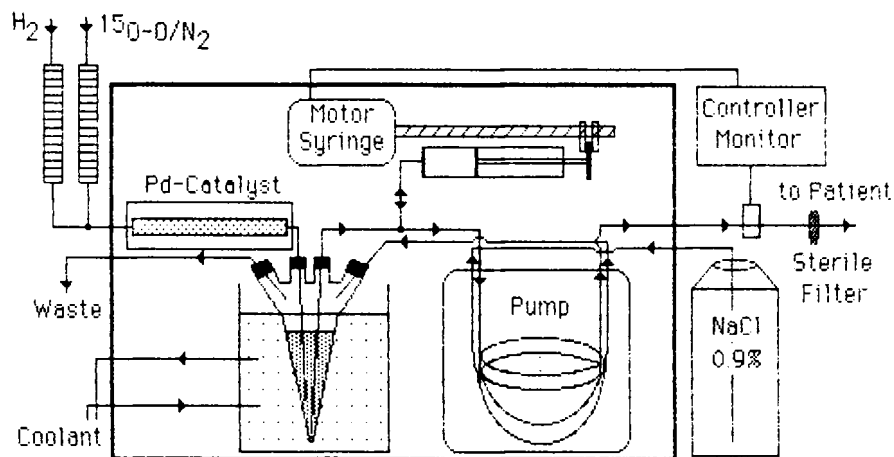


Fig. 1 System for constant infusion of ^{15}O -labelled water.

The target gas flow is kept at 200 ml/min, the Hydrogen flow at 10 ml/min. The oven Temperature is 150°C . The infusion rate is 4 ml/min. Under these conditions a beam current of $5\ \mu\text{A}$ is sufficient to deliver an activity level of 1–5 mCi/ml, depending on the reservoir in the 4 necked flask.

Assuring a constant infusion level for about 0.5 h periods necessitates control and adjustment equipment. However, the adjustment of a ^{15}O steady state system has complicated response characteristics. Increasing the flow on either the target gas side or the infusion side increases the delivered activity for a short time period, however, it depletes the activity level in the target gas or the infusion reservoir, causing a decrease of the delivered activity thereafter. Regulation of the beam current is much too slow to ensure a constant infusion level on the tail end. Therefore the stability of the activity level is controlled by two independent units. The first is located at the cyclotron beam current control system and provides a stable beam current. The second unit is a reservoir level control system and consists of a motor driven syringe which either dilutes or concentrates the reservoir in the 4 necked flask, according to the activity-level control monitor. Both system combined ensure a $\pm 2\%$ stable infusion level and an adjustment of the administered infusion level according to the patient's weight.

The shielding of the system allows it to be placed close to the PET imaging device. All long distances are spanned by gas transport and liquids are pumped with minimal dead volume losses, thereby keeping the total activity inventory as small as possible.

The infusion site can be chosen according to the investigation, i.e. at a foot vein for extravascular lung water measurements or the arm for CBF measurements. The inconvenience of wearing face masks and the associated leak probability is avoided also.

The potential hazard of bacterial contamination of the system is acknowledged. Therefore the system parts are sterilized before assembly, and sterility tests and apyrogenicity tests are carried out monthly. However, in three years of routine use, no bacterial or pyrogenic contamination has been found in any of the tests.

It should be mentioned that in target production of ^{15}O -water by bombardment of Nitrogen containing 2-4% Hydrogen (4) has been tested with this system also. However, the transport losses were quite high. In order to reach the same activity level as described above, the beam current had to be increased to 40 μA . Furthermore this method causes the production of considerable amounts of Ammonia in the target by radiolysis, which leads to a pH increase to 9-10 for the infusate 10 min after the production start.

Although steady state measurements with ^{15}O -water have recently been criticized because of some inherent limitations in accuracy, alternative procedures usually require an accurate measurement of the arterial input function (5). As long as no simple procedures are developed to obtain these data, steady state methods will be used in clinically oriented routine measurements for CBF and extravascular water. However, an alternative procedure could be developed, using either ^{15}O - or ^{11}C -Butanol. A study protocol for routine application of these compounds for CBF measurements is under development.

References:

1. Frackowiack, R.S.J., Lammertsma, A.A. In Reivich, M., Alavi, A., eds., Positron Emission Tomography. New York, Alan R. Riss Inc. 1985, pp153-181
2. Schober, O., Meyer, G.-J., Bossaller, C., Creutzig, H., Lichtlen, P.R., Hundeshagen, H., Eur. J. Nucl. Med. 10, 17-24 (1985)
3. Harper, P.V., Wickland, T., J. Labelled Compd. Radiopharm., 18, 186 (1981)
4. Vera Ruiz, H., Wolf, A. P., J. Labelled Compd. Radiopharm., 15, 185 (1978)
5. Huang, S.-C., Phelps, M.E., In Phelps, M.E., Mazziotta, J.C., Schelbert, H., eds., Positron Emission Tomography and Autoradiography. New York, Raven Press 1986, pp287-346

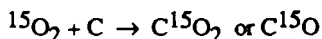
THE EDISON LAMP: O-15 CARBON MONOXIDE PRODUCTION IN THE TARGET.

JR VOTAW, MR SATTER, JJ SUNDERLAND, CC MARTIN, RJ NICKLES.

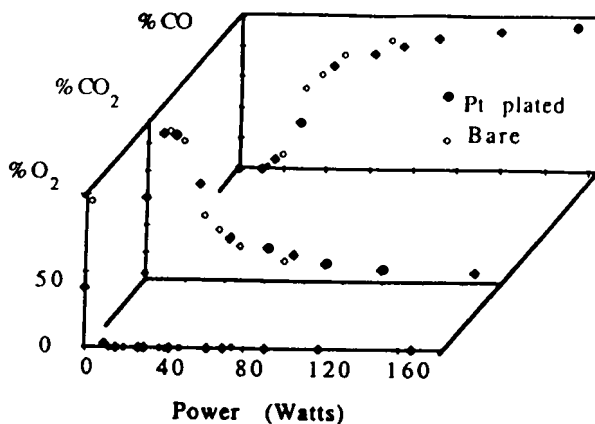
Department of Medical Physics, University of Wisconsin, Madison WI 53706

A target has been developed for the on line production of $C^{15}O$ in order to maximize the available activity for PET studies. The target, shown in figure 1, features an internal carbon filament which is heated to perform the conversion from $^{15}O-O_2$ to either $C^{15}O$ or $C^{15}O_2$. It was built to accommodate either static or flow through operation, and was tested as a static target with the $^{14}N(d,n)^{15}O$ reaction at 6 and 7 MeV on the University of Wisconsin EN Tandem Van de Graaff accelerator. By carrying out the experiment at the lower energies, the production of ^{11}C (via the $(d,\alpha n)$ reaction) is minimized. The conversion from $^{15}O-O_2$ to either $C^{15}O$ or $C^{15}O_2$ is achieved inside the target chamber by exposing the $^{15}O-O_2$ to a pyrolytic carbon filament heated by an electric current. After the initial success of a bare carbon filament, the experiment was repeated using a platinum plated filament in the hope that the platinum would act as a catalyst allowing the conversion reaction to $C^{15}O$ to take place at reduced temperatures. Results indicate that the Pt did not alter the conversion, but did greatly increase the temperature to which the filament could be heated and it also increased the filament lifetime.

The reaction of interest,



is very temperature dependent. The maximum conversion to $C^{15}O_2$ was found to be 98% of the produced activity at a power level of 13 Watts corresponding to a filament temperature of $500^\circ C$. At 170 watts ($T > 1800^\circ C$) and using the Pt coated filament, the produced target activity was 92% $C^{15}O$ and 8% $C^{15}O_2$. By varying the power supplied to the filament, the $^{15}O_2 / C^{15}O_2 / C^{15}O$ ratio may be altered between these extremes as shown in graph 1. The data below 70 Watts is consistent regardless of filament type but only the Pt plated filament is able to withstand the greater temperatures without burning out. The effect of the Pt is that it allows the filament to be taken to much higher temperatures for increased yields.



Graph 1. The relative ^{15}O labeled constituents of the target gas at end of bombardment as a function of power supplied to the filament. The three graphs sum to 100%.

For each separate test, the target was first evacuated then filled thick to the beam with a mixture of .03% O_2 in N_2 which is the composition of a standard N_2 tank of gas. The ratio was adjusted up to .5% O_2 with no noticeable effect in either the activity produced or in the ability to remove the activity from the target. Considering this and that the life of the filament is inversely related to the carrier oxygen level, future work will feature tank N_2 as the target gas.

To determine how fast the reaction takes place, several trials were taken while varying the irradiation time. It was found that the conversion was invariant over irradiation times ranging between 30 and 600 seconds indicating that the reaction was complete within seconds. Irradiations of 2 minutes are recommended as a compromise between producing enough ^{15}O and reducing the production of longer lived contaminating isotopes.

When the target is inverted (filament above beam strike) there is a significant drop in the production of C^{15}O . This indicates the importance of convection currents within the target and that the

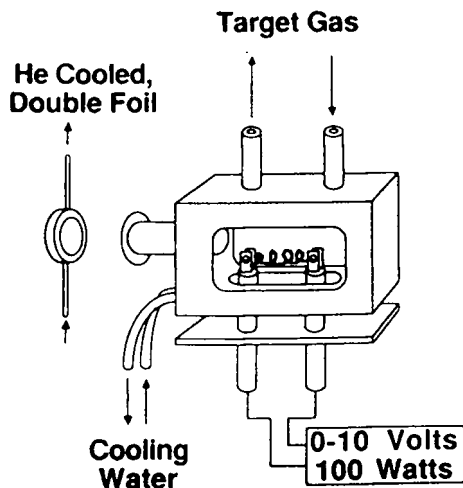


Figure 1. The C^{15}O production Edison Lamp target.

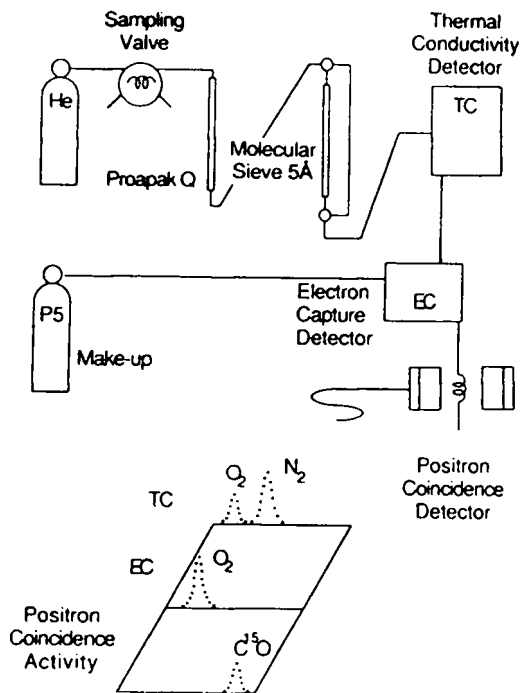


Figure 2. Gas chromatography system showing the three detectors used to unambiguously identify components of the target gas.

conversion reaction takes place at the surface of the carbon filament. By placing the filament at the bottom of the target and along its whole length, convection currents are maximized and the ^{15}O is more likely to come in contact with hot carbon and be converted to C^{15}O . Previous poor results with a small filament at the back of the target corroborate this hypothesis.

The composition of the target gas was measured post irradiation with gas radiochromatography employing two columns (Porapak Q and Molecular Sieve 5A) in switchable series with the three detectors shown below. In all studies, the O_2 , CO and CO_2 peaks, both stable and ^{15}O labeled, were clearly resolved as is demonstrated in figure 2. Concurrently, a sample of the target gas was placed in an extended range well counter¹ to measure the activity produced and to verify the radio-isotopic purity of the gas. These measurements show more than three decades of monoexponential decay indicating that the radio-peaks found in the gas chromatographic data are due to Oxygen-15.

Performing the conversion from ^{15}O to C^{15}O in the target eliminates the need for post irradiation charcoal furnaces and the additional time such an operation adds to the synthesis. This becomes increasingly important as we anticipate producing C^{15}O from a target of enriched $^{15}\text{N}\text{-N}_2$ target gas via the $^{15}\text{N}(p,n)^{15}\text{O}$ reaction after the arrival of a small proton only cyclotron. When this is

the case, the savings in time of one to three half-lives is extremely attractive. In addition to making static batches, taking advantage of the short conversion time within the target from $^{15}\text{O-O}_2$ to C^{15}O makes feasible the steady state production of C^{15}O . Recent results² have shown that by utilizing a flow rate of 4 ml/min, 17.5 mCi/min can be produced at a cost of \$1/min. In these experiments the STP target gas (200 psia) volume was 45 ml creating a target gas dwell time of 15 seconds which is adequate for conversion to take place. By running the edison lamp target at 90 Watts we expect to be able to make 16 mCi/min of C^{15}O at the same cost of \$1/min which would have been impossible had we not been able to perform the conversion inside the target.

With great pleasure the authors acknowledge generous support from the National Institute of Health in the form of grant RO1-CA33702. Support from the University of Wisconsin experimental nuclear physics research group in the form of accelerator beam time is also gratefully recognized.

¹Nickles RJ, Votaw JR: An Extended Range Well Counter. *IEEE Trans Nucl Sci* NS-32(1), 60 (1985).

²Wieland B, Hendry G, Abstract submitted to the Int'l Symp on Radiopharm. Chem., Boston MA, 1986. Personal Communication.

EFFICIENT, ECONOMICAL PRODUCTION OF OXYGEN-15 LABELED TRACERS WITH LOW ENERGY PROTONS

B.W. Wieland*, D.G. Schmidt†, G. Bida†, T.J. Ruth†, and G.O. Hendry*

*Computer Technology and Imaging, Inc., Berkeley, CA 94710

†UCLA School of Medicine, Division of Biophysics and Nuclear Medicine, Los Angeles, CA 90024

‡UBC/TRIUMF PET Program, University of British Columbia, Vancouver, BC V6T 1W5

The use of oxygen-15 labeled tracers for determination of tissue blood flow, blood volume, and oxygen utilization by Positron Emission Tomography (PET) will undoubtedly play a major role in securing the application of PET in Clinical Nuclear Medicine. Dynamic (1) and equilibrium (2) strategies using O-15 compounds have been employed in the evaluation of cerebral dysfunction (3). With the introduction of low energy (< 11 MeV), proton only accelerators (4) and an anticipated clinical PET patient schedule (5) of perhaps 15 studies/week, it was felt imperative to investigate the economic viability of O-15 production, which can only be provided via the $^{15}\text{N}(p,n)^{15}\text{O}$ nuclear reaction. An investigation of optimum target design and accelerator beam conditions for the efficient, low cost production of O-15 oxygen (batch and continuous flow modes) has been pursued and the preliminary results reported herein.

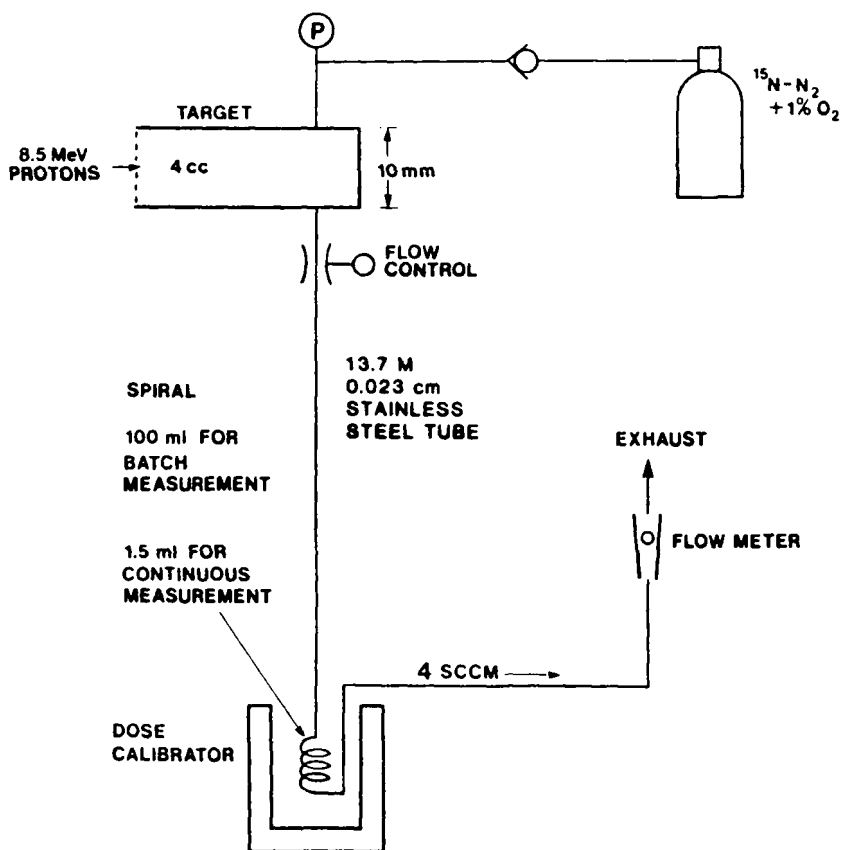


Figure 1. Experimental arrangement for $^{15}\text{O}_2$ production

TABLE 1. $^{15}\text{O}_2$ Production via $^{15}\text{N}(p,n)^{15}\text{O}$ at 8.5 MeV

Beam (μA)	Time (min)	Pressure with beam off (PSIA)	Flow (SCCM)	Activity in spiral (mCi)	Activity dispensing rate (mCi/min)	% Theo. ⁽⁶⁾	Cost ^{a)}
BATCH							
5	10	240	0	235	0	100	~\$20
10	10	250	0	450	0	95	~\$20
20	10	245	0	750	0	79	~\$20
FLOW							
5	10	225	4	1.7	4.5		1\$/min
10	10	215	4	3.3	8.8		1\$/min
15	10	205	4	5.0	13.3		1\$/min
20	10	200	4	7.7	19.0		1\$/min

a) Isotec, Inc., Dayton, OH (\$186/GRAM, 4/85).

A water cooled aluminum target chamber (ID = 10 mm, volume = 4 cm³) was designed in order to make efficient use of the 99+% enriched $^{15}\text{N}_2$ (+1% O_2 , v/v) target gas. The target assembly employed a 0.00254 cm aluminum vacuum window and a 0.00254 cm Havar target window. To further limit the $^{15}\text{N}_2$ inventory but maintain a comfortable saturation yield (6), a carbon degrader was used to reduce the proton beam energy on target to 8.5 MeV. The experimental arrangement used in these studies for continuous $^{15}\text{O}_2$ production is shown in Figure 1. The same arrangement was used for batch production except that a 0.081 cm ID delivery line and a 100 cm³ evacuated spiral was used. Results for the batch and continuous flow $^{15}\text{O}_2$ production are summarized in Table 1. Oxygen-15 gas samples were found to contain < 1% radionuclidic impurities (as $^{13}\text{N}_2$) and the radiochemical purity was ~98% as determined by radiogas-chromatography.

The conclusions provided by these initial experiments are straightforward: i) clinically useful quantities of 0-15 oxygen gas can be produced via $^{15}\text{N}(p,n)^{15}\text{O}$ and a proton energy of 8.5 MeV; ii) given an ambitious yet realistic weekly patient scenario of 15 studies (5), economics is not an issue. This work indicates that the economical production of 0-15 labeled water, carbon monoxide and carbon dioxide is now feasible.

- Mintun, M.A., Raichle, M.E., Martin, W.R.M., and Herscovitch, P., J. Nucl. Med., 25, 177 (1984).
- Frackowiak, R.S.J., Lenzi, G.-L., Jones, T., and Heather, J.D., J. Comput. Assist. Tomogr., 4, 727 (1980).
- a) Phelps, M.E., and Mazziotta, J.C., Science, 228, 799 (1985); b) Jones, T., Frackowiak, R., Wise, R., and Lenzi, G.-L., In Heiss, W.-D. and Phelps, M.E., eds., Positron Emission Tomography of the Brain, Heidelberg, Springer-Verlag, 1983, pp 107-112.

4. Straatman, M.G., Wieland, B.W., and Nickles, R.J., *Trans. Amer. Nucl. Soc.*, 50, 29 (1985).
5. Hawkins, R.A., and Phelps, M.E., *In Proceedings of the Workshop on Radiopharmaceutical Production Systems for Clinical Uses of Positron Tomography*, Washington, D.C., February 12, 1986, to be published.
6. Sajjad, M., Lambrecht, R.M., and Wolf, A.P., *Radiochim. Acta*, 36, 159 (1984).

AN ECONOMICAL TARGET FOR NITROGEN-13 PRODUCTION BY PROTON BOMBARDMENT OF A SLURRY OF C-13 POWDER IN 16-O WATER

G. Bida*, B.W. Wieland†, T.J. Ruth†, D.G. Schmidt*, G.O. Hendry†, and R.E. Keen*

*UCLA School of Medicine, Division of Biophysics and Nuclear Medicine, Los Angeles, CA 90024

†Computer Technology and Imaging, Inc., Berkeley, CA 94710

†UBC/TRIUMF PET Program, University of British Columbia, Vancouver, BC V6T 1W5

Compounds labeled with the short lived positron emitter ^{13}N have found widespread application in a number of disciplines (1). As concerns Positron Emission Tomography (PET), N-13 labeled ammonia has served as a readily available agent for imaging regional cerebral (2) and myocardial blood flow (3) and as a precursor for synthesis of various L- ^{13}N amino acids (4). Nitrogen-13 labeled ammonia is most commonly prepared by chemical reduction of the species resulting from proton irradiation of water (5). However, production of sufficient ^{13}N NH_3 to meet clinical demands using low energy (≤ 11 MeV) protons places undesirable constraints on the target. Although the $^{13}\text{C}(\text{p},\text{n})^{13}\text{N}$ reaction has a much higher saturation yield ($\sim 20 \times$ at 10 MeV), no method exists that involves proton irradiation of a C-13 enriched target material that is as simple, quantitative or as cost effective as the Devarda's reduction of proton irradiated water. Based on considerations of carbon particle size distribution, proton range and nascent N-13 atom recoil energies and hot atom chemistry in water (5), a target consisting of a slurry of C-13 powder in 0-16 water was investigated for production of N-13.

The target holder consisted of a water cooled, electroless nickel plated copper body fitted with a 0.00254 cm Havar beam window. A slurry of 99% enriched C-13 powder was pumped under pressure into the target volume (~ 250 mm³) and held in situ with a 10 μm pore SS frit at the target body exit, thus providing a stationary bed of C-13 powder through which water could be pumped. For N-13 production, the target was irradiated with a 10 MeV proton beam. Single pass flow of water through the carbon bed was maintained by a HPLC pump and the aqueous activity delivered through 14 m of 0.023 cm ID SS tubing to a collection vessel situated in a dose calibrator. Experimental conditions investigated and results of this initial study are summarized in Table 1. The conclusions from these data are: i) for the slurry target, the saturation N-13 yields are independent of dose rates, total doses and flow rates over the ranges investigated; and ii) the N-13 saturation yields for this target are roughly a factor of four higher than for H_2^{16}O only (consistent with the packing density and experimentally determined N-13 recoil fraction in water that derives from C-13). A conversion efficiency of aqueous N-13 activity to ^{13}N ammonia of 70-90% was observed. The ^{13}N NH_3 was identified by conversion to L- ^{13}N glutamate, via immobilized glutamate dehydrogenase and radio-HPLC analysis of the amino acid (Precolumn o-phthalaldehyde derivatization, Ultrasphere ODS, 5 μm , 4.6 x 150 mm i.d., 55% 100 mM potassium phosphate buffer, pH 7.4, and 45% MeOH; flow rate, 1.0 mL/min; fluorescence detector) (4).

The salient features of the C-13/ H_2^{16}O slurry target are: i) it provides sufficient aqueous N-13 for rapid conversion to ^{13}N NH_3 in clinically useful quantities; ii) beyond the initial target charge of enriched C-13 powder ($\sim \$20$ for this prototype), the cost is negligible; and iii) N-13 production is provided by both the $^{13}\text{C}(\text{p},\text{n})$ and $^{16}\text{O}(\text{p}, \alpha)$ reactions.

TABLE 1. ^{13}N Yields from Proton Irradiation of C-13 Powder/ H_2^{16}O Slurry Target vs 0-16 water only

Current (μA)	Time (min)	Flow Rate (cm^3/min)	Sat. N-13 Activity (mCi/ μA)	^{13}N Total aqueous collected (EOB) (mCi)
5	14	0.7	24.0	75
5	10	0.3	23.1	58
1	5	0.7	18.9	5.5
10	10	0.7	25.7	129
10	10	1.0	25.7	129
10	10	1.5	25.4	127
15	10	1.5	24.9	187
20	10	1.5	22.3	227
20	20	1.5	20.5	308
10	10	1.5	20.8	104
10	10	1.5	21.6	108
10	5	STATIC	6.61	20 ^a
15	5	"	6.60	29 ^a
20	5	"	5.86	35 ^a

a) Irradiation of 0-16 water only; all other entries are for the slurry target.

- See Chapters 11-20, In Root, J.W., and Krohn, K.A., Short-Lived Radionuclides in Chemistry and Biology, Adv. Chem. Ser. No. 197, American Chemical Society, 1981.
- Mazziotta, J.C., and Phelps, M.E., In Phelps, M.E., Mazziotta, J.C., and Schelbert, H.R., eds., Positron Emission Tomography and Autoradiography, New York, Raven Press, 1986, Ch. 11 and references therein.
- Schelbert, H.R., and Schwaiger, M., *ibid.*, Ch. 12.
- Barrio, J.R., Baumgartner, F.J., Henze, E., Stauber, M.S., Egbert, J.E., MacDonald, N.S., Schelbert, H.R., Phelps, M.E., and Liu, F.-T., *J. Nucl. Med.*, 24, 937 (1983).
- i) Parks, N.J., and Krohn, K.A., *Int. J. Appl. Radiat. Isot.*, 29, 754 (1978).
ii) MacDonald, N.S., Cook, J.S., Birdsall, R.L., McConnel, L.J., and Kuhl, D.E., *Trans. Amer. Nucl. Soc.*, 33, 927 (1979).
- Tilbury, R.S., and Dahl, J.R., *Radiat. Res.* 79, 22 (1979).

TECHNETIUM-99M AND INDIUM-111 LABELED LEUKOCYTES: IN VITRO AND IN VIVO EVALUATIONS, M.L. Thakur, F.A. White III, and M.T. Madsen, Thomas Jefferson University, Philadelphia, PA 19107

The use of ^{99m}Tc as a tracer for leukocytes remains attractive, and investigations continue for the development of new ^{99m}Tc agents that may label leukocytes efficiently. Recently Srivastava (1) reported that when leukocytes were incubated with 5-10 μg Sn^{2+} available in a glucoheptanate kit, washed and incubated again with $^{99m}\text{TcO}_4$ saline, the radioactivity was efficiently incorporated into the cells. He further reported that radioactivity was not eluted from the cells in vitro, and that the labeled autologous cells were accumulated in experimental abscesses in rabbits in quantities sufficient for gamma camera imaging.

We separated leukocytes from 30 ml venous blood from healthy human volunteers and labeled them in plasma, in saline, in the absence and presence of erythrocytes, and washed them repeatedly with plasma.

We then induced abscesses in a canine model by subcutaneous injection of turpentine, obtained 60 ml venous blood 18 hrs later and separated leukocytes by our standard procedure (2). Leukocytes were divided into two equal halves; cells in one portion were labeled with ^{111}In -Merc in plasma (3) and in the other portion with ^{99m}Tc as above in saline, following erythrocyte lysis. Both ^{111}In and ^{99m}Tc labeled cells were administered intravenously, and blood samples were drawn at 1, 2, 3, 4 hrs and at the time of sacrifice 18 hrs following cell administration. Abscesses were imaged with a gamma camera, equipped with low energy parallel hole or high energy parallel hole collimator set for ^{99m}Tc (140 keV, 20% window), or ^{111}In (247 keV, 20% window) gamma ray energy respectively. Equal numbers of counts were obtained for both types of images. Animals were then sacrificed with an over dose of 20% KCl and tissues dissected. Concomitant ^{99m}Tc and ^{111}In radioactivity was counted at a fixed geometry in an energy calibrated automatic well type scintillation counter. Using three standards of each radionuclide, an appropriate spill over correction factor was calculated. Percentages of radioactivity remained in circulation, released in plasma, and accumulated in whole liver, spleen, and kidney were then determined and abscess to tissue ratios were calculated for both tracers.

The glucoheptanate procedure labeled both human leukocytes and erythrocytes with equal efficiency in saline (60% and 70% respectively), but not in plasma (14% and 3% respectively). Unlike other ^{99m}Tc agents, the spontaneous elution of glucoheptanate labeled radioactivity, over a 24 hr period in vitro, was less than 10%.

The ^{99m}Tc agent however labeled canine leukocytes (10^8) less efficiently than it did human leukocytes and labeling efficiency varied between different animals (6.9%, 19.7%, 23.3%, and 42.3%), but was consistent between cell preparations from one animal (19.7%, 23.3%). The in vivo spontaneous elution of ^{99m}Tc was approximately 50%, as compared to 5% for ^{111}In .

Generally, the abscess to tissue ratios with ^{111}In were much higher than those with ^{99m}Tc ; the abscess/blood ratios for ^{111}In being 3 to 4 times higher than those with ^{99m}Tc .

These results, in dogs, indicate that ^{111}In still remains an attractive tracer for leukocytes.

References:

1. Srivastava S.C. Presented at the International Symposium on Radiopharmaceutical Chemistry, organized by the Indo-American and the Indian Soc. of Nucl. Med. Bangalore, Jan. 1986.
2. Thakur M.L., Coleman R.E. and Welch M.J., J. Lab. Clin. Med. 89 - 217 (1977).
3. Thakur M.L., McKenney S.L. and Park C.H., J. Nucl. Med. 26, 518 (1985).

NEW CHELATES FOR THE PREPARATION OF INDIUM AND GALLIUM RADIOPHARMACEUTICALS

C.J. Mathias, M.J. Welch, M.A. Green, J.A. Thomas, A.E. Martell*, and Y. Sun*
 Washington University School of Medicine, St. Louis, MO 63110 and *Department of
 Chemistry, Texas A&M University, College Station, TX 77843

The *in vitro* lipophilicity, electrophoretic behavior and *in vivo* biodistribution of the indium-111 complexes of new ligands with potential as indium and gallium radiopharmaceuticals were investigated. The ligands were N,N'-bis(2 hydroxy-benzyl)ethylenediamine-N,N'-diacetic acid (HBED), N,N'-bis(2-hydroxy-5-sulfo-benzyl)ethylenediamine-N,N'-diacetic acid (SHBED), N,N'-bis(5-deoxy-pyridoxyl)ethylenediamine-N,N'-diacetic acid (deoxy-PLED), N,N'-bis(2-hydroxy-3,5-di-methylbenzyl)-ethylenediamine-N,N'-diacetic acid (dimethyl HBED), N,N'-bis(2-hydroxy-5-dimethylbenzyl)-ethylenediamine-N-(2-hydroxyethyl)-N'-acetic acid (HBMA), and N,N'-bis(5-tert-butyl-2-hydroxy-3-methylbenzyl)-ethylenediamine-N,N'-diacetic acid [t-butyl (HBED)]. The ligands were synthesized and the complexes with indium-111 and (in the case of HBMA) gallium-67 prepared. The octanol water partition coefficient (P) were determined and the overall change on the complex evaluated by electrophoresis using cellulose electrophoresis strips (1,2). The log P and the electrophoretic mobility (relative to In-DTPA=1) of the complexes are given in Table 1. As anticipated the complexes with the higher log P has a lower electrophoretic mobility.

Biodistribution of the complexes were carried out in adult Sprague-Dawley rats over a time period of several hours. The lipophilic chelates of dimethyl HBED, t-butyl HBED, and HBMA cleared from the animals by the gastrointestinal tract, while the hydrophilic complex HBED, SHBED, and deoxy-PLED were cleared by the renal system. The most lipophilic compound studied (t-butyl HBED) showed the highest liver clearance, while for HBMA, a significant percentage (40%) of the activity was retained in the liver over a four hour time period. Stability studies showed that the In-HBMA complex has a much lower stability constant than the other ligands studied, suggesting that this complex may dissociate in the liver such that the radioactivity does not clear. The more lipophilic complexes may have a potential use as bifunctional chelates for labeling antibodies, since they have different properties from the ligands currently in use.

Table 1: Octanol/Water Partition Coefficients and Electrophoretic Mobility of Indium Complex Studies

Ligand	log P	Electrophoretic Mobility
	(In-DTPA = 1.0)	
DTPA	-2.9	1.0
HBED	-4.9	0.65
SHBED	-3.2	1.2
deoxy-PLED	-3.3	0.45
dimethyl HBED	-1.4	0.43
HBMA	1.7	0.27
t-butyl HBED	2.2	0.30

This work was supported in part by DOE Contract DE-AC02-77EV04318.

- Green, M.A., Welch, M.J., Mathias, C.J., et al: J. Nucl. Med. 26, 170 (1985).
- Green, M.A., Welch, M.J., Mathias, C.J., et al: Int. J. Nucl. Med. Biol. 12, 381 (1985).

SYNTHESIS AND LABELING OF TRIS-(2-SALICYLALDIMINOETHYL)AMINE WITH INDIUM AND GALLIUM

F.H. Liang, F. Virzi, R.C. Childs and D.J. Hnatowich

Department of Nuclear Medicine, University of Massachusetts Medical Center, Worcester, MA 01605

Recently, tris(5-methoxysalicylaldiminomethyl)ethane, a triiminotriphenol, was reported to form a neutral ^{68}Ga chelate which is potentially attractive for cardiac imaging (1). The triiminotriphenols provide three nitrogen lone electron pairs and three negative phenolic charges, thereby acting as hexadentate ligands to occupy the six coordination sites of trivalent metals such as gallium. We have investigated the use of another triiminotriphenol, tris-(2-salicylaldiminoethyl)amine (TITP), as a chelator for ^{111}In and ^{67}Ga . In addition to TITP, the 3-methoxy (3MeO-TITP) and the 5-methoxy (5MeO-TITP) analogs were each synthesized in one step from tris(2-aminoethyl)amine and unsubstituted, or 3-, or 5-methoxy salicylaldehyde. Elemental analyses (Table 1) of the chelates of each compound with indium trichloride or tris(acetylacetonato)gallium (III) are consistent with 1:1 complexes.

Table 1. Elemental analyses for TITP's and their indium and gallium chelates



Compound	Formula	C	H	N
TITP	C ₂₇ H ₃₀ N ₄ O ₃	70.58 (70.72)	6.53 (6.54)	12.18 (12.22)
5-MeOTITP	C ₃₀ H ₃₆ N ₄ O ₆	65.48 (65.68)	6.80 (6.61)	10.22 (10.21)
3-MeOTITP	C ₃₀ H ₃₆ N ₄ O ₆	65.38 (65.68)	6.35 (6.61)	10.10 (10.21)
In-TITP	C ₂₇ H ₂₇ N ₄ O ₃ ·In	56.99 (56.86)	4.96 (4.77)	9.58 (9.82)
In-3MeOTITP	C ₃₀ H ₃₃ N ₄ O ₆ ·In	54.51 (54.56)	4.94 (5.04)	8.39 (8.48)
In-5MeOTITP	C ₃₀ H ₃₃ N ₄ O ₆ ·In	54.39 (54.56)	4.94 (5.04)	8.39 (8.48)
Ga-TITP	C ₂₇ H ₂₇ N ₄ O ₃ ·Ga	62.01 (62.10)	4.85 (4.63)	10.23 (10.73)
Ga-3MeOTITP	C ₃₀ H ₃₃ N ₄ O ₆ ·Ga	58.34 (58.85)	5.08 (4.94)	9.02 (9.15)
Ga-5MeOTITP	C ₃₀ H ₃₃ N ₄ O ₆ ·Ga	58.47 (58.85)	5.11 (4.94)	8.96 (9.15)

Calculated values are in parentheses

Relative formation constants for indium and gallium were determined for each by adding solutions containing the chelator and EDTA in different molar ratios to either ^{111}In or ^{67}Ga . The distribution of the label between the chelator and EDTA was determined by paper chromatography after equilibrium was established. In this manner, the formation constant of each TITP for indium was found to be within an order of magnitude of that of EDTA, while for gallium the constants were one to two orders of magnitude lower than that of EDTA. Serum stability of the ^{111}In chelates of each TITP was determined by incubating in fresh human serum at 37°C followed by paper chromatographic analysis. The chelate of TITP itself

Table 2. Biodistribution of ^{111}In -labeled TITP's in normal mice at one hour post-intravenous injection*

	^{111}In -TITP	^{111}In -3MeOTITP	^{111}In -5MeOTITP
Blood	1.44 (0.39)	1.58 (0.34)	3.30 (0.54)
Heart	1.58 (0.34)	1.06 (0.24)	1.39 (0.24)
Lungs	2.82 (0.62)	1.00 (0.18)	2.00 (0.39)
Liver	21.24 (2.65)	16.07 (2.55)	9.80 (1.78)
Spleen	1.76 (0.25)	0.92 (0.19)	1.28 (0.22)
Kidneys	14.80 (1.68)	11.36 (2.37)	15.79 (2.11)
Stomach	2.24 (1.51)	1.34 (1.26)	1.77 (1.23)
Muscle	0.93 (0.17)	0.55 (0.09)	1.10 (0.17)
Bone	1.69 (0.27)	1.31 (0.31)	3.07 (0.60)
Brain	0.04 (0.01)	0.04 (0.01)	0.09 (0.05)

*Mean percent injected dose per gram (N = 5-6) normalized to a 25 gm animal with one standard deviation in parenthesis.

was found to be the most stable to dissociation under these conditions, losing only 8% of its label in 24 hours. Biodistributions of the ^{111}In chelates in normal mice (Table 2) obtained at one hour post-intravenous administration show similarities among the chelators, however the heart/blood ratio is most favorable for TITP and is similar to that reported for tris(5-methoxysalicylaldimino-methyl)ethane and ^{68}Ga (1). The favorable properties of the TITP chelates with ^{111}In and ^{67}Ga suggest that they may prove useful in the design of radiopharmaceuticals.

This work was supported in part by NIH grant CA33029 and DOE contract AC02-83ER60175.

1. Green M.A., Welch M.J., Mathias C.J., Fox K.A., Knabb R.M. and Huffman, J.C., *J. Nucl. Med.* 26 (1985) 170-180.

STABILITY STUDIES OF INDIUM-COMPLEXED
BIFUNCTIONAL CHELATES COUPLED TO PROTEIN

By

Kalyani M. Subramanian and Walter Wolf
Radiopharmacy Program, University of Southern California
Los Angeles, California. 90033

Abstract

Aminopolycarboxylic acids such as EDTA and DTPA form excellent complexes with trivalent metal ions. These chelating agents complexed to short-lived radionuclides of indium and gallium are used as radiopharmaceuticals in Nuclear Medicine. When such ligands are covalently bound to protein molecules they retain their metal binding ability that allows for easy radiolabelling of most proteins, including monoclonal antibodies. One question that needs to be addressed is whether the coupling of such ligands to a protein molecule alters the stability and (or) the formation constant of its metal chelate. Currently available methods to measure the stability constant of metal chelates in aqueous solution such as pH titration, polarography and spectrophotometry are not applicable to measure the stability constants of these bifunctional chelates when conjugated to a protein since they require conditions that are not compatible with the integrity of the protein. A simple method suitable for measuring the stability constants of metal complexes coupled to proteins is therefore required.

This report documents a method developed to determine the stability constants of indium chelates of aminopolycarboxylic acids NTA, EDTA, DTPA and TTHA, both in their free form and following coupling to a protein. This new method utilizes the displacement reaction between the indium chelates and ferric ions introduced in a nonprecipitable form. By measuring the position equilibrium constant 'K' of this reaction and knowing the stability constant 'B' of the corresponding ferric chelates,, the overall formation constants 'B' of the indium chelates were calculated. The radionuclide Indium-114m was used as a tracer for indium metal ion and new analytical methods were designed and used to determine the relative amounts of free and bound indium in equilibrium with ferric ion.

Human serum albumin was conjugated with EDTA and DTPA using their cyclic dianhydrides. A new method was developed to couple TTHA with HSA using Woodward's Reagent K.

The chelating agents coupled to HSA were complexed with indium and purified by dialysis, gel filtration or microcentrifugation. The stability constants of these indium complexes were determined at physiological pH using Fe-NTA as the source of ferric ion. The influence of pH conditions, concentration, molar ratios, and number of chelating groups attached to protein were studied to determine their effect on the overall stability constants of the above indium chelates both in their free form and when coupled to the protein. The results show that for free chelates, the values of overall stability constants determined in this work agreed well with published values. No significant differences could be observed between the stability constants of indium chelates in free form and when they are coupled to HSA.

The described new method for determining stability constants of indium chelates allows rapid determination of stability constants and may be applicable to other complexing agents. The analytical methods are also equally suitable to determine in vitro the status of indium in the bifunctional chelates attached to proteins.

ResultsComparison between the formation constant of the free chelates of indium and the chelates coupled to oroteinLog B values

<u>System</u>	<u>Free chelate</u>	<u>Protein coupled</u>
In-NTA	15.9 ± 0.19	---
In-EDTA	25.8 ± 0.21	25.9 ± .13
In-DTPA	28.5 ± 0.08	29.3 ± .11
In-TTBA	27.9 ± 0.18	26.0 ± 0.08

Stability constants of indium chelates

<u>Chelates(n)</u>	<u>log B</u>	<u>log B (literature value)</u>
In-NTA (9)	15.9 ± .19 at 22°C	16.9 , 15.9
In-EDTA (8)	25.8 ± .21 at 20°C	25.3 , 25.3
In-DTPA (6)	28.5 ± .08 at 20°C	29.0 , 28.4
In-TTBA (9)	27.9 ± .18 at 20°C	Not available

n = number of separate experiments

Effect of inert salt concentration on the stability constant of In-DTPA

DTPA-In-Fe : 1:1:1 Equilibrium

Concentration: 0.002 mM

Temperature: 20°C

<u>Salt added</u>	<u>Log B values</u>	
	<u>Ion Exchange Method</u>	<u>Paper Chromatography Method</u>
0.1M KCl	27.3 ± 0.22	27.6 ± 0.06
0.1M NaCl	27.3 ± 0.16	27.6 ± 0.01
0.1M KNO ₃ (Literature Data)		29.0
Without salt in this method		28.5±.08

APPLICATION OF PERTURBED ANGULAR CORRELATION MEASUREMENTS TO THE STUDY OF
In-111 LABELED PROTEINS. P.A. Jerabek, D. Mellenberg, J.K. Donahue, J.M.

Thomas, F.L. Otsuka, C.J. Mathias and M.J. Welch

Division of Radiation Sciences, Washington University School of Medicine, St. Louis, MO 63110

Over the past several years the technique of Perturbed Angular Correlation (PAC) of the gamma-ray cascade of Cd-111 following electron capture decay of In-111 has been shown to be a unique and interesting approach to obtain motional and structural information about molecules (1-4). The ability to monitor molecular motion by PAC is based upon previous studies showing that the experimentally determined integrated perturbation factor, G_2 , which estimates the degree of attenuation of the angular correlation, depends to a great extent on the magnitude of the molecular rotational correlation time (2,5). Thus PAC measurements can provide information concerning the tumbling rate of In-111 ions bound to molecules with different rotational correlation times.

We have applied this concept to study previously reported methods of labeling proteins using several In-111 labeled ligands (6). PAC measurements of free In-111 ion in aqueous solution gave a G_2 value of 0.90, characteristic of a fast tumbling rate of the unbound ion. When In-111 was bound to the protein transferrin, a G_2 value of 0.15 was measured, characteristic of the slow tumbling rate of In-111 bound to a large macromolecule. However, when In-111-DTPA ($G_2=0.69$) was bound to the protein human serum albumin (HSA), the G_2 value decreased to only 0.37. Measurements made of In-111-desferoxamine-HSA, and In-111-bromo-EDTA or In-111-DTPA bound to HDP1 antibody similarly gave higher G_2 values than expected. These results suggest that the nature of the binding of these ligands to proteins still affords some motional freedom of the attached ligand. It is interesting to note that similar chelating techniques have been used to attach gadolinium to proteins (7) and the proton relaxation enhancement of the protein-DTPA-Gd complex is similar to that of Gd-DTPA, again suggesting motional freedom.

PAC measurements were also made to monitor the rate of exchange between several different In-111-labeled ligands and a ligand bound to HSA. A study of the exchange of In-111-HBED (N,N'-bis(2-hydroxybenzyl)ethylenediamine-N,N'-diacetic acid) and DTPA-HSA showed that essentially all of the In-111 becomes bound to DTPA-HSA over a time of 10-12 days. Conversely, no exchange was observed between In-111-DTPA-HSA and HBED over a time of 7 days. These results agreed with those determined by conventional column chromatography. Other studies of exchange rate measurements by PAC will be presented.

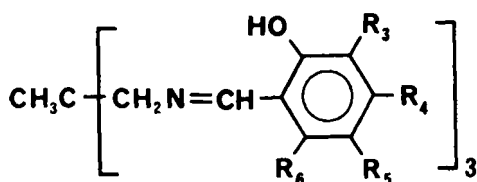
1. Leipert, T.K., Baldeschwieler, J.D. and Shirley, D.A., *Nature*, 220, 907 (1968).
2. Meares, C.F., Sundberg, M.W., and Baldeschwieler, J.D., *Proc. Nat. Acad. Sci. U.S.A.*, 69, 3718 (1972).
3. Shirley, D.A., *J. Chem. Phys.*, 53, 465 (1970).
4. Hwang, K.J. and Mauk, M.R., *Proc. Nat. Acad. Sci. U.S.A.*, 74, 4991 (1977).
5. Marshall, A.G. and Meares, C.F. *J. Chem. Phys.*, 56, 1226 (1972).
6. Otsuka, F.L. and Welch, M.J. *Int. J. of Nucl. Med. Biol.* 1986 (in press)
7. Unger E.C., Totty W.E., Neufeld, D., et al. *Med at Investigative Radiol.* 20, 693 (1985).

SYNTHESIS AND BIODISTRIBUTION OF A SERIES OF LIPOPHILIC GALLIUM-67
TRIS(SALICYLALDIMINE) COMPLEXES

Mark A. Green.

Departments of Radiology and Medicinal Chemistry, University of Minnesota,
Minneapolis, Minnesota 55455, U.S.A.

The development of radiopharmaceuticals labeled with generator-produced gallium-68 may facilitate more widespread use of PET imaging by reducing the need for nuclides that require in-house cyclotron production. Tracers for evaluation of regional cerebral and myocardial perfusion would be especially valuable. The synthesis and characterization of an uncharged and lipophilic gallium-68 chelate complex, $^{68}\text{Ga}[(5\text{-MeOsal})_3\text{tame}]$, has been reported elsewhere (1,2). It was shown that this agent can be used to produce PET images of the heart which show a linear correlation between gallium-68 uptake and regional myocardial perfusion; however, it behaves neither as a freely diffusible tracer nor a microsphere analog and is thus not suitable for quantitation of myocardial perfusion. Reported here is the synthesis of a series of closely related complexes and a comparison of their biodistributions in rats.



LIGAND	R ₃	R ₄	R ₅	R ₆
H ₃ [(sal) ₃ tame]	H	H	H	H
H ₃ [(3-MeOsal) ₃ tame]	OCH ₃	H	H	H
H ₃ [(4-MeOsal) ₃ tame]	H	OCH ₃	H	H
H ₃ [(5-MeOsal) ₃ tame]	H	H	OCH ₃	H
H ₃ [(4,6-(MeO) ₂ sal) ₃ tame]	H	OCH ₃	H	OCH ₃
H ₃ [(3-EtOsal) ₃ tame]	OC ₂ H ₅	H	H	H

Figure 1. Tris(salicylaldimines) investigated as gallium chelating ligands.

TABLE 1. Octanol/Saline (pH 5.2) Partition Coefficients, P, for the ^{67}Ga -Salicylaldimine Complexes Studied.

Complex	log P
$^{67}\text{Ga}[(\text{sal})_3\text{tame}]$	1.60 ± 0.05
$^{67}\text{Ga}[(3\text{-MeOsal})_3\text{tame}]$	1.65 ± 0.05
$^{67}\text{Ga}[(4\text{-MeOsal})_3\text{tame}]$	2.35 ± 0.05
$^{67}\text{Ga}[(5\text{-MeOsal})_3\text{tame}]$	1.45 ± 0.05
$^{67}\text{Ga}[(4,6\text{-(MeO)}_2\text{sal})_3\text{tame}]$	3.0 ± 0.1
$^{67}\text{Ga}[(3\text{-EtOsal})_3\text{tame}]$	2.7 ± 0.1
$^{67}\text{Ga}(\text{acac})_3$	2.0 ± 0.1

TABLE 2. Biodistribution of $^{67}\text{Ga}[(\text{sal})_3\text{tame}]$ in Rats.

	% Injected Dose per Organ				
	1 minute	5 minutes	30 minutes	60 minutes	240 minutes
Blood	7.1 ± 1.7	3.0 ± 0.3	0.83 ± 0.19	0.50 ± 0.05	0.29 ± 0.03
Heart	1.3 ± 0.2	0.49 ± 0.07	0.09 ± 0.02	0.034 ± 0.007	0.015 ± 0.003
Lungs	1.1 ± 0.4	0.53 ± 0.08	0.14 ± 0.04	0.094 ± 0.017	0.050 ± 0.016
Liver	28. ± 5.	41. ± 4.	64. ± 5.	75. ± 12.	73. ± 11.
Spleen	0.42 ± 0.06	0.24 ± 0.09	0.05 ± 0.01	0.024 ± 0.006	0.015 ± 0.004
Kidneys	8.2 ± 0.6	4.8 ± 0.6	0.94 ± 0.14	0.48 ± 0.04	0.24 ± 0.08
Brain	0.045 ± 0.011	0.025 ± 0.003	0.012 ± 0.004	0.007 ± 0.001	0.004 ± 0.002

Values shown represent the mean of four rats (161-201 g).

TABLE 3. Biodistribution of $^{67}\text{Ga}[(3\text{-EtOsal})_3\text{tame}]$ in Rats.

	% Injected Dose per Organ			
	1 minute	5 minutes	30 minutes	60 minutes
Blood	6.7 ± 1.1	4.2 ± 1.7	1.28 ± 0.07	0.96 ± 0.16
Heart	1.4 ± 0.3	0.45 ± 0.08	0.11 ± 0.01	0.06 ± 0.01
Lungs	2.0 ± 0.9	0.83 ± 0.22	0.27 ± 0.03	0.20 ± 0.03
Liver	24. ± 2.	26. ± 3.	16. ± 2.	12. ± 1.
Spleen	0.43 ± 0.09	0.21 ± 0.02	0.06 ± 0.01	0.04 ± 0.01
Kidneys	6.4 ± 1.4	2.4 ± 0.4	0.52 ± 0.06	0.30 ± 0.08
Brain	0.044 ± 0.008	0.028 ± 0.007	0.011 ± 0.002	0.008 ± 0.002

Values shown represent the mean of four rats (167-192 g).

TABLE 4. Biodistribution of $^{67}\text{Ga}[(4,6\text{-}(\text{MeO})_2\text{sal})_3\text{tame}]$ in Rats.

	% Injected Dose per Organ			
	1 minute	5 minutes*	30 minutes	60 minutes
Blood	6.0 ± 2.0	2.7 ± 0.4	2.2 ± 0.3	1.4 ± 0.1
Heart	2.0 ± 0.1	0.99 ± 0.13	0.53 ± 0.04	0.35 ± 0.03
Lungs	1.8 ± 0.2	1.9 ± 0.5	0.66 ± 0.09	0.43 ± 0.08
Liver	31. ± 8.	32. ± 3.	25. ± 4.	16. ± 2.
Spleen	0.40 ± 0.11	0.22 ± 0.02	0.25 ± 0.03	0.18 ± 0.05
Kidneys	5.40 ± 0.14	2.40 ± 0.16	1.6 ± 0.2	1.1 ± 0.2
Brain	0.033 ± 0.007	0.024 ± 0.003	0.024 ± 0.001	0.017 ± 0.002

Values shown represent the mean of four (*three) rats (178-208 g).

TABLE 5. Biodistribution of $^{67}\text{Ga}[(4\text{-MeOsal})_3\text{tame}]$ in Rats.

	% Injected Dose per Organ		
	1 minute*	5 minutes*	30 minutes
Blood	4.8 ± 0.5	3.5 ± 0.2	2.2 ± 0.1
Heart	1.1 ± 0.2	0.55 ± 0.08	0.30 ± 0.03
Lungs	1.3 ± 0.7	0.75 ± 0.14	0.45 ± 0.04
Liver	18. ± 5.	24. ± 3.	14. ± 1.
Spleen	0.30 ± 0.04	0.29 ± 0.01	0.15 ± 0.01
Kidneys	4.8 ± 0.6	2.4 ± 0.4	1.2 ± 0.1
Brain	0.039 ± 0.014	0.033 ± 0.004	0.027 ± 0.002

Values shown represent the mean of four (*three) rats (175-203 g).

TABLE 6. Biodistribution of $^{68}\text{Ga}(\text{acac})_3$ in Rats.

	% Injected Dose per Organ	
	5 minutes	30 minutes*
Blood	46. ± 7.	37. ± 3.
Heart	1.0 ± 0.1	0.81 ± 0.15
Lungs	7.6 ± 0.8	5.2 ± 0.7
Liver	3.4 ± 0.7	3.5 ± 1.2
Spleen	0.37 ± 0.08	0.57 ± 0.12
Kidneys	1.3 ± 0.3	1.4 ± 0.5
Brain	0.16 ± 0.04	0.16 ± 0.04

Values shown represent the mean of four (*three) rats (189–205 g).

The series of tris(salicylaldimine) ligands in Figure 1 were prepared by condensation of the appropriate salicylaldehyde derivative with 1,1,1-tris-(aminomethyl)ethane (3). On a macroscopic scale these ligands react with tris(acetylacetonato)gallium(III) in ethanol to afford 1:1 gallium:tris-(salicylaldimine) complexes as high melting solids (m.p. > 320°C). All exhibit parent ion peaks in their electron-impact mass spectra. The gallium-67 complexes of these ligands were prepared by reaction of the ligand with gallium-67 acetylacetonate in ethanol. All the tris(salicylaldimine) ligands produced lipophilic Ga-67 complexes, as evidenced by the measured octanol/saline partition coefficients (Table 1.).

The biodistributions of these complexes were determined in rats following intravenous injection of filtered (0.2 μm PTFE membrane) 20% ethanol:80% saline solutions (Tables 2–5.). As a control experiment, the biodistribution of gallium-68 acetylacetonate was also determined (Table 6.). The distribution of the salicylaldimine complexes differ markedly from their acetylacetonate precursor. The latter remains predominately in the blood pool, consistent with the expected formation of gallium-transferrin by ligand exchange. No significant differences were observed between the in vivo behaviors of $^{67}\text{Ga}[(5\text{-MeOsal})_3\text{tame}]$ (2), $^{67}\text{Ga}[(4\text{-MeOsal})_3\text{tame}]$, $^{67}\text{Ga}[(3\text{-EtOsal})_3\text{tame}]$, and $^{67}\text{Ga}[(4,6\text{-}(\text{MeO})_2\text{sal})_3\text{tame}]$, despite the variation in their lipophilicities. All were rapidly removed from circulation by the liver and slowly excreted. None penetrated the blood-brain barrier. The distribution of the parent complex, $^{67}\text{Ga}[(\text{sal})_3\text{tame}]$, is similar to that of the alkoxy-substituted derivatives, except the radiometal does not clear from the liver in the time span studied. This prolonged retention of gallium in the liver probably indicates decomposition of the salicylaldimine complex, resulting either in binding of the metal to liver macromolecules or precipitation of gallium hydroxide.

1. Green, M.A., Welch, M.J., and Huffman, J.C., *J. Am. Chem. Soc.*, **106**, 3689, (1984).
2. Green, M.A., Welch, M.J., Mathias, C.J., Fox, K.A.A., Knabb, R.M., and Huffman, J.C., *J. Nucl. Med.*, **26**, 170, (1985).
3. Fleischer, E.B., Gembala, A.E., Levy, A. and Tasker, P.A., *J. Org. Chem.*, **36**, 3042, (1971).

EFFECT OF DETERGENTS (TWEEN 80, TRITON X-100, AND SODIUM DODECYL SULFATE) ON PLATELET LABELING WITH LIPOID SOLUBLE IN-111 COMPLEXES AND PLATELET VIABILITY

M.K. Dewanjee and S.T. Mackey.
Mayo Clinic and Foundation, Rochester, MN 55905

To prevent adhesion of In-111 oxine to container, the detergent Tween-80 (T80) is added at 100 PPM level.(1-2) We have studied the effect of various dose levels of T80, Triton X-100 (T100), and sodium dodecyl sulfate (SDS) to study the effect on membrane permeability at low detergent concentration, membrane derangement at higher concentration and effect on platelet survival.(3-5) Structures of the three detergents are shown in Figure 1A. The formation of In-tropolone-detergent micelle is shown in Figure 1B. One microcurie of In-111 oxine (50 µg oxine) and In-111 tropolone (15 µg) were mixed with 10, 50, and 100 µg of T80, T100, and SDS. Aliquots of In-tropolone combining variable amounts of T80, T100, and SDS were incubated with 150×10^6 canine platelets for 5, 10, 30, and 60 minutes and uptake (%) in platelets were tabulated:

Detergent (µg)	In-111 tropolone							
	5 min.		10 min.		30 min.		60 min.	
	T80	T100	T80	T100	T80	T100	T80	T100
0	51±6	61±2	59±3	75±5	58±3	74±1	65±2	82±1
10	59±1	64±1	53±1	67±1	65±2	76±1	64±2	82±1
50	49±3	71±1	54±1	68±2	54±5	75±1	57±4	80±1
100	31±3	12±1	44±1	11±1	54±6	17±5	45±5	13±1

At low concentration, T80 and T100 increase the kinetics of uptake due to In-111 tropolone-detergent micelle formation, whereas at higher concentration due to membrane alteration the uptake decreases. Similar results were obtained with In-111 oxine uptake in presence of T80 and T100. In addition platelet survival as determined in dogs were not affected at 100 µg of T80 ($T_{1/2}$: 58 ± 10 hr control vs 55 ± 12 hr T80 group). T80 at low concentration appears nontoxic to labeled platelets. At higher concentration, the detergents solubilize membranes and are toxic to cells. SDS appears more damaging to membrane lipids and proteins leading to higher Indium loss at longer incubation time.

DETERGENTS

Name	Structure	Type
A. Polyoxyethylene sorbitol esters (Tween)	<p>No. of polyoxyethylene = $x + y + z + w$.</p>	Non-ionic
B. Triton X-100		Non-ionic
C. Sodium dodecyl-sulphate (SDS)		Anionic

Figure 1A. Structure of two nonionic detergents, Tween, Triton and an anionic detergent SDS.

Tween-80, ¹¹¹In-oxine, protein interaction
Polyoxyethylene sorbitol esters (Tween)

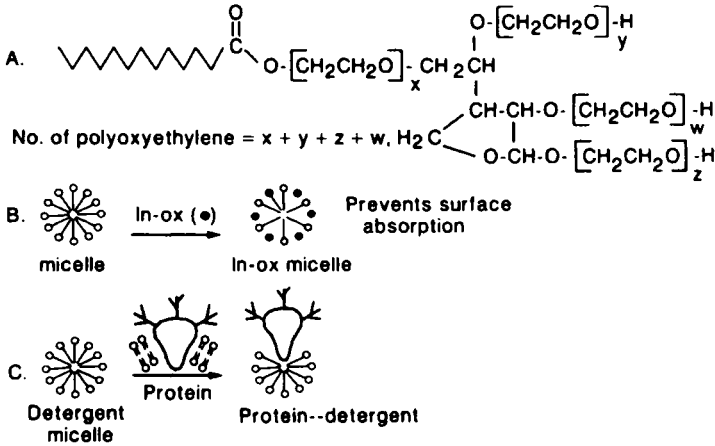


Figure 1B. Formation of In-111 tropolone-detergent micelle and possible effect on loss of membrane lipid and protein at high concentration.

- (1) Thakur, M.L., Welch, M.J., Joist, J.H., and Coleman, R.E., *Thromb Res*, **9**, 345 (1976)
- (2) Dewanjee, M.K., Rao, S.A., and Didisheim, P., *Indium-111 tropolone, a new high-affinity platelet label: preparation and evaluation of labeling parameters*, *J Nucl Med*, **22**, 981 (1981).
- (3) Package insert for In-111 oxine, *Amersham Corp., Arlington Heights, Illinois 60005*.
- (4) Helenius, A., and Simons, K., *Biochem Biophys Acta*, **415**, 29 (1975).
- (5) Attwood, D., and Florence, A.T., *Surfactant Systems*, Chapman and Hall, London, 1-39, 1983.

INDIUM-111 COMPLEXES OF PHENOLIC AMINOCARBOXYLATES FOR EXTENDED BILIARY SCINTIGRAPHY

F.C. Hunt

Isotope Division, Australian Atomic Energy Commission, Lucas Heights Research Laboratories, PMB Sutherland NSW 2232, Australia

Despite its unfavourable radiation emissions and dosimetry characteristics, ^{131}I -Rose Bengal is still used for a number of hepatobiliary investigations, particularly for diagnosis of biliary atresia and neonatal hepatitis (1). The delayed excretion of radiopharmaceutical in such cases precludes the use of the short-lived $^{99\text{m}}\text{Tc}$ -HIDA compounds.

Several attempts have been made to find an improved radiopharmaceutical for delayed hepatobiliary studies, for example HIDA compounds have been labelled with the longer lived ruthenium-97 (2). In an earlier study, the metal-chelating dye, phenolphthalein complexone was labelled with ^{111}In (3).

At the last Symposium, ^{67}Ga -complexes of the the phenolic aminocarboxylic acids EHPG and HBED (Figure 1) were described which have biliary excretion characteristics suitable for delayed studies (4). In the present study these chelators containing lipophilic substituents were complexed with ^{111}In , which has superior imaging properties.

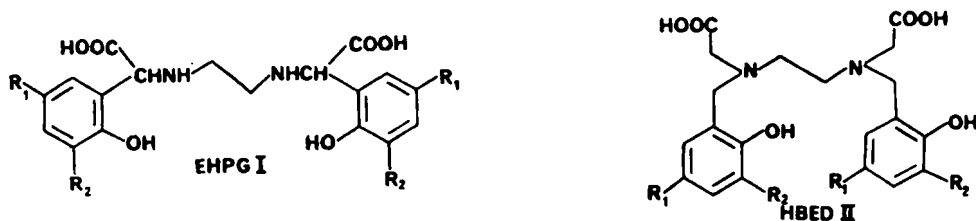
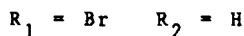
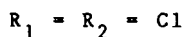


Figure 1. Structural formulae of the phenolic aminocarboxylates



The indium complexes were prepared by ligand exchange from ^{111}In -citrate. Analysis by reverse-phase HPLC showed complete complexation and mostly single radiochemical species present in the case of the HBED complexes, and multiple species present in the case of EHPG, which can be partly attributed to the presence of chiral isomers.

Biodistribution studies in mice (Table 1) showed substantial biliary excretion with both series of complexes, with biodistribution patterns similar to $^{99\text{m}}\text{Tc}$ -HIDA complexes. Gamma camera scintigraphy of the compound with the greatest biliary output In-di-Cl-HBED is shown in Figure 2. The gallbladder is visualised and there is little hepatic retention at 2 hour post injection.

Table 1. Biodistribution of Indium-111 Phenolic Aminocarboxylates*

EHPG R1	R2	Blood	Liver	GIT+GB	Kidneys	Urine
Cl	H	0.8 ± 0.1	6.9 ± 1.6	74.3 ± 2.1	2.2 ± 0.4	8.1 ± 0.5
Cl	Cl	0.4 ± 0.1	21.3 ± 1.9	71.7 ± 1.6	1.8 ± 0.1	1.1 ± 0.4
Br	H	2.4 ± 0.1	11.4 ± 0.8	60.9 ± 1.5	5.3 ± 0.5	8.8 ± 2.8

HBED	H	0.5 ± 0.2	2.3 ± 0.2	61.1 ± 1.6	1.3 ± 1.3	28.3 ± 1.5
Cl	Cl	0.2 ± 0.01	5.5 ± 0.4	88.4 ± 0.6	0.2 ± 0.01	2.7 ± 0.6
Br	H	0.6 ± 0.1	9.8 ± 4.1	76.5 ± 5.2	4.9 ± 0.2	7.6 ± 1.3

*Percentage of injected dose per organ. Means ± SD for 3 mice

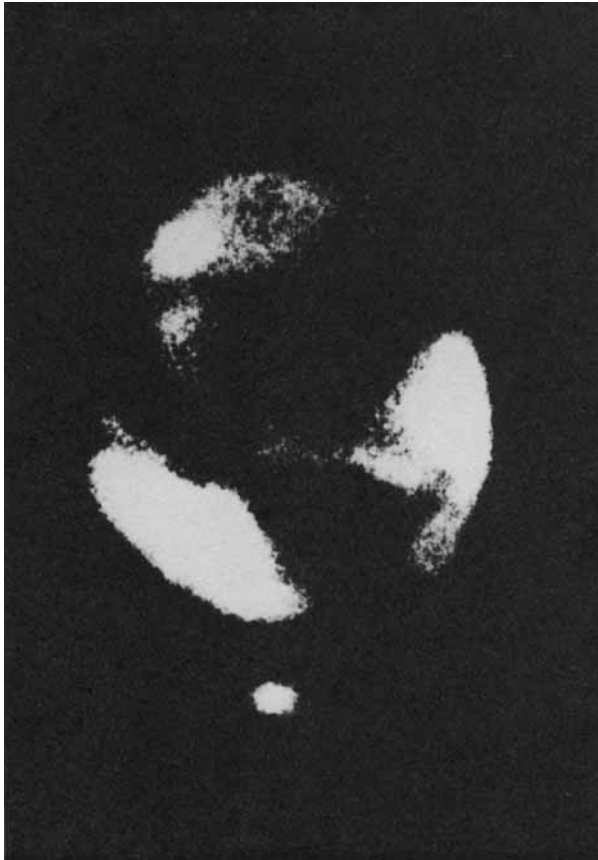


Figure 2. Scintigraphy of ^{111}In -dichloro-HBED in a rabbit

Indium-111 phenolic aminocarboxylates are therefore potential replacements for ^{131}I -Rose Bengal for extended hepatobiliary studies.

1. Antico, V.F; Denhartog P; Ash, J.M; Gilday, D,L; and Houle, S; Clin. Nucl. Med; 10, 171 (1985).
2. Srivastava, S.C; and Meinken G.E; In Proceedings Fifth International Symposium on Radiopharmaceutical Chemistry, Science University of Tokyo, Tokyo, 1984, p 57.
3. Lin, M.S; Radiology, 123, 783 (1977)
4. Hunt, F.C; In Proceedings Fifth International Symposium on Radiopharmaceutical Chemistry, Science University of Tokyo, Tokyo, 1984, p 13.

EXCITATION FUNCTIONS RELEVANT TO THE PRODUCTION OF SHORT-LIVED β^+ -EMITTING RADIOISOTOPES OF BROMINE

S.M. Qaim, G. Stöcklin

Institut für Chemie 1 (Nuklearchemie), Kernforschungsanlage Jülich GmbH, 5170 Jülich, FRG

The radioisotopes ^{75}Br ($T_{1/2} = 1.6$ h) and ^{76}Br ($T_{1/2} = 16.1$ h) have found applications in PET studies and the radioisotopes ^{78}Br ($T_{1/2} = 6.5$ min) and $^{77\text{m}}\text{Br}$ ($T_{1/2} = 41.5$ min) are potentially useful β^+ emitters. Methods of production of some of those radioisotopes were reviewed (1); several gaps in the production data were observed.

Excitation functions were measured by the stacked-foil technique for the first time for the reactions $^{75}\text{As}(\alpha, n)^{78}\text{Br}$ ($T_{1/2} = 6.5$ min) and $^{75}\text{As}(\alpha, 2n)^{77\text{m}}\text{Br}$ ($T_{1/2} = 4.5$ min) up to $E_\alpha = 28$ MeV. Thin samples used for measurements were prepared by an electrolytic deposition of arsenic on Cu-backing. A fast removal of radiobromine from the Cu-matrix activity was performed to be able to identify the short-lived products. The excitation functions are shown in Fig. 1. From these data the thick target yields for the formation of ^{78}Br and $^{77\text{m}}\text{Br}$ were calculated. The thick target saturation yield of ^{78}Br over the energy range $E_\alpha = 28 \rightarrow 10$ MeV amounts to 481 MBq (13 mCi)/ μA . A 30 min irradiation with 28 MeV α -particles at 25 μA could lead to (theoretically) about 12 GBq (325 mCi) ^{78}Br .

The two major processes for the production of ^{75}Br , viz. $^{75}\text{As}(^3\text{He}, 3n)^{75}\text{Br}$ and $^{76}\text{Se}(p, 2n)^{75}\text{Br}$, demand a medium sized cyclotron (cf. refs. 1–5). Attempts to use the $^{78}\text{Kr}(p, \alpha)^{75}\text{Br}$ reaction in the energy range of $E_p = 16 \rightarrow 12$ MeV resulted in low yields (6). We investigated the $^{74}\text{Se}(d, n)^{75}\text{Br}$ reaction which can possibly be used at low energy cyclotrons. Excitation function was measured up to $E_d = 14$ MeV using 31.4 % enriched ^{74}Se . The thick target yields of ^{75}Br calculated from the preliminary cross-section data are given in Table 1. The yield expected from the $^{74}\text{Se}(d, n)^{75}\text{Br}$ reaction over the energy range of $E_d = 10 \rightarrow 7$ MeV is higher than that from the $^{78}\text{Kr}(p, \alpha)^{75}\text{Br}$ reaction for $E_p = 16 \rightarrow 12$ MeV.

TABLE 1. Theoretical Thick Target Yield of ^{75}Br calculated from the Excitation Function of the $^{74}\text{Se}(d, n)^{75}\text{Br}$ Reaction*

Energy range (MeV)	Thick target yield of ^{75}Br MBq/ μAh	(mCi)
14 \rightarrow 7	555	(15)
12 \rightarrow 7	370	(10)
10 \rightarrow 7	185	(5)

*assuming that 99 % enriched ^{74}Se is used.

Assuming that 99 % enriched ^{74}Se is used as target material and that the target can withstand a deuteron beam current of about 15 μA (cf. 5) for 3 h the theoretically expected yield of ^{75}Br over the energy range of $E_d = 10 \rightarrow 7$ MeV would amount to about 5.5 GBq (~ 150 mCi). Experimental batch yield would be lower and thus possibly not sufficient for large scale PET applications. A baby cyclotron (with $E_p = 17$ MeV; $E_d = 10$ MeV) thus can produce only limited quantities of ^{75}Br via either of the two investigated reactions $^{78}\text{Kr}(p, \alpha)^{75}\text{Br}$ and $^{74}\text{Se}(d, n)^{75}\text{Br}$. If at all the $^{74}\text{Se}(d, n)^{75}\text{Br}$ process may be preferable since a solid target is easier to handle than a gas target (both ^{78}Kr and ^{74}Se being very expensive). In contrast to a baby cyclotron, if a machine with a higher deuteron energy (for example ~ 14 MeV) is used, the yield of ^{75}Br from the $^{74}\text{Se}(d, n)^{75}\text{Br}$ process increases sharply and is then comparable to that from the $^{75}\text{As}(^3\text{He}, 3n)^{75}\text{Br}$ reaction. The cost of the 99 % enriched target material would be approximately US \$ 30000. The level of ^{76}Br impurity should be low since it would be formed from ^{76}Se , the amount of which in highly enriched ^{74}Se is very small.

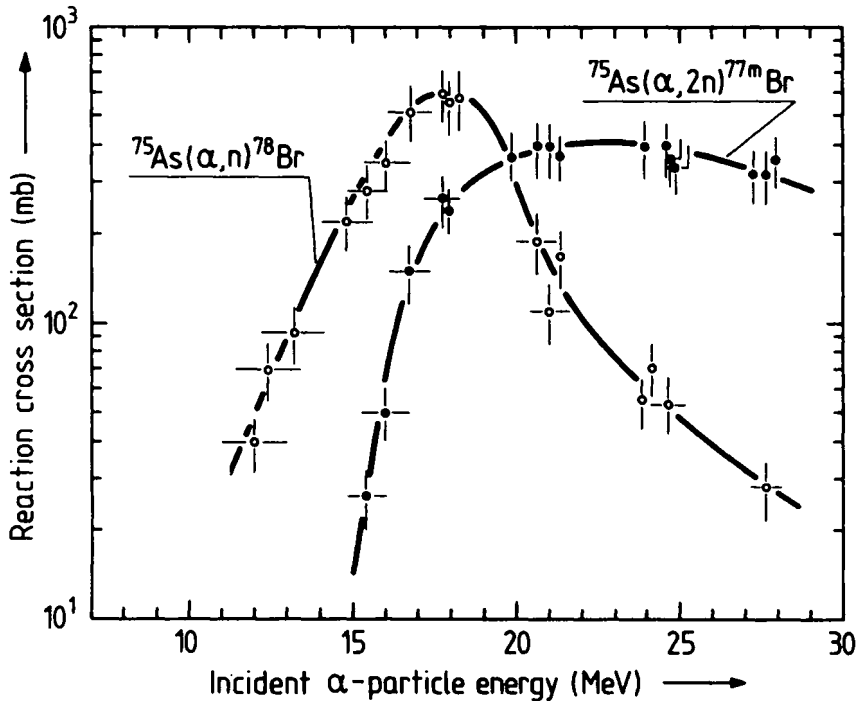


Figure 1. Excitation functions of the $^{75}\text{As}(\alpha, n)^{78}\text{Br}$ and $^{75}\text{As}(\alpha, 2n)^{77\text{m}}\text{Br}$ reactions. The errors in cross sections include both statistical and systematic errors. Typical deviations in energies in various regions are also given.

1. Qaim, S.M. and Stöcklin, G., *Radiochimica Acta* **34**, 25 (1983)
2. Weinreich, R., Alfassi, Z.B., Blessing, G. and Stöcklin, G., in *Nuklearmedizin, Supplement 17*, F.K. Schattauer Verlag GmbH, Stuttgart (1980) pp 202-205
3. Paans, A.M.J., Welleweerd, J., Vaalburg, W., Reiffers, S. and Woldring, M.G., *Int. J. Appl. Radiat. Isotopes* **31**, 267 (1980)
4. Blessing, G., Weinreich, R., Qaim, S.M. and Stöcklin, G., *Int. J. Appl. Radiat. Isotopes* **33**, 333 (1982)
5. Kovács, Z., Blessing, G., Qaim, S.M. and Stöcklin, G., *Int. J. Appl. Radiat. Isotopes* **36**, 635 (1985)
6. Friedman, A.M., De Jesus, O.J., Harper, P. and Armstrong, C., *J. Label. Compd. Radiopharm.* **19**, 1427 (1982)